Role of the cannabinoid receptor 2 in the development of surgical neuropathic pain

Dissertation zu Erlangung des Doktorgrades
(Dr. rer. nat.)
Mathematisch-Naturwissenschaftliche Fakultät
Rheinische Friedrich-Wilhelms-Universität Bonn

vorgelegt von
Elisa Nent

Bonn
August 2017

Angefertigt mit Genehmigung der Mathematisch – Naturwissenschaftlichen Fakultät der Rheinischen Friedrich – Wilhelms Universität Bonn

1. Gutachter : Prof. Dr. A. Zimmer
2. Gutachter : Prof. Dr. M. Pankratz

Tag der Promotion: 14.12.2017
Erscheinungsjahr: 2018

Abbreviations

AA	Arachidonic acid
2-AG	2-arachidonoyl glycerol
AEA	Arachidonoyl ethanolamine (Anandamide)
ANOVA	Analysis of variance
ATP	Adenosine triphosphate
BCP	Beta-caryophyllene
BDNF	Brain-derived neurotrophic factor
bp	Base pair
BSA	Bovine serum albumin
CB1	Cannabinoid receptor 1
CB2	Cannabinoid receptor 2
CBD	Cannabidiol
CCL2	C-C motif chemokine ligand 2
CCR2	C-C motif chemokine receptor 2
CGRP	Calcitonin-gene related peptide
cm	Centimeter
CNS	Central nervous system
contra	Contralateral
COX-2	Cyclooxygenase-2
CX3CR1	Fractalkine receptor
CYP	Cytochrome P450
DAG	Diacylglycerol
Daglα	Diacylglycerol lipase α
DAPI	4',6-diamidino-2-phenylindole
dH_2O	Deionized H_2O

DMEM	Dulbecco's modified eagle medium
DMSO	Dimethyl sulfoxide
DNA	Deoxyribonucleic acid
DRG	Dorsal root ganglia
DSE	Depolarization-induced suppression of excitation
DSI	Depolarization-induced suppression of inhibition
eCB	Endocannabinoid
ECS	Endocannabinoid system
EDTA	Ethylene glycol tetraacetic acid
EtOH	Ethanol
ERK	Extracellular signal-related kinase
FAAH	Fatty acid amid hydrolase
FCS	Fetal calf serum
FITC	Fluorescein isothiocyanate
FL	Floxed (flanked by loxP sites)
g	Gravitational force
g	Gram
GABA	γ-aminobutyric acid
GFP	Green fluorescent protein
GPCR	G-protein coupled receptor
h	Hour
HBSS	Hank's buffered salt solution
HCl	Hydrochloric acid
Iba1	Ionized calcium-binding adapter molecule 1
IHC	Immunohistochemistry
IL	Interleukin
iNOS	Inducible nitric oxide synthase
i.p.	Intraperitoneal

ipsi	Ipsilateral
IR	Infrared
JAK-STAT3	Janus kinase- signal transducer and activoator of transcription 3
JNK	c-JUN N terminal kinase
kb	Kilobase
kDa	Kilodalton
kg	Kilogram
lig	Ligated
LOX	Lipoxygenase
loxP	“locus of X-ing over” in phage P1
LPS	Lipopolysaccharide
LTD	Long-term depression
LTP	Long-term potentiation
M	Molar
m	Meter
MAGL	Monoacylglycerol lipase
MAPK	Mitogen-activated protein kinase
mg	Milligram
min	Minutes
MIP	Mirror-image pain
Ml	Milliliter
mM	Millimolar
mRNA	Messenger RNA
ms	Milliseconds
MS	Mass spectrometry
n	Number (sample size)
NAPE	N-acyl-phosphatidylethanolamine
NAPE-PLD	NAPE-phospholipase D

NeuN	Neuronal nuclear antigen
nM	Nanomolar
NMDA	N-methyl-D-aspartate
NO	Nitroc oxide
ns	Not significant
ng	Nanogram
PAG	Periaqueductal grey
PBS	Phosphate buffered saline
PCR	Polymerase chain reaction
PE	Phosphatidylethanolamine
PEA	Palmitoylethanolamide
PFA	Paraformaldehyde
PG	Prostaglandins
PKA	Protein kinase A
PKC	Protein kinase C
PLC	Phospholipase C
PPAR	Peroxisome-proliferator activated receptor
PSNL	Partial sciatic nerve ligation
RNA	Ribonucleic acid
RT	Room temperature
RVM	Rostral ventromedial medulla
s	Second
SEM	Standard error of the mean
SNRI	Serotonin-noradrenaline reuptake inhibitor
T	Temperature
TCA	Tricyclic antidepressants
THC	Δ9-tetrahydrocannabinol
TLR	Toll-like receptor

TNBS	Trinitrobenzene sulfonic acid
TNF-α	Tumor necrosis factor - alpha
Tris	Tris (hydroxymethyl) aminomethane
TRP	Transient receptor potential
TRPV1	Transient receptor potential vanilloid 1
U	Unit
VTA	Ventral tegmental area
WHO	World Health Organization
WT	Wild type
µl	Microliter
µM	Micromolar

Summary

When normal nociceptive pain becomes chronic, it loses its protective function and causes a general pain hypersensitivity. Neuropathic pain is one type of chronic pain, which is caused by various diseases or physical injury of the somatosensory nervous system. The two main symptoms include hyperalgesia, describing increased sensitivity to pain, or allodynia, the sensation of pain after an innocuous stimulation. These symptoms result from a maladaptive plasticity of the nociceptive system. In recent years, many studies could confirm a contribution of the endocannabinoid system in nociception. In particular, the CB2 receptor is known be located on immune cells and to regulate inflammation. Since inflammation of the somatosensory nervous system is a key component of neuropathic pain, I was interested in the pain phenotype of mice with a constitutive or conditional CB2 deletion. Previous studies demonstrated that mice with a constitutive CB2 deletion (CB2KO) develop increased mechanical allodynia on the non-injured side after induction of neuropathic pain through partial sciatic nerve ligation.

I analyzed neuropathic pain development in conditional CB2 knockout mice, lacking the CB2 receptor in myeloid cells (e.g. microglia and macrophages, CB2-LysM) or in neurons (CB2-Syn) only. CB2-LysM mice showed the same enhanced allodynia on the non-injured side as observed in CB2KO animals. This effect was not measured in CB2-Syn mice. I could confirm this finding through histological studies measuring microgliosis in the dorsal horn of the lumbar spinal cord. Microgliosis was increased on both sides of the spinal cord in CB2KO and CB2-LysM mice. To confirm the cellular distribution of CB2, I used CB2-GFP mice, which reveal a GFP signal in all CB2-expressing cells. A strong expression was found in the sciatic nerve, dorsal root ganglion and lumbar spinal cord that colocalized with microglial marker Iba1 but not with neuronal marker synapsin. These results indicate the expression of the CB2 receptor on microglia cells.

The CB2 receptor can be activated through the two main endocannabinoids 2-AG and anandamide. I investigated the contribution of Daglα the main synthesizing enzyme for 2-AG, in thermal, mechanical and neuropathic pain behavior. Contrary to our expectations, mice lacking Daglα showed the same pain phenotype as normal WT animals. I suspect an 2-AG independent activation of CB2 during neuropathic pain, which would serve to counteract the inflammation.

Table of Contents

1 Introduction

1.1 Pain

Nociception is an essential process to warn the organism against tissue damage. In case of an injury, peripheral sensory nerve fibers, called nociceptors, transduce thermal, mechanical or chemical pain stimuli into an electrical signal, which is sent to the central nervous system (Basbaum et al. 2009). Peripheral nociceptors have their cell bodies located in the dorsal root ganglia (DRG) and branch into the periphery and the dorsal horn's laminae I - V of the spinal cord. These nociceptors are called primary afferent neurons and have a pseudo-unipolar morphology, since their axonal branches are directed to the spinal cord and to the peripheral tissue. Three different types of nociceptors exist: Aδ nociceptors are myelinated and have a medium sized diameter, transmitting acute, fast mechanical, chemical, or thermal pain. This is in contrast to Aβ fibers, which have a large diameter and conduct mechanical innocuous stimuli such as light touch. The other type of nociceptors are C fibers. These fibers have a small diameter and are unmyelinated. Therefore, they conduct signals in a slow manner. C-fibers are polymodal and transduce heat or mechanical stimuli but do also react to innocuous sensations (see Figure 1) (Meyer et al. 2006). Each type of nociceptor expresses a different set of channels that are specific for a certain stimulus. Heat stimuli, for example, are transduced via the transient receptor potential vanilloid 1 (TRPV1) (Caterina et al. 1997). Mechanical pain stimuli are thought to be transduced by TRPV4 and TRP Ankyrin 1, but research to confirm these findings is still ongoing (Dubin & Patapoutian 2010). The principle pathway of pain transduction is as follows : in peripheral nerve terminals, the pain stimulus is transduced into an electrical signal or a so-called receptor potential, leading to the depolarization of the nociceptor. Thus, voltage-gated ion channels are activated and generate action potentials that are conveyed to synapses in the dorsal horn of the spinal cord. These synapses end at second order neurons, which transmit the signal to different regions of the brain, including the thalamus, somatosensory cortex, amygdala or the insular cortex (Kandel et al. 2000).

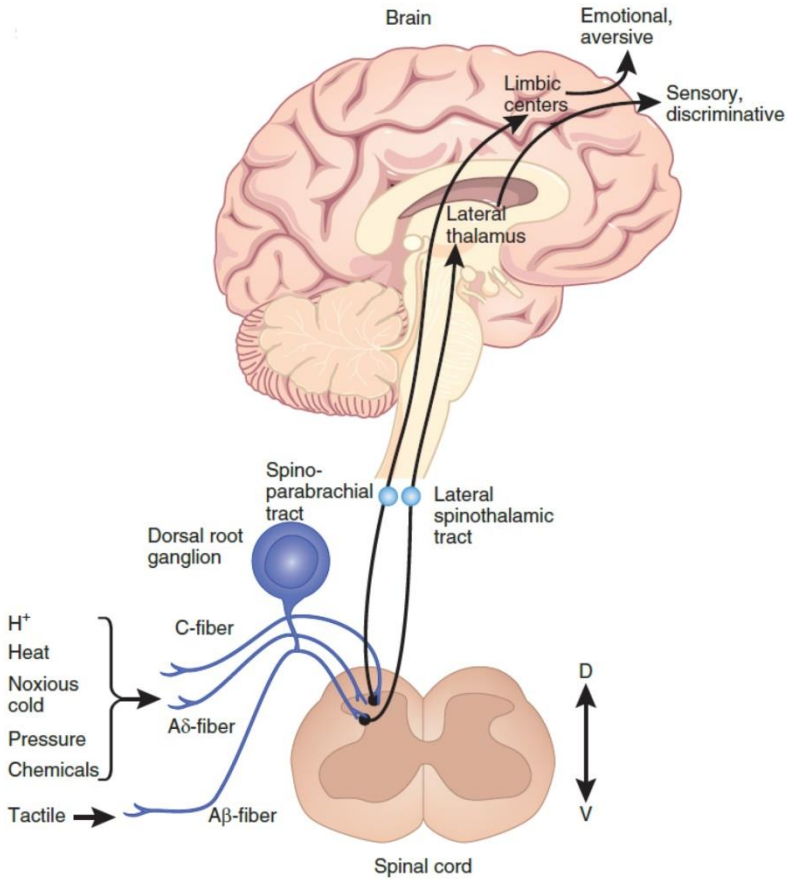

Figure 1 Pain circuit. Noxious or tactile stimuli are recognized by nociceptors in the periphery. The signal is then transferred via C-, Aδ, or Aβ- fibers to the dorsal spinal cord, where nociceptors signal to second order neurons. These neurons are directed to the thalamus and to the cortex via the spinoparabrachial tract or the lateral spinothalamic tract (modified from Kuner, 2010.)

1.2 Neuropathic pain

When pain exceeds its protective function and resides for months or longer, it transforms into chronic pain. Nowadays, up to 10% of the general population is affected by chronic neuropathic pain (Van Hecke et al. 2014). This type of persistent pain often results from injuries to the somatosensory nervous system or diseases such as diabetes mellitus, arthritis, multiple sclerosis or cancer (Treede et al. 2008). Many patients suffering from chronic neuropathic pain experience a general hypersensitivity, including symptoms such as spontaneous pain, an increased sensitivity to a painful stimulus (hyperalgesia), or a painful sensation to a normally innocuous stimulus (allodynia) (Woolf & Mannion 1999). Yet, current therapies still fail to completely abolish the pain but rather reduce the symptoms. Existing pharmacotherapies act by inhibiting nociceptor activity but do not

prevent disease progression. Additionally, most therapeutics induce severe side effects in patients (Attal et al. 2010). A better understanding of the molecular mechanisms is needed for the development of an adequate therapy.

1.2.1 Pathophysiological mechanisms

In case of a peripheral nerve injury, complex peripheral and central sensitization processes occur, rendering the nerve to an increased state of excitability and hypersensitivity. This is caused by the release of endogenous factors, such as neurotransmitters, lipids, cytokines, peptides or inflammatory mediators from injured neurons at the site of injury, which attract and activate resident and infiltrating immune cells. Moreover, proalgesic factors will bind nerve terminals surrounding the damaged neuron to increase their sensitivity, resulting in a reduced firing threshold and ectopic discharges of these neurons. This phenomenon is called peripheral sensitization and is in part responsible for the typical symptoms of spontaneous pain and allodynia. The elevated firing rate of peripheral primary afferent neurons overstimulates second order neurons in the spinal cord and induces synaptic plasticity, mainly through the activation of glutamate receptors (Maldonado et al. 2016). This maladaptive, neuroplastic change of the respective synapses between first and second order neurons is called central sensitization. The succeeding disruption in homeostasis in the spinal cord causes resident glia cell, like microglia to transform into their reactive state, including morphological changes and an increased transcription of inflammatory genes(Kierdorf & Prinz 2013).

1.2.2 Neuroinflammation in neuropathic pain

An important key player in the pathophysiological mechanisms of chronic pain, besides peripheral nociceptors and second-order neurons, is the innate immune system. In recent years, it has become of great interest in a majority of studies covering the mechanisms of neuropathic pain. Many components of the immune system are involved in the neuroinflammatory processes of this disease. In the following part, the most significant components regarding this study will be covered, although many more are involved in chronic pain pathology.

Among the inflammatory mediators that are released by injured neurons are vasoactive molecules such as calcitonin gene- related peptide (CGRP), bradykinin, substance P and

nitric oxide, which cause hyperemia and swelling to support immune cell infiltration at peripheral sites (Scholz & Woolf 2007). Moreover, secreted cytokines activate the extracellular signal-related (ERK) mitogen-activated protein kinase (MAPK) in Schwann cells, which leads to a degradation of their myelin sheath (Napoli et al. 2012). This process is part of the Wallerian degeneration that occurs to the distal parts of the damaged axon to prepare for regrowth (Gaudet et al. 2011). Resident mast cells then start to degranulate and release histamine, serotonin, nerve growth factor, and leukotrienes, which in turn attract circulating neutrophils. This type of granulocyte recruits immune cells, like macrophages during the first 24h and is responsible for the early development of hyperalgesia in neuropathic pain (Perkins & Tracey 2000). The infiltration of immune cells at the site of nerve injury is critical to the development of neuropathic pain (Clark et al. 2013). Additionally, some proinflammatory factors like TNF-α are able to travel along the axon retrogradely to the DRG's and anterogradely from the DRG to the spinal cord, where they can activate glia cells or induce disruption of the blood - spinal cord – barrier (Shubayev et al. 2010). This in turn facilitates the infiltration of immune cells, like macrophages and T lymphocytes to central sites. CCL2, (Kiguchi et al. 2010) as well as TNF-α, IL-1β, IL-10 (Üçeyler et al. 2007) were found to be upregulated in the DRG after nerve injury. Other signal molecules, like IL-6, brain-derived neurotrophic factor (BDNF), adenosine triphosphate (ATP), glutamate, substance P, and calcitonin gene-related peptide (CGRP) are also released into the dorsal horn (Ren & Dubner 2010).

Glia cells of the spinal cord like microglia and astrocytes are consequently activated by the released signal molecules. IL-6 for example, activates microglia in the spinal cord via the Janus kinase-signal transducer and activator of transcription 3 (JAK-STAT3) pathway (Dominguez et al. 2010). ATP on the other hand binds purinergic receptors, like the P2X4 receptor on microglia, which is upregulated after neuropathic pain induction (Tsuda et al. 2003). Activated microglia then secrete BDNF (Tsuda & Inoue 2016) and IL-1β. Released IL-1β facilitates the phosphorylation of NMDA receptors in neurons, thereby changing synaptic strength and promoting hyperalgesia (Guo et al. 2007). Microglia in the dorsal spinal cord can also be activated by fractalkine (CX3CL1), CCL2 or Toll-like receptors (TLR) (see Figure 2) (Scholz & Woolf 2007), which can induce an upregulation and release of proinflammatory cytokines (Trinchieri & Sher 2007).

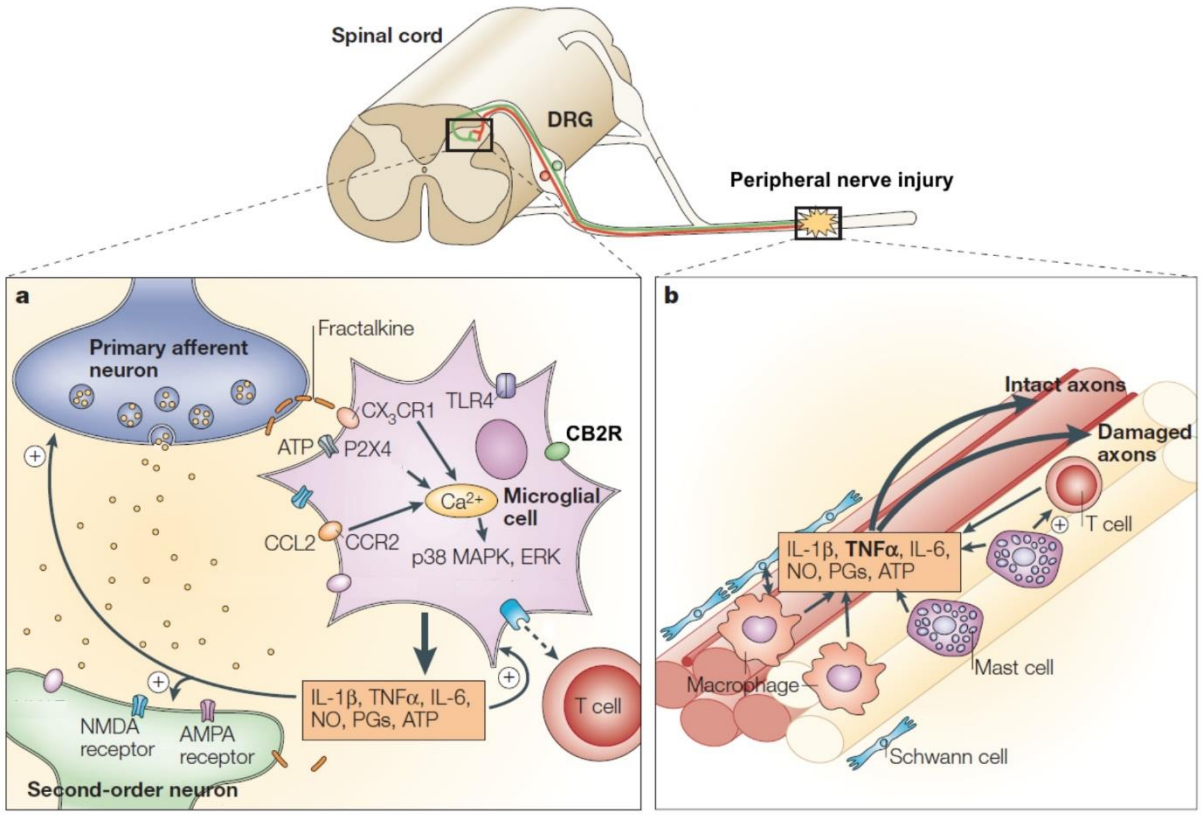

Figure 2 Molecular mechanisms after peripheral nerve injury. a) Primed nociceptors release cytokines or transmitters that activate microglia, which are surveilling the spinal cord. Activated microglia release proinflammatory cytokines like interleukin 1β (IL-1β), tumor necrosis factor-α (TNFα), interleukin-6 (IL-6), nitric oxide (NO), prostaglandins (PGs) or adenosine triphosphate (ATP) and express several receptors such as the ionotropic purinoceptor P2X4, Toll-like receptor 4 (TLR4), fractalkine receptor (CX_3CR1), chemokine (C-C motif) receptor 2 (CCR2) and the cannabinoid receptor 2 (CB2R). Activation of some of these receptors induces an increase in calcium levels and activation of the p38 mitogen-activated protein kinase (MAPK), extracellular signal-regulated kinase (ERK) pathway. **b)** Injured neurons release proinflammatory factors that recruit Schwann cells, mast cells, macrophages and T cells among others. These cells release IL-1β, TNFα, IL-6, NO, PGs and ATP to induce hypersensitivity in the injured nerve fibers. Eventually, proinflammatory factors are transported retrogradely to the neuronal cell bodies in the dorsal root ganglion (DRG) and further to the spinal cord to induce further inflammation and increased sensitivity. (modified from Marchand, 2005)

Overall, many immunological processes at peripheral and central sites are contributing to the development of neuroinflammation and neuropathic pain. Moreover, innate immune cells play a significant role and regulation of these immune cells can determine development and progression of the disease.

A recurring phenomenon of chronic pain is the so-called mirror-image pain (MIP), which only has been described in few publications so far. It was first described in 1990, when MIP was observed in rats after PSNL (Seltzer et al. 1990). A review by Koltzenburg described the mirror-image pain as a contralateral pain, with a lower magnitude and a briefer time course than on the injured, ipsilateral side (Koltzenburg et al. 1999). Important to note is the fact that an induction of MIP does not always occur and strongly

depends on the utilized experimental animal and pain model. For example, MIP was never observed in WT mice after partial sciatic nerve ligation and this is important to mention as in many studies investigating pain, WT mice serve as control animals. Moreover, only specific experimental models such as chronic construction injury can induce contralateral pain. It is believed, that the severeness of the pain model influences the development of MIP (Jancalek 2011). Models with an increased inflammatory response are more likely to induce mirror-image pain. In a study by Milligan, contralateral MIP was induced only through an intense immune activation at the ipsilateral sciatic nerve, which was blocked by addition of a glial inhibitor or antagonists for interleukin-1, tumor necrosis factor or interleukin-6 (Milligan et al. 2003). Whether the immune response happens only at central levels or as well at peripheral sites, remains unclear and is possibly as well dependent on the experimental model. Glia cells for example can be also active in MIP in the peripheral nervous system. Cheng and colleagues observed satellite glia cells that surround DRG neurons to be activated and release nerve growth factor (NGF) in the contralateral DRG after spinal nerve ligation in rats (Cheng et al. 2015). Many mechanisms are still vague and some findings are contradictory, as seen in a publication from 2015, which showed a inhibitory rather than a proinflammatory effect of microglia and IL-1. IL-1β expression was colocalized with microglia in the spinal cord and increased after carrageenan injection, a mouse model to induce a peripheral inflammation. In contrast to the findings of Milligan, inhibition of microglial activation or IL-1 receptor induced an earlier development of MIP in these animals (Choi et al. 2015). An involvement of the immune system is evident but a clear mechanism of contralateral pain induction is still missing.

1.2.3 Treatment

Various therapies are available for patients suffering from neuropathic pain, including antidepressants, anticonvulsants, opioid analgesics, cannabinoids, NMDA antagonists, and topical medication (Szczudlik et al. 2014). Tricyclic antidepressants (TCA) and serotonin-noradrenaline reuptake inhibitors (SNRI) are among the antidepressant drugs. Inhibition of noradrenaline and serotonin reuptake results in an increased activation of the descending antinociceptive pathway, which is composed of inhibitory projections from the brainstem to the spinal cord (Marks et al. 2009). Anticonvulsants, like pregabalin

or gabapentin are used to diminish the hyperexcitability in neuropathic nociceptors. Through the antagonizing effects of pregabalin to voltage-gated Ca^{2+} channels, calcium influx is reduced and signal transmission of overactive sensory neurons is disturbed (Verma et al. 2014). Topical agents like lidocaine are used to block voltage-gated sodium channels and to stop propagation of action potentials in sensory neurons (Attal et al. 2000). NMDA receptor antagonists, like ketamine are as well used to block signal transduction in hypersensitive nociceptors (Niesters et al. 2014). An overall inhibitory effect on sensory neurons that is causing a decrease in hypersensitivity, is induced by opioids, endogenous molecules that act on G-protein coupled receptors (GPCR) (Stein 2013). Another class of endogenous molecules acting on GPCR are endocannabinoids. In the recent years, endocannabinoids were found to have many beneficial effects on various neurological diseases, like multiple sclerosis, Huntington's disease, Alzheimer's disease and chronic pain (Kendall & Yudowski 2017). A detailed view on the physiological and pathological mechanisms of the cannabinoid receptor 2 (CB2), will be given in the following parts.

1.3 The Endocannabinoid System

In recent years, the medical use of the *Cannabis sativa* plant has been approved in several European countries, as well as in more than half of the U.S. states (Bifulco & Pisanti 2015). Nowadays, medical marijuana is widely used to alleviate symptoms in chronic diseases such as multiple sclerosis, chronic pain, AIDS or cancer (Koppel et al. 2014). *Cannabis sativa*, which was used already for centuries not only for medical purposes but also for recreational use, acts through its components Δ^9-tetrahydrocannabinol (THC) or cannabidiol (CBD). THC is known to activate the seven transmembrane G-protein coupled cannabinoid receptor 1 (CB1) (Devane et al. 1988) and cannabinoid receptor 2 (CB2) (Matsuda et al. 1990), the two main receptors of the endocannabinoid system.

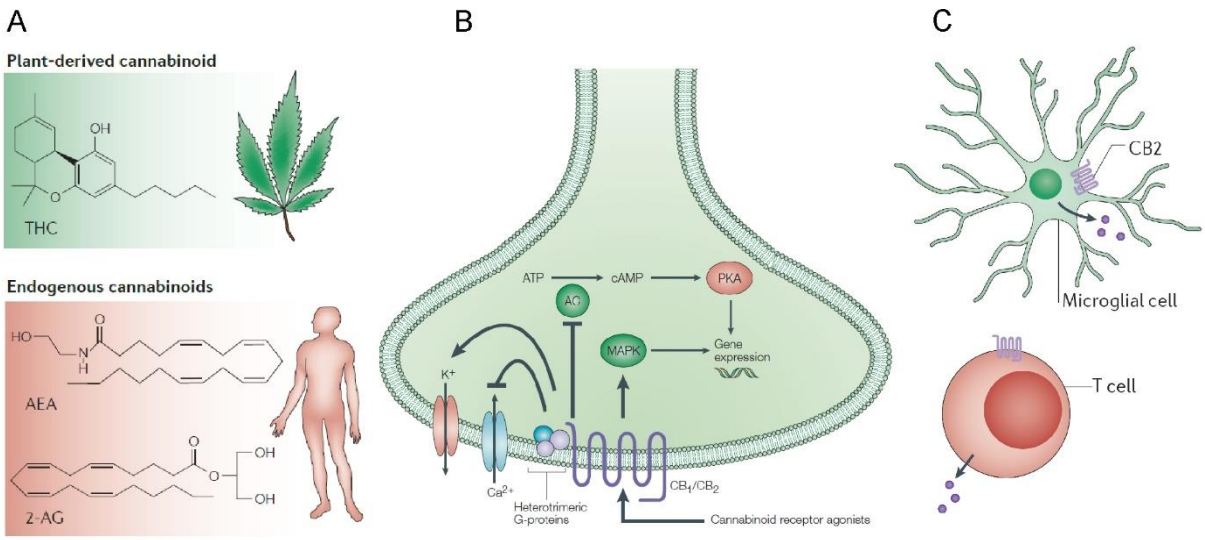

Figure 3 The endocannabinoid system. A Exogenous cannabinoids like the plant-derived Δ^9–tetrahydrocannabinol (THC) or the endogenous cannabinoids N-arachidonoylethanolamine (AEA) and 2-arachidonoylglycerol (2-AG) bind to the cannabinoid receptors 1 and 2. **B** Activation of these G-protein coupled receptors inhibits adenylate cyclase (AC) which leads to a reduction of cyclic AMP (cAMP) and inactivation of the protein kinase A (PKA) or stimulation of the mitogen-activated protein kinase (MAPK). Additional effects of CB1 activation in neurons are the reduction of calcium levels and opening of inwardly rectifying K channels to reduce neurotransmitter release. **C** The CB2 receptor is most abundantly expressed in immune cells of the periphery like T cells or in the central nervous system on microglia. Expression of CB2 is generally low but gets upregulated after neuroinflammation (modified from Di Marzo, 2004; Di Marzo, 2015; Velasco, 2012)

Both receptors are coupled to $G_{i/o}$ or $G_{q/11}$ and elucidate an inhibitory action on the expressing cell. Activation of the receptor induces dissociation of the $G_{\beta\gamma}$ subunit, which then results in phosphorylation of MAPK as well as ERK1/2, p38 MAPK, and JUN N-terminal kinases (JNK). Interaction of the $G_{i/o}$ protein with the activated CB1 or CB2 receptor inhibits adenylyl cyclase, which reduces cyclic AMP-protein kinase A (PKA) signaling. Moreover, CB1 receptor activation leads to opening of inwardly rectifying K^+ channels and inhibits L-, N- and P/Q-type voltage-gated Ca^{2+} channels (Howlett et al. 2010). Both mechanisms reduce neurotransmitter release and signal transduction (see Figure 3).

These two receptors can be also activated by the endogenous ligands of the ECS, 2-arachidonoylglycerol (2-AG) (Mechoulam et al. 1995) and N-arachidonoylethanolamine (anandamide, AEA) (Devane et al. 1992). Both endocannabinoids are synthesized on demand from membrane lipid precursors by specific enzymes. 2-AG is produced by diacylglycerol lipase (Dagl) α and β from arachidonic-acid containing diacylglycerol (DAG) (see Figure 4) (Sugiura et al. 2002). Anandamide is mainly synthesized by the N-acyltransferase (NAT) and the N-acyl-phosphatidylethanolamine-specific phospholipase D (NAPE-PLD) from phosphatidylethanolamine (Di Marzo et al. 1994).

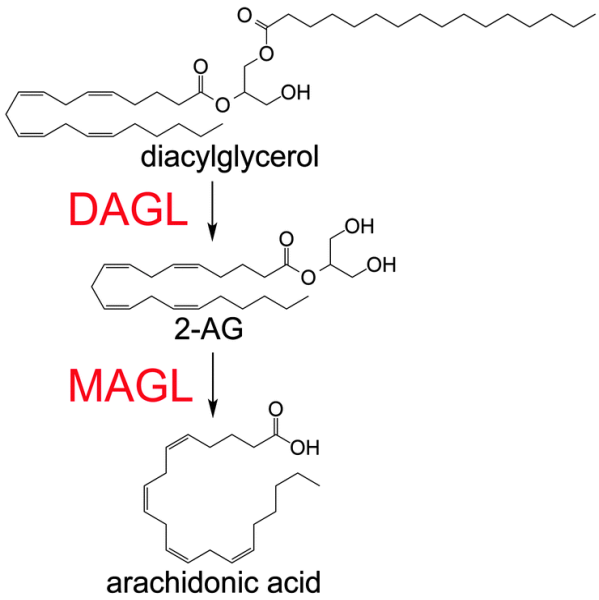

Figure 4 Synthesis and degradation of 2-AG. The diacylglycerol lipase (Dagl) or synthesizes 2-arachidonoylglycerol (2-AG) from diacylglycerol through hydrolysis. 2-AG is afterwards degraded by monoacylglycerol lipase (MAGL) to arachidonic acid.(modified from Kohnz et al. 2014)

Since the endocannabinoids are primarily produced at the postsynapse and bind to CB1 receptors located at the presynapse, they are called retrograde messengers, causing depolarization-induced suppression of inhibition (DSI) and excitation (DSE) in short-term synaptic plasticity as well as long-term potentiation (LTP) or depression (LTD) during learning and memory (Chevaleyre et al. 2006). Endocannabinoid signaling is inactivated by receptor internalization of reuptake and degradation of the ligands. 2-AG is degraded by monoacylglycerol lipase (MAGL) to arachidonic acid (Dinh et al. 2002). Fatty acid amide hydrolase (FAAH) degrades AEA to arachidonic acid and ethanolamine (Di Marzo et al. 1994). Alternative routes of degradation include oxidation through cyclooxygenase-2 (COX-2), lipoxygenases (LOXs), and cytochrome P450 (CYPs). Other possible components of the endocannabinoid system may be the orphan GPCR GPR55 and GPR18 as well as the peroxisome proliferator activated receptors (PPAR) α and γ transient receptor potential vanilloid type-1 (TRPV-1) (Maccarrone et al. 2014).

The CB1 receptor is expressed i. e. in the adrenal gland, heart, lung, prostrate, bone marrow, thymus, testis and tonsils but most abundantly in the central nervous system and on nociceptors in the periphery (Fine & Rosenfeld 2013). In the CNS, CB1 is found in high levels in the spinal cord, the brainstem, basal ganglia, hippocampus, neocortex and cerebellum (Marsicano & Kuner 2008). CB1 receptors modulate synaptic plasticity and influence thereby learning and memory. Moreover, they play a role in homeostatic

functions such as sedation or appetite stimulation but CB1 regulates as well perception, motor control and mood (Hashimotodani et al. 2007). The CB2 receptor is found primarily on immune cells, like T lymphocytes or macrophages in the periphery or microglia in the central nervous system. Interestingly, CB2 receptor expression was recently proposed on neurons in the hippocampus (Stempel et al. 2016), where CB2 activation induced a long-lasting hyperpolarization of hippocampal principle neurons in the CA2/ CA3 region. Nevertheless, the major functions of the CB2 receptors comprise pain modulation and regulation of the immune system. A detailed description of the CB2 receptor in neuroinflammation and neuropathic pain will be given in the following part.

1.4 ECS in neuropathic pain and neuroinflammation

The role of the endocannabinoid system in pain and neuroinflammation has been extensively studied in the recent years. For example, anandamide was shown to be a full agonist for TRPV1 and might induce pain modulating activity (De Petrocellis et al. 2001).

1.4.1 The endocannabinoids in neuropathic pain

Elevated anandamide and 2-AG levels were measured in spinal cord, periaqueductal grey (PAG), and rostral ventromedial medulla (RVM) in neuropathic rats (Petrosino et al. 2007). Moreover, peripheral AEA levels but not 2-AG levels were as well increased in the ipsilateral hind paw after nerve ligation in rats (Jhaveri et al. 2007). In the CNS, AEA might act through the activation of the CB2 receptor on microglia. Malek and colleagues showed that anandamide induced a shift from the M1 phenotype to M2 in microglia culture after stimulation with LPS (Malek et al. 2015). Surprisingly, mice with a genetic deletion of the fatty acid amide hydrolase, the main degrading enzyme for anandamide, did not show any difference in neuropathic pain behavior, although pharmacological blockage of FAAH produced consistent analgesic effects (Nadal et al. 2013). Comparable to this was the discovery that MAGL knockout mice did not show atypical neuropathic pain, but pharmacological MAGL blockage induced antinociception (Schlosburg et al. 2010). MAGL blockage results in elevated 2-AG levels, which was shown to exhibit anti-hyperalgesic and anti-allodynic effects in the case of CNS injury (Panikashvili et al. 2001). Release of 2-AG by DRG neurons can be stimulated by bradykinin (Gammon et al. 1989). Next to

neurons, microglia are as well able to secrete 2-AG. Microglial 2-AG levels is dependent on Ca^{2+} levels and P2X7 receptor activation by ATP (Witting et al. 2004). After 2-AG binds microglial CB2 receptors, microglial motility, proliferation and migration is induced (Carrier et al. 2004). 2-AG is synthesized by Daglα, which was highly expressed in the soma of TRPV1 – positive neurons after spared nerve injury (Giordano et al. 2012). The other 2-AG synthesizing enzyme is Daglβ. After inhibition of Daglβ, 2-AG levels are reduced and LPS-induced TNF-α release by macrophages is decreased (Hsu et al. 2012). To sum up, endocannabinoids and their synthesizing and degrading enzymes take an important role in regulation of neuropathic pain.

1.4.2 The CB1 receptor in neuropathic pain

Another interesting contributor of the endocannabinoid system for pain modulation might be the CB1 receptor, since it is expressed on nociceptors and in several CNS regions, such as the PAG, RVM, cortex, and spinal cord. Nevertheless, constitutive CB1 receptor knock-out mice did not develop increased neuropathic pain (Nadal et al. 2013) but did develop anxiety and depression during neuropathic pain (Rácz et al. 2015). Only when CB1 was conditionally deleted in nociceptors, increased neuropathic pain developed (Agarwal et al. 2007). These results were confirmed by the pharmacological activation of CB1 and CB2 receptor, which induced antinociceptive effects (Nadal et al. 2013). Additionally, administration of an inverse agonist of the CB2 receptor or blockage of the CB1 receptor showed an increased hypersensitivity (Rahn & Hohmann 2009). The disadvantage of CB1 receptor activation as an antinociceptive therapeutic lies in its side effects. Because of its wide distribution in the CNS, CB1 receptor activation induces psychomimetic effects, as seen after the consumption of THC (Kalant 2004). Therefore, pharmacological treatment with CB1 receptor agonists are only recommended in severe cases, where the antinociceptive benefits outweigh the psychomimetic effects.

1.4.3 The CB2 receptor in neuropathic pain

Since the CB2 receptor has an important immunomodulatory role and is known to be upregulated in pathological tissue, it came into focus in several studies covering neuroimmunological diseases (Atwood & Mackie 2010). Indeed, CB2 activation was

shown to be analgesic and anti-inflammatory in several animal models of pain (Anand et al. 2009). One of the first studies proving the relevance of the CB2 receptor in the regulation of pain was performed by Calignano and colleagues in 1998. Systemic and intraplantar administration of palmitoylethanolamide (PEA) induced antinociception in the formalin test, which was blocked by a CB2 receptor antagonist (Calignano et al. 1998). This study confirmed the influence of the CB2 receptor, although PEA is no direct CB2 agonist and possibly acts through a different mechanisms. Following studies utilizing CB2 receptor agonists (i.e. HU308) further proved the antinociceptive effects induced by the CB2 receptor (Hanus et al. 1999). Moreover, systemic administration of the CB2 agonist GW405833, another CB2 for 3-5 weeks after PSNL, reduced mechanical hyperalgesia. Additionally, this effect was blocked after the addition of a CB2 receptor antagonist and absent in CB2 receptor knockout mice (Whiteside et al. 2005). More studies about the effects of CB2 receptor selective agonists in pain development are reviewed by Guindon and Hohmann (Guindon & Hohmann 2008). CB2 receptor expression in the CNS is relatively low in healthy tissue but upregulated after induction of pathological pain states. More specifically, upregulation of the CB2 receptor was detected in the lumbar spinal cord in microglia and astrocytes in neuropathic rats (Zhang et al. 2003) but as well in TRPV1-positive nociceptors located in human DRG's (Anand et al. 2008).

Activation of the CB2 receptor results in reduced secretion of proinflammatory cytokines in macrophages and mast cells (Pacher & Mechoulam 2011) and simultaneously stimulates release of anti-inflammatory mediators. This was shown by the release of antinociceptive β-endorphins by keratinocytes after CB2 receptor activation through the agonist AM1241 (Ibrahim et al. 2005). In the spinal dorsal horn, CB2 receptor activation was shown to reduces MAPK phosphorylation, which affected BDNF levels and reduced allodynia (Landry et al. 2012). When CB2 receptor was overexpressed, mechanical hypersensitivity in neuropathic mice was attenuated. On the contrary, CB2 knockout mice develop a robust neuropathic pain and a mirror-image pain i.e. increased sensitivity on the hindpaw contralateral to the nerve ligation. Moreover, CB2KO mice showed an enhanced microgliosis on the contralateral dorsal horn (Racz et al. 2008a). This effect might have been triggered through microglia activation and interferon-γ release. Double knockout mice of interferon-γ and CB2 did not develop contralateral pain after nerve ligation. Additionally, cultured microglia decreased interferon-γ dependent upregulation of the proinflammatory gene iNOS and CCR2 after stimulation with the CB2 agonist JWH-

133 (Racz et al. 2008b). These studies strongly suggest a regulation of microglia and inflammation in neuropathic pain by the CB2 receptor. In another study, the phytocannabinoid beta-caryophyllene (BCP) which is a natural agonist of the CB2 receptor, induced reduction of mechanical allodynia and spinal neuroinflammation after PSNL and thereby could reduce the development of neuropathic pain. Besides, BCP also alleviated inflammatory pain responses in a formalin test and was more efficient than subcutaneously injected CB2 agonist JWH-133(Klauke et al. 2014). Overall, many studies hint towards an anti-inflammatory effect of the CB2 receptor, which is primarily induced by glia cells or immune cells of the innate immune system. Importantly, CB2 was able to alleviate inflammatory and chronic pain without inducing psychoactive side effects as seen after CB1 receptor activation (Ikeda et al. 2013)(Landry et al. 2012).

1.4.4 Leptin in neuropathic pain

In the last years, several studies revealed an impact of leptin on the immune system, the endocannabinoid system, and on neuropathic pain. Leptin is an adipokine, which is known to regulate food intake, body weight, and maintains energy homeostasis. *ob/ob* mice are deficient for the leptin gene "obese" (ob) and develop obesity and abnormalities in reproduction, hematopoiesis, insulin secretion, and in the immune system (La Cava & Matarese 2004). One of the first connections between leptin and the ECS was found in the regulation of food intake, where leptin was shown to negatively regulate endocannabinoid levels in the hypothalamus (Di Marzo et al. 2001). Independent from food intake, Maeda and colleagues discovered a link between leptin and neuropathic pain in 2009. Adipocytes released leptin in injured peripheral nerves, which then stimulated macrophages and supported neuropathic pain development. Additionally, macrophages were shown to express the leptin receptor. Administration and stimulation of peritoneal macrophages with leptin could restore the loss of allodynia in leptin-deficient *ob/ob* mice (Maeda et al. 2009). Just recently, leptin was as well linked to the CB2 receptor in traumatic brain injury, where the neuroprotective effects of leptin were reduced after administration of AM630, a CB2 receptor antagonist (Lopez-Rodriguez et al. 2016). Surprisingly in this study, leptin was shown to have anti-inflammatory effects, in contrast to the proinflammatory actions mediated by leptin in macrophages. Another connection between the CB2 receptor and leptin was discovered just recently, showing an upregulation of the leptin receptor in CB2 deficient mice at the ipsilateral sciatic nerve

after partial sciatic nerve ligation (unpublished observation). Whether leptin has a beneficial effect on neuropathic pain is still unclear, but a regulation between the CB2 receptor and leptin in neuropathic pain is highly possible.

As a conclusion, it is not surprising that cannabinoids were used as pain medication already for the last 20 centuries by India, China, Greece, Rome and Israel (Iversen 2007). Nowadays, cannabis was proved in several studies and through different routes to be more or less effective for the treatment of chronic pain (Jensen et al. 2015). Most studies showed an improvement in pain as well as in sleep without severe side effects (Lynch & Campbell 2011). Actually, side effects of cannabis are stated to be not more severe than in other pain therapies (Ware et al. 2004), but cannabis should only be prescribed, if other pain medication fails to induce analgesia (see Reviews for more details: (Boychuk et al. 2015)(Maldonado et al. 2016)).

1.5 Aim

The aim of this thesis was to study the contribution of the CB2 receptor of mice in neuropathic pain. Previous studies showed the development of contralateral pain in CB2KO mice after nerve ligation. The cellular mechanisms involved in this effect are, however, unknown. Thus, I was aiming to reveal the cellular localization of CB2 that is important for the development of neuropathic pain and especially contralateral pain. One aim was therefore to analyze neuropathic pain in constitutional and conditional CB2 knockout mice by measuring mechanical allodynia, microgliosis in the spinal cord and immune cell infiltration of the sciatic nerves. Since it is still under debate, which impact the cellular localization of CB2 has during neuropathic pain, I was also aiming to determine the cellular distribution of CB2 by analyzing nervous tissue of the recently generated CB2-GFP mouse strain. I hypothesize that CB2 is located on microglia and that mice, which have a microglial CB2 deletion exhibit a stronger inflammation, comparable to CB2KO mice.

The second part of my project concentrated on the contribution of the Daglα enzyme in the development of neuropathic pain. Daglα is the main synthesizing enzyme for 2-AG, one of the two endocannabinoids binding the CB2 receptor. It was shown before that 2-AG modulates neuropathic pain development in mice and therefore I was interested in the role of Daglα in neuropathic pain. My aim for this was to analyze pain

behaviour in Daglα KO mice. Therefore, I measured mechanical allodynia after PSNL, thermal pain, and inflammatory pain sensitivity in these mice.

2 Materials

2.1 Equipment

Technical instrument	Company
Analgesia meter hot plate	TSE Systems
Analytical balance	BP 121 S, Sartorius
Animal shaver	Isis GT420, Aesculap
Cell strainer 40µm	BD Falcon
Centrifuges	Biofuge fresco, Heraeus Instruments
	Biofuge pico, Heraeus Instruments
	Biofuge stratos, Heraeus Instruments
	Megafuge 1.0R, Heraeus Instruments
Cold-light source	KL1500 LCD, Schott
Cryostat	CM3050S, Leica GmbH
Flow cytometer	FACS Canto II, BD Biosciences
Hargeaves apparatus	Ugo Basile
Incubator	Be-Ed-Fd, Bindner
Laminar flow hood	Herasafe, Kendro
Liquid handling platform	Janus®, Perkin Elmer
Magnetic stirrer	MR 3001 K, Heidolph, Fisher
Microscopes	
Light microscope	Axioskop 40, Zeiss
Fluoresence microscope	Axiovert Imager M2, Zeiss
Confocal microscope	LSM SP8, DMI 6000 CS, Leica
Needle 27G x 1/2	BD Microlance™ 3
pH meter	inoLab, WTW
Perfusion pump	Reglo Digital MS-4/8, Ismatec
Real-time PCR cycler	LightCycler® 480 Instrument II, Roche
Scalpel	Feather Safety Razor CO., LTD.

Technical instrument	Company
Spectrophotometer	NanoDrop 1000, Thermo scientific
Sterilizing oven	Varioklav 25T, H+P Labortechnik
Prolene suture 5-0, for wound closing	Ethicon
Braid silk suture 7-0, for nerve ligation	Natsume Seisakusho
Syringe 1 ml	Clexane, Transcoject®
Tissue homogenizer	Precellys 24, Bertin Technologies
Vaporizer for Isoflurane	ISOFLO, Eickmeyer
Vortexer	Vortex-Genie 2, Scientific Industries
Von Frey aesthesiometer	Ugo Basile
Von Frey filaments	Touch Test Sensory Evaluators, Stoelting
Von Frey grid	Ugo Basile
Fluosorber	Table Top Single Animal Anaesthesia System, Harvard Apparatus

2.2 Chemicals and reagents

2.2.1 Chemicals

Chemicals	Company
0.9% Saline	Braun
Albumin Bovine Fraction V, pH 7.0 standard grade, lyophil. (BSA)	Serva
APC Streptavidin	Biolegend
Betaisodona	Mundipharma
Citric acid monohydrate	Promega
Cooling Spray	Roth
DAPI Fluoromount-G®	SouthernBiotech
DMEM	Gibco Life Technologies
Donkey Serum	VWR
EDTA disodium salt, dehydrate	Calbiochem
Ethanol	Otto Fischar GmbH &Co KG
FC Block CD16/32	Biozol
Fetal calf serum	PAA cell culture company
Fluoromount-G®	SouthernBiotech
HBSS	Gibco Life technologies
Hepes	Sigma-Aldrich
Hydrochloride acid	Sigma-Aldrich
Isoflurane	Abott GmbH
10% Ketamin	Medistar
2-Methylbutan/ Isopentan	Sigma-Aldrich
OCT Compound	Sakura Finetek
Oxygen	Linde
PapPen	Vector Laboratories
Paraformaldehyd	Sigma-Aldrich

Chemicals	Company
PercP-Cy™ 5.5 Streptavidin	BD Pharmingen
Sucrose, for microbiology	Sigma-Aldrich
Triton X-100	Sigma Aldrich
Tris Base	Roth
TRIzol® Reagent	Thermo Fisher
Tween20	Sigma-Aldrich
2% Xylazine	Ceva Tiergesundheit GmbH

2.2.2 Buffers and solutions

If not stated otherwise all buffers and solutions were prepared with dH_2O and all chemicals were purchased from Applichem, Life Technologies, Merck, Carl Roth or Sigma-Aldrich.

Buffers and solution	Composition	Application
Blocking Solution • for GFP IHC	10% (v/v) Normal Donkey Serum 0.5% PBST 0.33% FC Block in PBS	Immunohisto-chemistry
• for Iba1 IHC	10% (v/v) Normal Donkey Serum 0.1% PBST in PBS	
Citrate buffer	10 mM Citric acid 0.05% (v/v) Tween 20 adjusted to pH 6.0	Immunohisto-chemistry
Enzyme Mix for sciatic nerve tissue	1 U/µl DNase I 0.5% Collagenase type 4 0.01 U/µl Elastase	Flow Cytometry
Collection Buffer	1 M HEPES in DMEM	Flow Cytometry
Facs Buffer	0.5 M EDTA in PBS	Flow Cytometry
Inactivation Buffer	20% FCS in HBSS	Flow Cytometry
Paraformaldehyde (PFA) 4%	4% (w/v) Paraformaldehyde in PBS	Fixation of brain tissue

Buffers and solution	**Composition**	**Application**
Permeabilization Solution		Immunohistochemistry
0.5% PBST	0.5% (v/v) Triton X-100 in PBS	
0.1% PBST	0.1% (v/v) Triton X-100 in PBS	
Phosphate buffered saline (PBS) 10x	10.5 mM KH_2PO_4 1551 mM NaCl 29.6 mM Na_2HPO_4-$7H_2O$ adjusted to pH 7.4	General Use

2.2.3 Enzymes and antibodies

Antibody	Type	Host	Product Number	Company
Anti-CD11b APC	Monoclonal	Rat	170112	eBioscience
Anti-CD11b FITC	Monoclonal	Rat	101206	Biozol
Anti-CD45 eFluor® 450	Monoclonal	Rat	48-0451	eBioscience
Anti-CD45 FITC	Monoclonal	Rat	103107	Biozol
Anti-CD45 PE	Monoclonal	Rat	103106	Biozol
Anti-CD45 PerCP/Cy™ 5.5	Monoclonal	Rat	103132	Biozol
Anti-GFP	Polyclonal	Goat	Ab6673	Abcam
Anti-Iba1	Polyclonal	Rabbit	019-19741	Wako
Anti-Leptin Receptor	Polyclonal	Goat	AF497	R&D Systems
Anti-Ly-6B.2 APC	Monoclonal	Rat	MCA771A647	AbD Serotec
Anti-Ly-6C Biotin	Monoclonal	Rat	557359	BD Pharmingen
Anti-Ly-6G PE	Monoclonal	Rat	12-5931	eBioscience
Anti-Mouse Macrophage (F4/80)	Monoclonal	Rat	CL8940AP	Cedarlane
Anti-NeuN Biotin	Monoclonal	Mouse	MAB377B	Millipore
Anti-Goat Cy™3	Polyclonal	Donkey	705-166-147	Jackson ImmunoResearch, INC.
Anti-Rabbit AlexaFluor® 647	Polyclonal	Donkey	A31573	Life Technologies
Anti-Rat AlexaFluor® 488	Polyclonal	Donkey	A21208	Life technologies

Serum / Enzyme	Company
Elastase	Worthington
Normal donkey serum (ab7475)	Abcam
Normal goat serum (ab7481)	Abcam
Proteinase inhibitor complete mini	Roche
Collagenase type 4	Worthington
DNase I	Roche

2.3 Software

Software	Company
Adobe Photoshop	Adobe Systems, 2011, USA Cs5.1, Version 12.1
AxioVision LE	Carl Zeiss, Germany, Version 4.8.2
Flowjo	Tree Stars Inc., USA, Version 9.5.2
ImageJ	Wayne Rasband, NIH, USA, Version 1.47
Leica Application Suite X	Leica, Germany, Version 3.0.0
Mendeley	Mendeley Ltd., USA, Version 1.16.3
Microsoft Office Professional Plus 2013	Microsoft, 2012, USA
NanoDrop	NanoDrop 1000, Version 3.7
Prism	GraphPad Software, Inc., 2012, USA, Version 6.01

3 Methods

3.1 Animals

For the following experiments, constitutive and conditional CB2KO and DaglαKO mouse lines were used. Wildtype (WT) or floxed (FL) littermates were used as control animals. All animals were bred on a C57BL/6J background. Mice were kept under specific pathogen free conditions (SPF) and were housed with a 24 h light-dark circle (12 h light, 12 h dark). All mice were group-housed in cages with up to five littermates and had *ad libitum* access to food and water. All animals were 2 - 5 months of age at the time of the experiments.

3.1.1 Constitutional and conditional CB2 deletion

Used CB2KO mice had a deletion in the coding exon of the *Cnr2* gene, thus inactivating the CB2 receptor, as described previously (Buckley et al. 2000). CB2KO mice were bred homozygously in our animal facility. In the CB2-Syn mouse, Cre recombinase is expressed under the synapsin 1 promoter, which is specifically expressed in neurons (Zhu et al. 2001). As a consequence, the Cre recombinase is only active and excises parts of the *Cnr2* gene in neuronal cells (Stempel et al. 2016). CB2-LysM mice have a conditional deletion in all myeloid cells, since the Cre recombinase is active in cells expressing the lysozyme M gene. This mouse line has a CB2 deletion in 30-40 % of microglia and macrophages

3.1.2 CB2-GFP

CB2-GFP mice were used to localize CB2 receptor expression. The GFP open reading frame was cloned downstream of a CB2 promoter (Schmöle et al. 2015). The resulting offspring expressed functional CB2 receptors and a strong GFP signal in all CB2 expressing cells. CB2-GFP mice were backcrossed for at least five generations to a C57BL/6J background.

Table 1 Transgenic mice Used mouse strains with their official name, abbreviation, genetic modification and literature reference, if published.

Name	Abbreviation	Modification	Reference
B6.cg Cnr2 tm1Zim	CB2KO	Deleted part in coding exon of *Cnr2*	(Buckley et al. 2000)
B6.cg Cnr2 tm2Zim	CB2-FL	ORF in exon 2 of *Cnr2* is flanked by two loxP sites	(Stempel et al. 2016)
Lyz2 tm1(cre)lfo	LysM-Cre	Cre recombinase expressed under lysozym M gene promoter	(Clausen et al. 1999)
Tg(Syn1-cre)671Jxm	Syn-Cre	Cre recombinase expressed under synapsin 1 gene promoter	(Zhu et al. 2001)
B6.cg Cnr2 tm2Zim x Lyz2 tm1(cre)lfo	CB2-LysM	CB2-FL crossed with LysM-Cre mice	unpublished
B6.cg Cnr2 tm2Zim x Tg (Syn1-cre)671Jxm	CB2-Syn	CB2-FL crossed with Syn-Cre mice	(Stempel et al. 2016)
B6.cg Tg(Cnr2-GFP)1Zim	CB2-GFP	GFP ORF cloned downstream of CB2 promoter	(Schmöle et al. 2015)
B6.cg Dagla tm1Zim	Daglα FL	Exon 1 of *Dagla* gene is flanked by two loxP sites	(Jenniches et al. 2016)
Tg(Pgk1-cre)1Lni	PGK1-Cre	Cre recombinase expressed under *Pgk1* promoter	(Lallemand et al. 1998)
B6.cg-Dagla tm1Zim x Tg(Pgk1-cre)1Lni	Daglα KO	Daglα FL crossed with Pgk1-Cre mice	(Jenniches et al. 2016)

3.1.3 Daglα KO

Constitutive Daglα KO mice were tested for pain sensitivity. Daglα KO mouse resulted from crossing mice containing two loxP sites flanking the exon 1 of the *Dagla* gene (Daglα FL) (Ternes 2013) with mice expressing the Cre recombinase ubiquitously under the *Pgk1* promoter (Pgk1-Cre) (Lallemand et al. 1998). Consequently, Daglα KO mice have a constitutive deletion of the *Dagla* gene (Jenniches et al. 2016).

All animal experiments were approved by the local committee for animal health (LANUV NRW) and followed the guidelines of the German Animal Protection Law. (AV 84-02.04.2014.A258, AV 87-51.04.2014.A393, AV 84-02.04.2014.A443)

3.2 Behavioral Experiments

3.2.1 Partial sciatic nerve ligation (PSNL)

To induce a sciatic nerve injury, the partial sciatic nerve ligation (PSNL) method was used, as described previously (Rácz et al. 2015). Mice were anesthetized with 2-3% isoflurane gas and ⅓ - ⅔ of the left sciatic nerve was tightly ligated with a 7-0 braid silk suture. This resulted in a robust development of mechanical allodynia with its peak on day 14 post ligation. Sham operated mice underwent the surgery without ligation of the sciatic nerve to serve as controls (see Figure 5 A/B).

3.2.2 Von Frey

Mechanical allodynia was tested with manual von Frey filaments (Stoelter) using the up-down method described previously (Dixon 1965) or the automated von Frey aesthesiometer (Ugo Basile) . Mice were habituated on a metal grid for 1 h on three days prior to the first measurement and 1 h directly before each assessment (see Figure 4 C). All mice were tested before and 3, 7, 10 and 14 days after PSNL. Either von Frey filaments of different strengths were applied against the plantar surface of both hind paws until the filament bent (see Figure 4 D) or the automated aesthesiometer was placed under the plantar surface of the hind paw and a filament elevated with increasing force. Shaking, licking or paw withdrawal was considered as a nociceptive response. The aesthesiometer automatically calculated the force at which the animal reacted. In case of the manual von

Frey filaments, force was calculated using the up-down method by Chaplan (Chaplan et al. 1994).

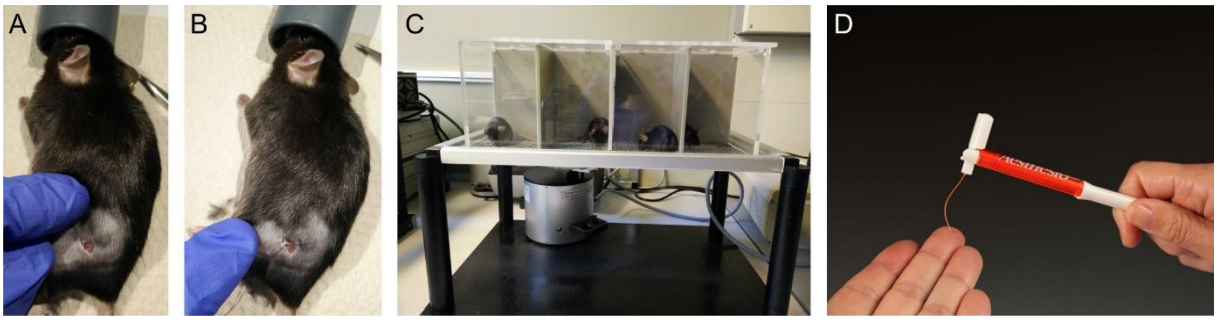

Figure 5 Neuropathic pain model. Mice were anesthetized to perform a sham surgery (A) or a partial sciatic nerve ligation (B) to induce neuropathic pain. Mechanical allodynia was assessed for each mouse in both hind paws (C) with von Frey filaments (D) (modified from Danmic Global, LLC).

3.2.3 Up-down method

In the up-down method, measurement was started with a filament of medium strength (3.61). Depending on the response, filaments with a higher or lower strength were varied. In case of a positive nociceptive response, weaker filaments were taken. Consequently, stronger filaments were used in case of no response. The measurement was finished after the fourth filament used, following a positive response. By recording the sequence of responses and the value of the last used filament, the force could be calculated, at which in 50% of the cases a reaction would occur (Chaplan et al. 1994).

3.2.4 Hot Plate

The hot plate test (Eddy & Leimbach 1953) was used to assess thermal nociception in Daglα KO and WT mice. Mice were placed on a hot surface (52°C) and trapped by a round plastic cylinder. Latency (s) until the first signs of nociceptive behavior such as shaking, licking or jumping was measured. Either after jumping, which was considered as a sign for most painful behavior, or after 30 s, the experiment was stopped and the mouse was transferred back to its cage. Latency until the first sign of pain and until each of the different behaviors was calculated and compared between genotypes with Graphpad Prism.

3.2.5 Formalin Test

In the formalin test, the acute inflammatory reaction of the mice was assessed (Walker et al. 1999). Mice were habituated in small transparent boxes for 15 – 30 min prior to the experiment. To induce inflammation, 20 µl of 5% formalin was injected into the left hind paw of the animal. For comparison and as a control, the same amount of a vehicle (saline) was injected into the right hind paw as well. Subsequently, the mouse was placed into a small plastic box and recorded with a camera for 45 min. After the experiment, all mice were sacrificed to prevent further suffering of the animals. The video material was then analyzed for nociceptive behavior of the mice: the video was stopped every ten seconds and nociceptive behavior, such as shacking, licking or jumping was considered as a positive value (1). No reaction to the injection was documented as a negative value (0). All values were added for every minute and the mean was calculated for each genotype. The results were divided into the early and acute inflammatory phase (0 – 5 min) or the late and tonic inflammatory phase (15 – 40 min).

3.2.6 Hargreaves test

To analyze thermal hypersensitivity, Daglα KO and WT mice underwent the Hargreaves test (Hargreaves et al. 1988). Mice were habituated one day before testing and on the day of the experiment for 1 h on a plantar setup in small Plexiglas chambers. The mobile infrared heat source of the Hargreaves apparatus (Ugo Basile) was placed under the hind paw of a mouse and a radiant heat beam (infrared) with an intensity of 40 IR induced thermal pain in the plantar surface of the hind paw. After retraction, the device measured automatically the withdrawal latency (s). Both sides were assessed each three times and the mean withdrawal latency was calculated. All values from both genotypes were compared in Graphpad Prism.

3.3 Immunohistochemistry

3.3.1 Tissue Preparation

For the immunohistological experiments, tissue was collected at 14 days post-surgery using the same procedure. Ligated and sham operated animals were anaesthetized with a mixture of 10% ketamine and 5% xylazine, diluted in 0.9% saline. Mice were

intracardially perfused with ice-cold phosphate-buffered saline (PBS) for 5 min and with 4% paraformaldehyde (PFA) for 15 min at a speed of 4 ml / min. The tissue samples (lumbar spinal cord, sciatic nerves, DRGs, spleen or brain) were isolated and post fixated overnight at 4°C in 4% PFA. On the next day, tissue was transferred to 30% sucrose and incubated again up to one week at 4°C for cryopreservation. Tissue samples were then embedded in O.C.T. compound, cooled down on dry ice and frozen to -80°C. Subsequently, 14 µm thick sections were cut at a cryostat, collected on object slides and stored at -20°C until use.

3.3.2 Iba1 staining

To measure microgliosis in the dorsal horn, lumbar spinal cord sections of CB2KO, CB2-LyM, CB2-Syn and floxed CB2 animals were used. Frozen slides were dried at 37°C for 30 min, encircled with a PapPen and washed for 5 min in PBS buffer. For permeabilization, slides were incubated in 0.1% PBST for 15 min at room temperature (RT). To block unspecific binding sites of the secondary antibody, slides were transferred to a blocking solution (Blocking solution for Iba, see 2.2.2) for 2 h at RT. Primary anti-Iba1 antibody was diluted 1:500 in 10% donkey serum and 0.1% PBST, added to the tissue and left for incubation overnight at 4°C. To increase antibody binding, slides were heated on the next day to 37°C for 2 h and consequently washed 3 times, 10 min each with 0.1% PBST. Bound primary antibodies were visualized by addition of a fluorophore coupled secondary antibody (anti-rabbit AlexaFluor® 647), which was diluted 1:1000 in 0.1% PBST and incubated for 2 h at RT in the dark. Unbound antibodies were washed off 3 times with each 10 min of PBS. Before mounting, slides were washed in MilliQ water to remove any remaining salts. Slides were then mounted in DAPI Fluoromount G, covered and sealed. Stained slides were stored at -20°C until analysis.

3.3.3 GFP staining

Since the expression of CB2 is generally low and thus GFP is only weakly expressed, we used anti-GFP antibodies to amplify the GFP signal. To localized the expression of GFP, a double staining of GFP with either Iba1 or NeuN was performed. In the beginning, slides were dried at 37°C for 30 min and encircled with a PapPen. After a 5 min washing step with PBS, antigen retrieval was achieved by incubating the slides in citrate buffer for 40

min at 70°C. Slides were then washed again for 5 min in PBS and cell membranes were permeabilized with 0.5% PBST for 1 h at RT. Next, slides were washed again for 3 times 10 min each with PBS and unspecific binding sites were blocked with blocking buffer (Blocking buffer for GFP, see 2.2.2) for 2 h at RT. Afterwards, slides were washed 3 x 10 min with PBS, and incubated with the primary antibodies (anti-GFP, 1:1000 with either anti-Iba1, 1:500 or anti-NeuN-Biotin, 1:200) diluted in 0.025% PBST, at 4°C overnight. On the next day, primary antibodies were washed off 3 times, 10 min each, with PBS. The secondary antibodies were diluted in 0.025% PBST (anti-goat Cy™3, 1:1000 with either anti-rabbit AlexaFluor® 647, 1:1000 or APC Streptavidin, 1:300), added to the slides and incubated in the dark for 2 h at RT. Unbound secondary antibody was washed off again by 3 times PBS washing, 10 min each and a final washing step in MilliQ water. Slides were then mounted in DAPI Fluoromount G, covered and sealed. Stained sections were stored at -20°C until analysis.

3.3.4 Leptin staining

To stain the spinal cord and sciatic nerves for the leptin receptor, a similar protocol as for the Iba1 staining was used. Primary antibodies against leptin receptor (diluted 1:40) and against F4/80 (diluted 1:100), a common macrophage marker, were used. Utilized secondary antibodies comprised anti-Goat Cy™ (diluted 1:250) and anti-Rat AlexaFluor® 488 (diluted 1:250). Stained tissue was stored at -20°C until analysis.

3.3.5 Image acquisition and analysis

Iba1 staining in spinal cord tissue of WT, CB2KO, CB2-LysM and CB2-Syn mice was analyzed with ImageJ software. For this, sections of both dorsal horns in the lumbar spinal cord were imaged with a confocal laser microscope (LSM SP8, DMI 6000 CS, Leica) using the same settings for laser intensities and gain in all spinal cord slides. Images were then imported to ImageJ and the green channel, representing the Iba1 signal, was analyzed. The threshold was adjusted once per genotype until most microglia but least background was visible and these threshold values were then applied for all images of the same genotype. To quantify the stained area, all particles with size > 1 – infinity and a circularity of 0 - 1 were analyzed. The resulting values represented stained Iba1 area in percent and

were compared between both treatments within the same genotype. Per genotype, 3-4 animals were analyzed with each 3-4 sections of the dorsal horn on each side.

3.4 Flow Cytometry

3.4.1 Isolation of cells

For the analysis of macrophages and neutrophils in the sciatic nerves and spinal cord of WT and CB2KO animals, a slightly adapted protocol from Nadeau (Nadeau et al. 2011) was used. In this procedure, mice were anaesthetized and quickly perfused with 20 ml ice-cold PBS solution to wash out most blood cells. Both sciatic nerves were isolated and cut into small segments. Tissue samples were transferred to tubes containing collection buffer and were kept light-protected on ice during the whole procedure. All tubes were centrifuged at 4500 rpm and the supernatant was discarded. Cell pellets were dissolved in a collagenase/ DNase- / elastase mix for sciatic nerve tissue (see 2.2.2 Buffers and solutions). Samples were incubated at 37°C for 60-90 min. The reaction was stopped with inactivation buffer and samples were further dissolved either by pipetting or applying the solution through a small needle. To filter the samples, a 40 µm cell strainer was used twice and washed with FACS buffer afterwards. Filtered samples were centrifuged at 6000 rpm for 5 min. The remaining pellet was washed with PBS and centrifuged again.

3.4.2 Flow cytometry staining

Samples were centrifuged and the remaining pellet was blocked for 15 min with Fc Block. After an additional centrifugation step, cells were stained with antibodies against the surface markers in a dilution of 1:200. Antibodies incubated for 15 min and were washed with FACS buffer by an additional centrifugation step. Pellets (except for single stained cells) were incubated for another 15 min in secondary antibodies or Streptavidin solution and washed again in FACS buffer with an additional centrifugation step. All cell pellets were dissolved in FACS buffer, measured at a FACS Canto II flow cytometer and analyzed with FlowJo software.

3.5 Measurement of endocannabinoids

Spinal cords of ligated and sham operated Daglα KO, CB2KO and WT animals were collected 14 days post ligation and immediately frozen to -80°C. Extraction and quantification of endocannabinoids was performed by Dr. Laura Bindila (Prof. Beat Lutz, Institute of Physiological Chemistry, University Medical Center, Mainz) as previously described (Lomazzo et al. 2015). Endogenous 2-AG, AEA and AA levels were measured employing a 5500 QTrap® triple-quadrupole linear ion trap mass spectrometer (AB SCIEX). The endocannabinoid levels were quantified and normalized according to the relative protein weight, which was isolated.

3.6 Statistical Analysis

All data are presented as mean ± standard error of the mean (SEM). Data was calculated and analyzed by ImageJ (v1.47), Microsoft Excel (Office 2013) or Graphpad Prism (v.6.0c). If not stated otherwise, statistical analysis was calculated through multiple t-tests using the Holm-Sidak method or two-way ANOVA followed by a Bonferroni's post-hoc test or a Tukey's post-hoc test. Significance levels were set to $p \leq 0.05$. Stars represent statistical significance as followed: * $p \leq 0.05$, ** $p \leq 0.01$, *** $p \leq 0.001$.

4 Results

4.1 Localization of CB2 receptor expression

An important aim of this study was to localize the expression of the CB2 receptor in healthy and inflamed nervous tissue of mice. Since expression of CB2 is known to be relatively low in healthy nervous tissues (Schmöle et al. 2015) and existing antibodies against CB2 are not specific enough (Marchalant et al. 2014), many experiments failed to determine specific cellular location of CB2 receptor expression. Recently, the CB2 receptor was detected via RNAscope ISH in hippocampal neurons (Stempel et al. 2016). To determine, whether the CB2 receptor is expressed on neurons or microglia (or both) with regard to neuropathic pain, I utilized the simple approach of analyzing the CB2-GFP

mouse line. For this, I concentrated on tissue that is relevant for the pain processing, such as the spinal cord, DRG and sciatic nerves

4.1.1 Expression of GFP under the CB2 promoter

The GFP-CB2 mouse expresses GFP under the CB2 receptor promoter and was previously shown to help identifying CB2 receptor expressing tissue (Schmöle et al. 2015). To validate and localize the expression of CB2 receptors in mice suffering from experimentally induced neuropathic pain, I stained for GFP in tissue slices of CB2-GFP mice 14 days after PSNL (Figure 6-9). First, I analyzed spleen tissue, as I expected a higher expression of CB2 in the spleen than in nervous tissue. The high expression of the CB2 receptor in spleen tissue was described before (Buckley et al. 2000) and was used here to validate the GFP expression in CB2-GFP mice. In contrast to WT mice, CB2-GFP mice display a strong expression of GFP in the spleen, independent from ligation or sham surgery (Figure 6). Subsequently, pain relevant tissue was analyzed to detect any differences in CB2-GFP expression resulting from PSNL procedure (Figure 7). Tissue from WT mice served as a negative control to validate the GFP signal in CB2-GFP mice. A strong GFP signal was detected in ipsilateral sciatic nerve (SN) tissue of ligated CB2-GFP animals, whereas contralateral sciatic nerves or nerves of sham treated animals exhibited a weak or no GFP signal.

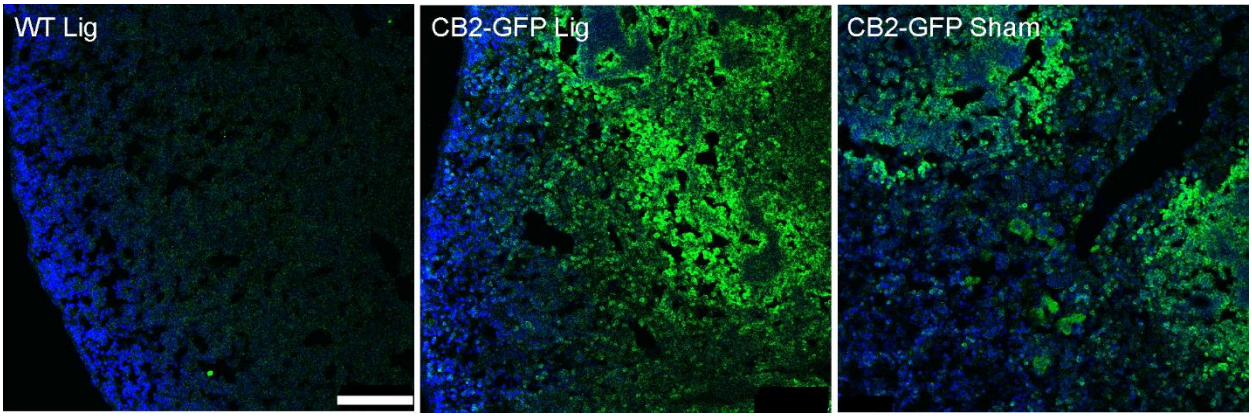

Figure 6 Expression of the CB2 receptor in spleen. Representative GFP expression under a CB2 promoter is shown in ligated and sham treated CB2-GFP mice 14 days post PSNL. Ligated WT animals served as a control. GFP was stained with green fluorescent antibody in spleen and is detectable in ligated (Lig) and sham CB2-GFP animals. Cell nuclei were stained by DAPI (blue) (scale = 100µm).

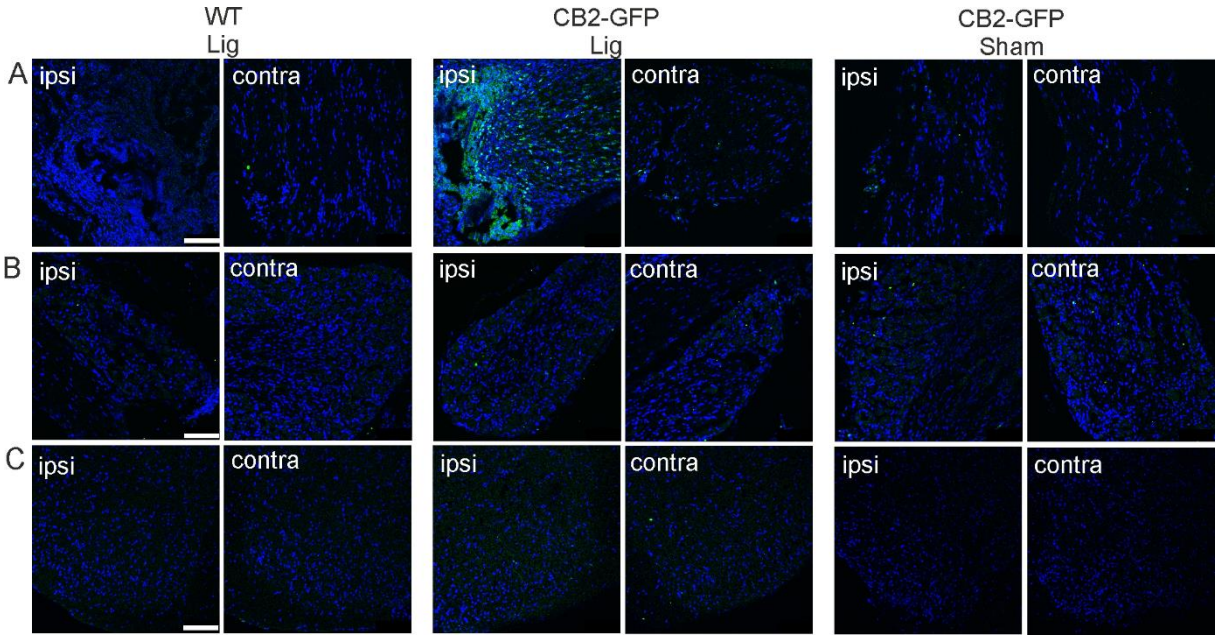

Figure 7 Expression of the CB2 receptor in nervous tissue. Representative stainings of GFP (green) in the sciatic nerve (A), dorsal root ganglia (B) and lumbar spinal cord (C). GFP expression under a CB2 promoter is shown in ligated and sham treated CB2-GFP mice 14 days post PSNL. Ligated WT animals served as a control. Cell nuclei were stained with DAPI (blue) (scale = 100µm).

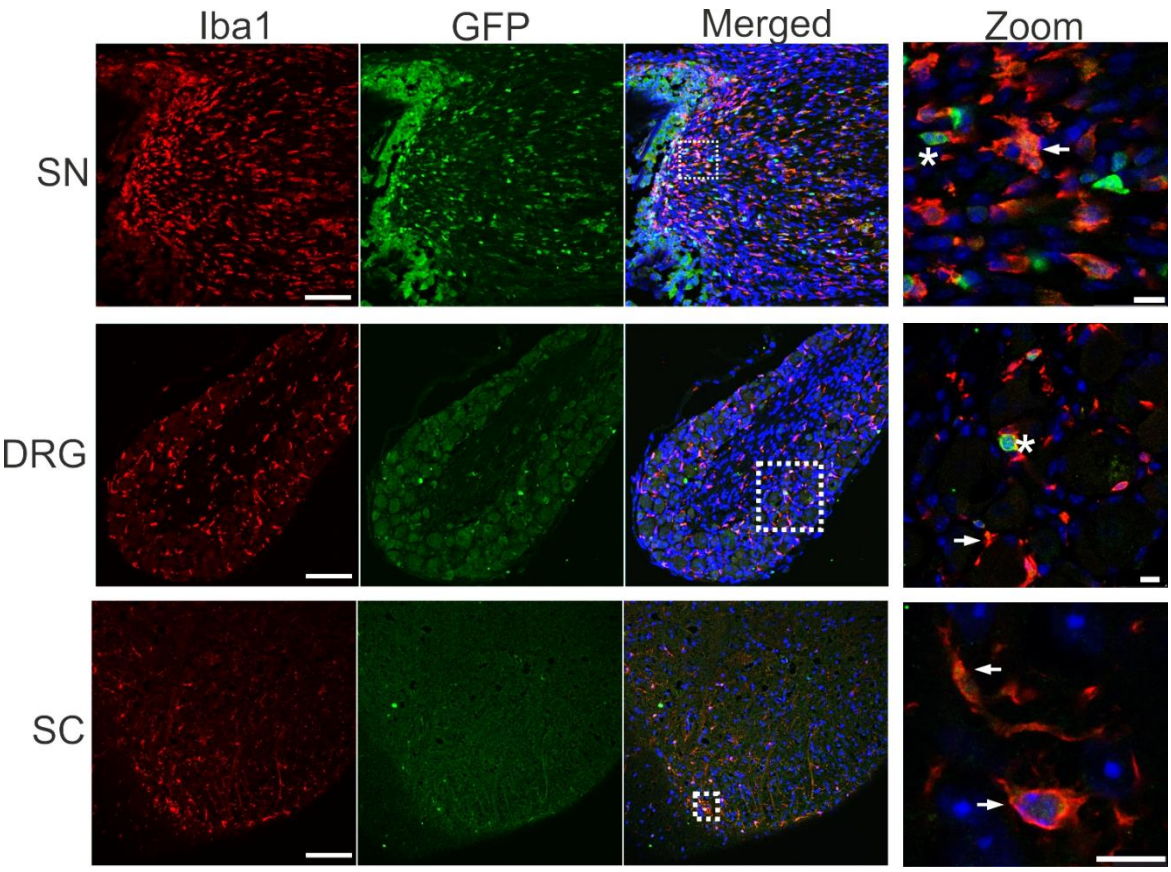

Figure 8 Coexpression of GFP with Iba1. Representative staining of ligated GFP-CB2 animals 14 days post PSNL in ipsilateral sciatic nerve, ipsilateral DRG, and ipsilateral lumbar spinal cord. GFP (green) colocalized with Iba1 (red), shown by white arrows. Some cells did express GFP but not Iba1 (white stars). Cell nuclei were stained with DAPI (blue) (scale = 100µm, Zoom scale = 10µm).

A weak expression of CB2-GFP was detected in ligated CB2-GFP mice sections of dorsal root ganglia (DRG) (Figure 7 B) or the dorsal horns of lumbar spinal cord (SC) (Figure 7 C). Control stainings of WT mice in sciatic nerves, DRG or spinal cord showed no GFP signal in any sections (Figure 7).

4.1.2 Localization of CB2-GFP in nociceptive tissue

After validating the GFP expression in CB2-GFP mice, a double staining of GFP with Iba1 or NeuN was performed to analyze colocalization of GFP with either myeloid cells (Iba1), such as macrophages and microglia, or neurons (NeuN) (Figure 8 and 9, respectively). Since GFP signal was strongest in ligated, ipsilateral tissue (see Figure 7), I only stained for colocalization in ipsilateral SN, DRG and SC tissue of ligated CB2-GFP mice 14 days after PSNL. Double staining with Iba1 (Figure 8) revealed a colocalization of GFP and Iba1 in sciatic nerves, DRG and spinal cord tissue.

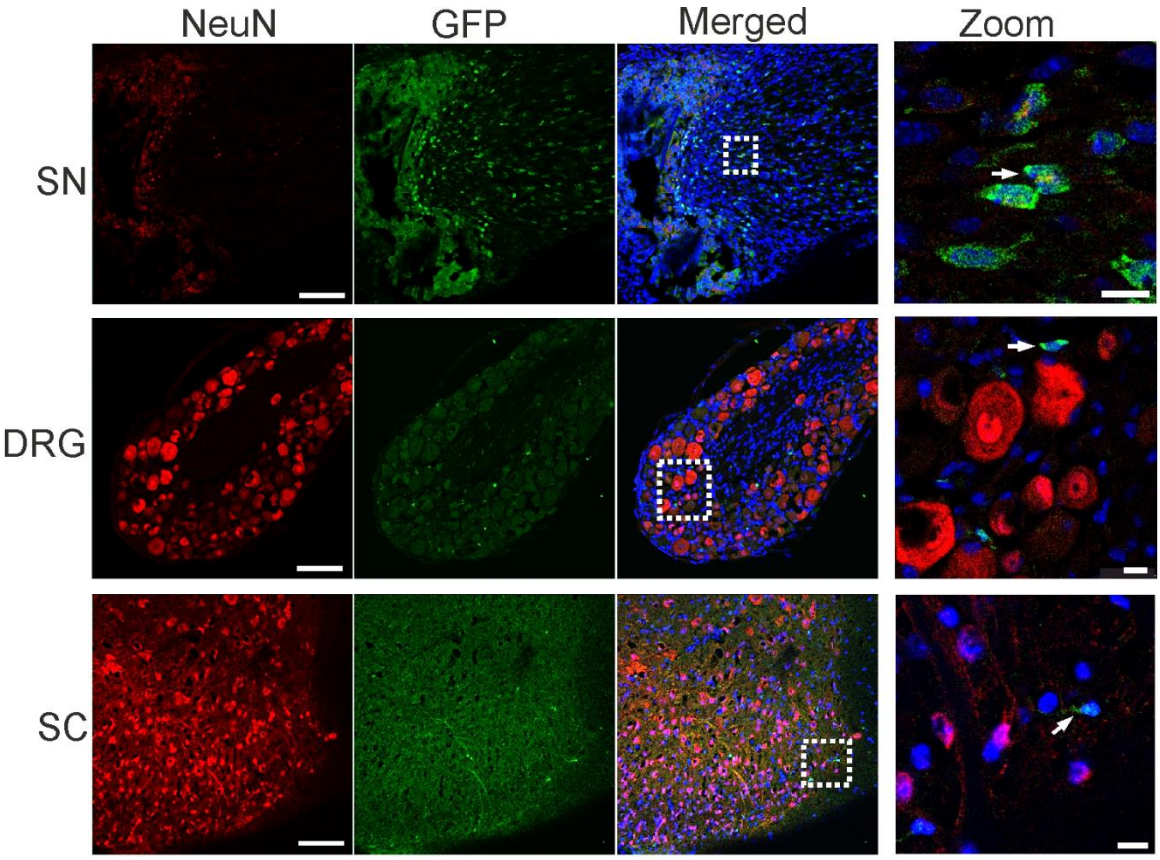

Figure 9 Coexpression of GFP with NeuN. Representative staining of ligated GFP-CB2 animals 14 days post PSNL in ipsilateral sciatic nerve, ipsilateral DRG, and ipsilateral lumbar spinal cord. GFP (green) did not colocalize with NeuN (red). Arrows show GFP expressing cells. Cell nuclei were stained by DAPI (blue) (scale = 100µm, Zoom scale = 10µm).

When I co-stained GFP with NeuN (Figure 9), I detected no colocalization in any of the three tissue types (see zoomed images). Additionally, some cells displayed a strong GFP signal but were lacking any Iba1 or NeuN staining. Control stainings of ligated WT animals with GFP and Iba1 or NeuN did not reveal any GFP signal or colocalization (Figure 10).

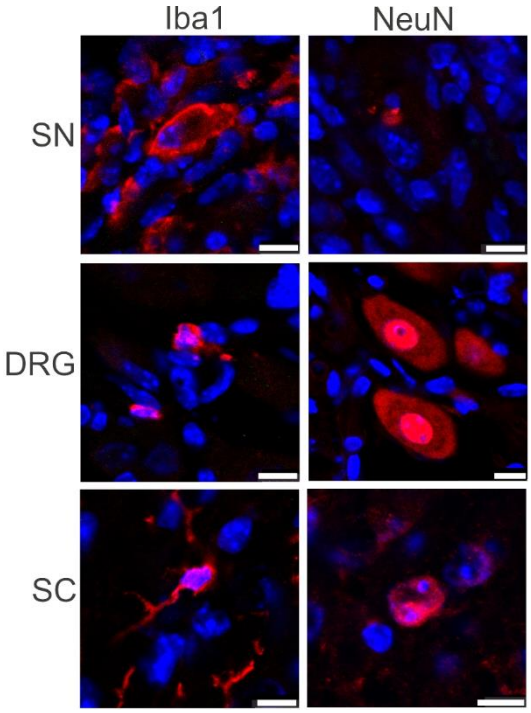

Figure 10 Control stainings of GFP with Iba1 or NeuN in ligated WT animals 14 days post PSNL. Ipsilateral sciatic nerves, ipsilateral dorsal root ganglia and ipsilateral lumbar spinal cord were stained for GFP (green) with Iba1 (red, left panel) or with NeuN (red, right panel). Cell nuclei were stained with DAPI (blue) (scale = 10 µm).

4.2 Cellular CB2 receptor expression in inflammatory tissue

To further prove the significance of CB2 receptor expression on microglia and macrophages, in contrast to neurons, I evaluated different conditional CB2KO mice for their behavior during inflammation. Therefore, I analyzed mechanical allodynia after PSNL in complete CB2KO mice and conditional CB2-LysM or CB2-Syn mice, lacking the CB2 receptors in myeloid cells or neurons, respectively.

4.2.1 Behavioral analysis of neuropathic pain development in CB2KO mice

First I compared mechanical allodynia of WT with CB2KO animals. Beginning on day 3 after PSNL, all ligated mice showed nociceptive responses on the ipsilateral hind paw (Figure 11). WT mice displayed a strong *treatment* effect [$F_{1,60} = 292.1$, $p < 0.0001$] and a

treatment x *time* interaction [$F_{4,60}$ = 21.81, p < 0.0001]. Mechanical threshold of ligated WT mice decreased on day 3 and stayed constant until day 14.

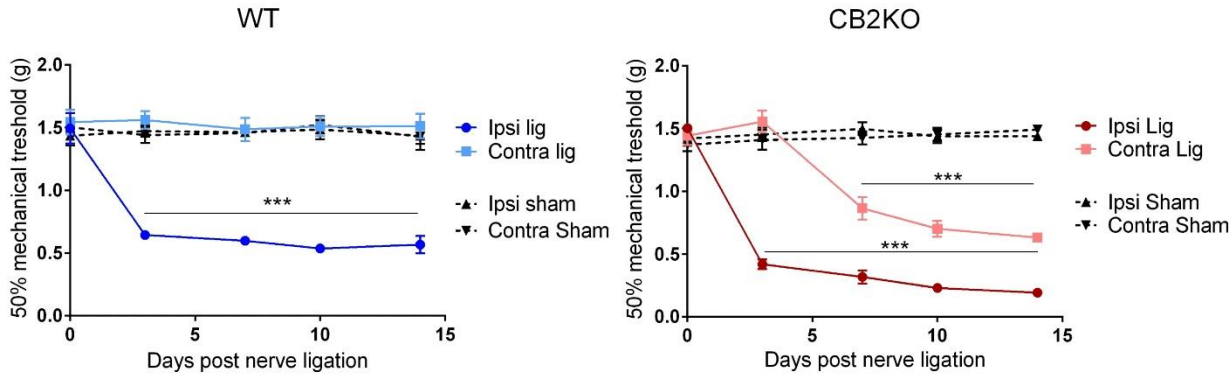

Figure 11 Mechanical allodynia of WT and CB2KO mice assessed with von Frey filaments basal and during 14 days post PSNL in ipsi- and contralateral hind paws. Ligated CB2KO and WT mice showed increased ipsilateral hypersensitivity. Additionally, ligated CB2KO mice developed contralateral hypersensitivity in contrast to ligated WT mice. When compared to sham treated animals, ligated CB2KO animals showed a significant decreased mechanical threshold on both, ipsi- and contralateral side. n = 7-8 Statistical significance was determined with a two-way ANOVA and a Bonferroni's post-hoc test. Stars represent differences between ligated and sham animals. *p < 0.05, ** p < 0.01, ***p < 0.001, Error bars show SEM

Ligated CB2KO mice also developed an increased mechanical allodynia on the ipsilateral side that lasted for 14 days (Figure 11) [*treatment* $F_{1,70}$ = 1063, p < 0.0001]. Additionally, the contralateral hind paw of ligated CB2KO mice displayed signs of neuropathic pain as well, beginning on day seven [*treatment* $F_{1,70}$ = 92.41, p < 0.0001]. Both sides displayed significant *treatment* x *time* interaction [ipsi: $F_{4,70}$ = 80.45, p < 0.0001; contra: $F_{4,70}$ = 26.56, p < 0.0001]. In contrast, ligated WT animals did not develop any signs of contralateral mechanical allodynia at any time point. No *treatment* effect was detectable [$F_{1,60}$ = 1.114, p = 0.2955]. Sham treated animals did not develop any mechanical allodynia on the ipsi- or contralateral side.

4.2.2 Behavioral analysis of neuropathic pain development in CB2-LysM mice

After validation of the pain phenotype in CB2KO mice, which showed increased mechanical allodynia on the contralateral side, I was interested to further specify the cellular localization of CB2 in neuropathic pain. Since the immunohistochemical data of CB2-GFP mice indicated an expression on microglia and macrophages, I generated mice with a myeloid-specific CB2 deletion using the Cre/ loxP recombination system. In this system, the Cre recombinase excises a DNA sequence, which is flanked by two loxP sites

through site-specific recombination (Hoess & Abremski 1984). Floxed CB2 mice (CB2-FL) contain two loxP sequences that flank the open reading frame of exon 2 in the *Cnr2* gene (Stempel et al. 2016). For the generation of conditional CB2-LysM mice, CB2-FL mice were crossed with mice that express the Cre recombinase under the myeloid–specific promoter for the lysozyme gene M (LysM). The resulting offspring has a conditional CB2 deletion in microglia, macrophages and granulocytes (Clausen et al. 1999).

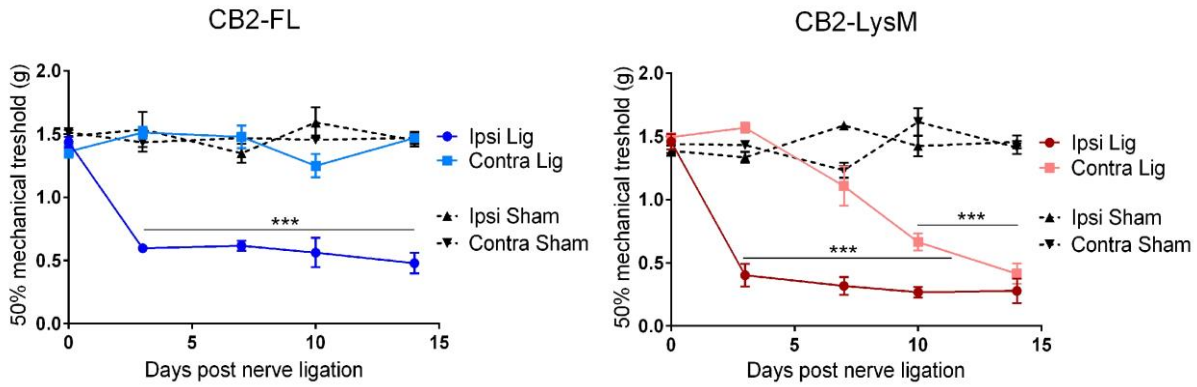

Figure 12 Mechanical allodynia of CB2-FL and CB2-LysM mice measured in ipsi- and contralateral hind paws basal and during 14 days post PSNL. Ligated CB2-LysM mice developed increased ipsilateral hypersensitivity when compared to ligated CB2-FL animals. Moreover, ligated CB2-LysM animals showed signs of contralateral mechanical allodynia. Compared to sham treated animals, ligated CB2-LysM mice displayed significant reductions of mechanical threshold on ipsi- and contralateral sides. n = 7 on day 0, 7, 14 and n = 4 on day 3, 10. Statistical significance was determined with a two-way ANOVA and a Bonferroni's post-hoc test. Stars represent differences between ligated and sham animals. * $p < 0.05$, ** $p < 0.01$, ***$p < 0.001$, Error bars show SEM

At the age of 8-12 weeks, mechanical allodynia of CB2-LysM mice was tested after PSNL. Neuropathic pain development in CB2-LysM mice was similar to CB2KO animals (Figure 12). Increased ipsilateral mechanical allodynia started on day 3 and was constant until day 14. A strong *treatment* effect was revealed for the ipsilateral hind paw [CB2-LysM: $F_{1,48} = 427.9$, $p < 0.0001$; CB2-FL: $F_{1,48} = 249.7$, $p < 0.0001$]. The contralateral side developed a similar pain response as seen in CB2KO mice, starting on day 7 after nerve ligation until day 14 [*treatment* $F_{1,48} = 45.69$, $p < 0.0001$]. Both sides showed a significant *time* x *treatment* effect [ipsi: $F_{4,48} = 41.46$, $p < 0.0001$; contra: $F_{4,48} = 20.42$, $p < 0.0001$]. Again, mechanical allodynia in control mice only developed on the ipsilateral side [*treatment* $F_{1,48} = 249.7$, $p < 0.0001$] and remained on basal levels on the contralateral side [*treatment* $F_{1,48} = 2.225$, $p = 0.1423$].

4.2.3 Behavioral analysis of neuropathic pain development in CB2-Syn mice

To determine whether CB2 on neurons is relevant for the development of neuropathic pain, CB2-Syn mice were analyzed as well for mechanical allodynia.

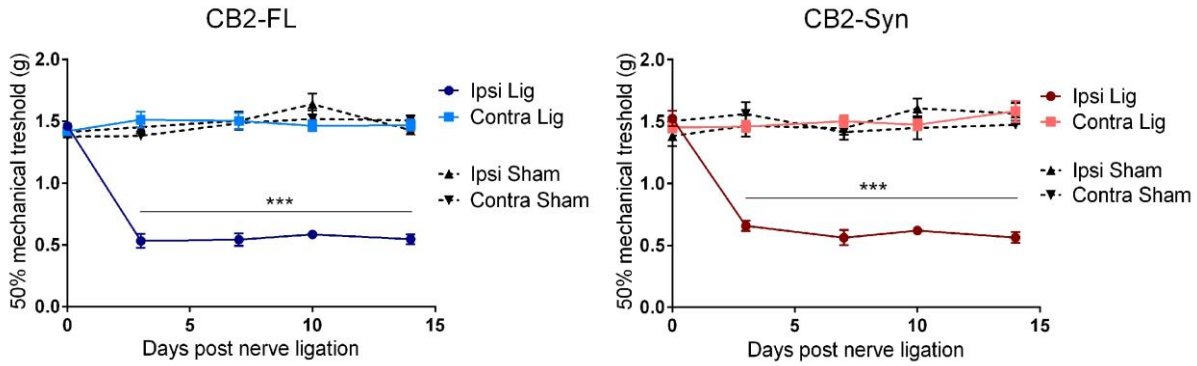

Figure 13 Mechanical allodynia of CB2-FL and CB2-Syn mice. Hind paws were measured ipsi- and contralateral, basal and during 14 days post PSNL. Ligated CB2-Syn mice and CB2-FL mice developed ipsilateral hypersensitivity starting on day 3 after PSNL. These reductions were statistical significant when compared to sham treated mice No change in mechanical allodynia was observed on the contralateral side for both genotypes. n = 8 Statistical significance was determined with a two-way ANOVA and a Bonferroni post-hoc test. Stars represent differences between ligated and sham animals. *p < 0.05, ** p < 0.01, ***p < 0.001, Error bars show SEM

In CB2-Syn mice (Fig 13), mechanical allodynia was detected only on the ipsilateral side, similar as in ligated CB2-FL mice [*treatment* CB2-Syn: $F_{1,70} = 294.3$, $p < 0.0001$; CB2-FL: $F_{1,70} = 534.1$, $p < 0.0001$] and remained constant until day 14. The interaction of *time* x *treatment* revealed a significant effect for the ipsilateral hind paw of both genotypes [CB2-Syn: $F_{4,70} = 27.23$, $p < 0.0001$; CB2-FL: $F_{4,70} = 28.63$, $p < 0.000$]. There was no significant *treatment* effect for the contralateral sides of both genotypes [CB2-Syn: $F_{1,70} = 0.1315$, $p = 0.7180$; CB2-FL: $F_{1,70} = 0.4214$, $p = 0.5184$].

4.2.4 Comparison of the behavioral analyses between all genotypes

Finally, von Frey data of all analyzed CB2 knockout mice was compared, to display phenotypic differences. When comparing mechanical allodynia of all ligated genotypes, the differences on the ipsi- and contralateral sides between all genotypes become obvious (Figure 14). Moreover, a strong *genotype* effect was revealed by two-way ANOVA for both sides [ipsi: $F_{3,124} = 29.35$, $p < 0.0001$; contra: $F_{3,124} = 59.21$, $p < 0.0001$].

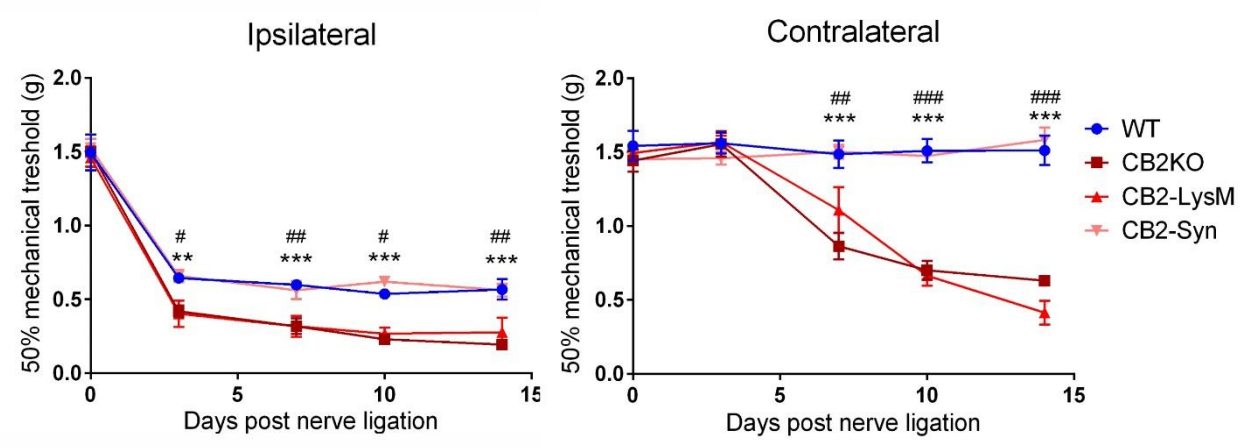

Figure 14 Mechanical allodynia measured in ligated WT, CB2KO, CB2-LysM and CB2-Syn mice on both sides basal and during 14 days post PSNL. Mechanical threshold of previous experiments from CB2KO, CB2-LysM and CB2-Syn were combined to be compared between genotypes. CB2KO and CB2-LysM mice showed a significant decreased mechanical threshold on both, ipsi- and contralateral side, compared to WT animals. n = 4 - 8 Statistical significance was determined with a two-way ANOVA and multiple t-tests using the Holm-Sidak method for each day. Stars represent differences between CB2KO and WT mice. Hashtags indicate significance between CB2-LysM and WT mice. *p < 0.05, **p < 0.01, ***p < 0.001 # p < 0.05, ## p < 0.01 ### p < 0.001, Error bars show SEM.

CB2KO and CB2-LysM mice developed an increased mechanical allodynia on the ipsilateral side after nerve ligation. Multiple t-tests showed statistical significance for CB2-LysM and CB2KO throughout all days on the ipsilateral side, when compared to WT animals [CB2KO: Day 3 p = 0.00353, Day 7 p = 0.00034, Day 10 and Day 14 p < 0.0001; CB2-LysM: Day 3 p = 0.03875, Day 7 p = 0.00564, Day 10 p = 0.02194, Day 14 p = 0.00445]. After analyzing the contralateral side with multiple t-tests, a significant difference for CB2KO compared to WT mice was revealed [Day 7, Day 10 and Day 14 p < 0.0001]. A similar significant reduction of mechanical threshold on the contralateral side was observed in CB2-LysM mice [Day 7 p = 0.00423, Day 10 and Day 14 p < 0.0001].

4.2.5 Molecular analysis of neuropathic pain development in cell-specific CB2 receptor KO mice

To confirm the stronger development of neuropathic pain in CB2KO and CB2-LysM mice, I analyzed Iba1 expression, as a marker for microgliosis, in the dorsal horn of the lumbar spinal cord in WT, CB2KO, CB2-LysM and CB2-Syn mice (Figure 15).

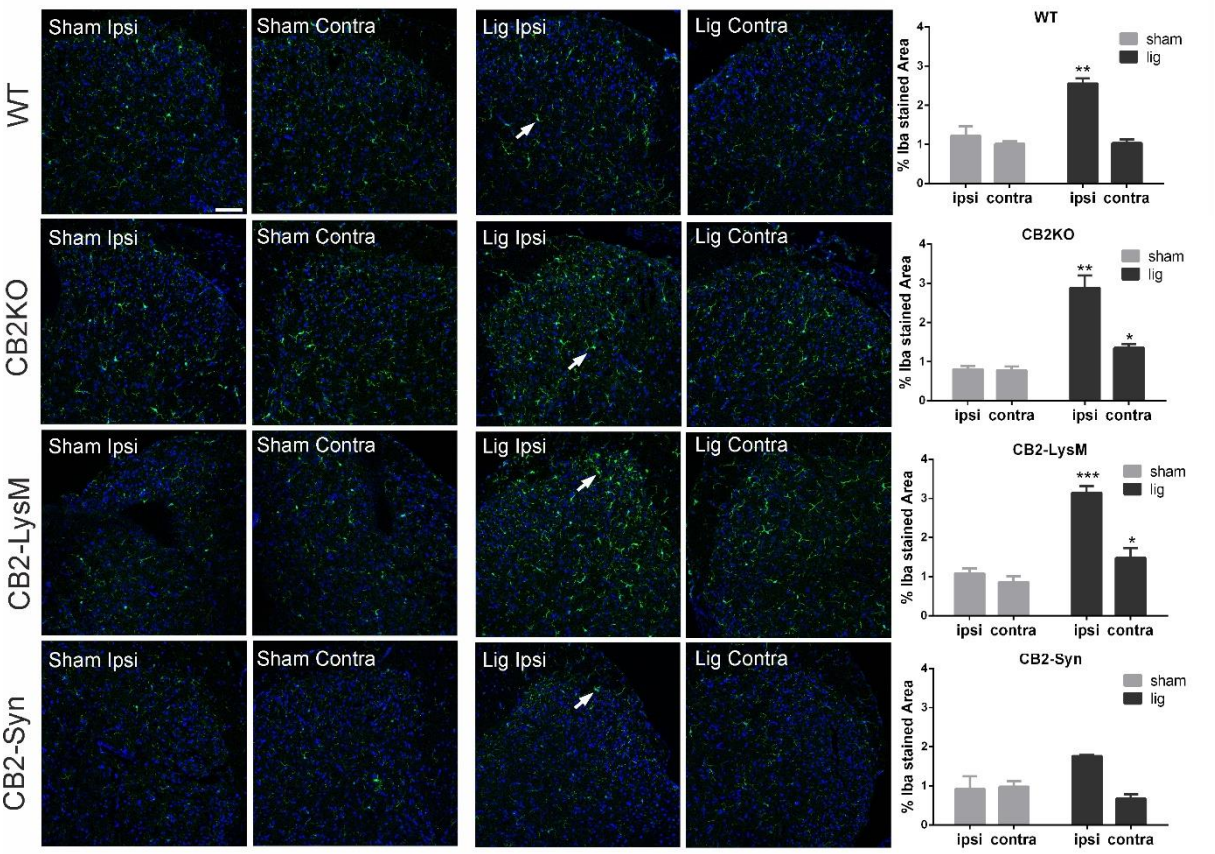

Figure 15 Expression of microglia in the dorsal horn . Microglia were stained with Iba1 (green) in both sides of the dorsal horn in the lumbar spinal cord. Representative stainings of Iba1 in CB2KO, WT, CB2-LysM and CB2-Syn mice 14 days after PSNL (lig) or sham surgery (sham). Cell nuceli were stained with DAPI (blue). Arrows indicate Iba1 expressing cells (scale = 75µm). Analysis of Iba1 stained area in percent shows increase of Iba1 expression after ligation ipsilateral (WT, CB2KO and CB2-LysM) and contralateral (CB2KO, CB2-LysM). n = 3-4. Statistical significance was determined with multiple t-tests using the Holm Sidak Method. Stars represent differences between ligated and sham animals. *p < 0.05, **p < 0.01, ***p < 0.001, Error bars show SEM.

When I analyzed Iba1 stained areas, all mice showed a profound increase in Iba1 signal on the ipsilateral side after nerve ligation [WT p = 0.0076; CB2KO p = 0.0032; CB2-LysM p < 0.0001; CB2-Syn p = 0.0598], whereas CB2-Syn mice failed to induce a statistical significant difference of Iba1 expression post PSNL. Additionally, CB2KO as well as CB2-LysM mice displayed increased expression of the microglia marker Iba1 on both sides, ipsilateral and contralateral [CB2KO p = 0.0175; CB2-LysM p = 0.0425]. This was in contrast to WT mice, which did not exhibit an increased Iba1 signal on the contralateral side following nerve ligation [WT p = 0.9301]. Sham treated animals did not display any increased expression of Iba1 in both, ipsi- and contralateral sides of the dorsal horns.

To confirm the different development of neuropathic pain in WT and CB2KO mice, I analyzed infiltrating immune cells in the sciatic nerve on day 3 after PSNL (Figure 16). First, expression of CD45 as a marker for leukocytes was analyzed. Around 65% - 75% of all viable cells in ipsilateral ligated samples were found to be $CD45^+$ (Figure 17 B).

Whereas the contralateral sides contained almost no CD45⁺ cells, I detected around 20% of these cells in ipsilateral sham samples. When I analyzed the results for statistical significance with a two-way ANOVA, I measured a significant *treatment* effect for the ipsilateral side [$F_{1,12}$ = 96.96, p < 0.0001] but no *genotype* effect [$F_{1,12}$ = 0.0867, p = 0.7741]. This was in contrast to the contralateral side, which showed a statistical significant *genotype* effect [$F_{1,12}$ = 5.999, p = 0.0306] but not *treatment* effect [$F_{1,12}$ = 4.603, p = 0.0531]. Multiple comparisons between the samples on the ipsilateral side revealed that the amount of CD45⁺ cells significantly increased after nerve ligation for both genotypes [WT p < 0.0001; CB2KO p = 0.0003] but did not show any statistical significance between the genotypes [WT vs. CB2KO p = 0.8605].

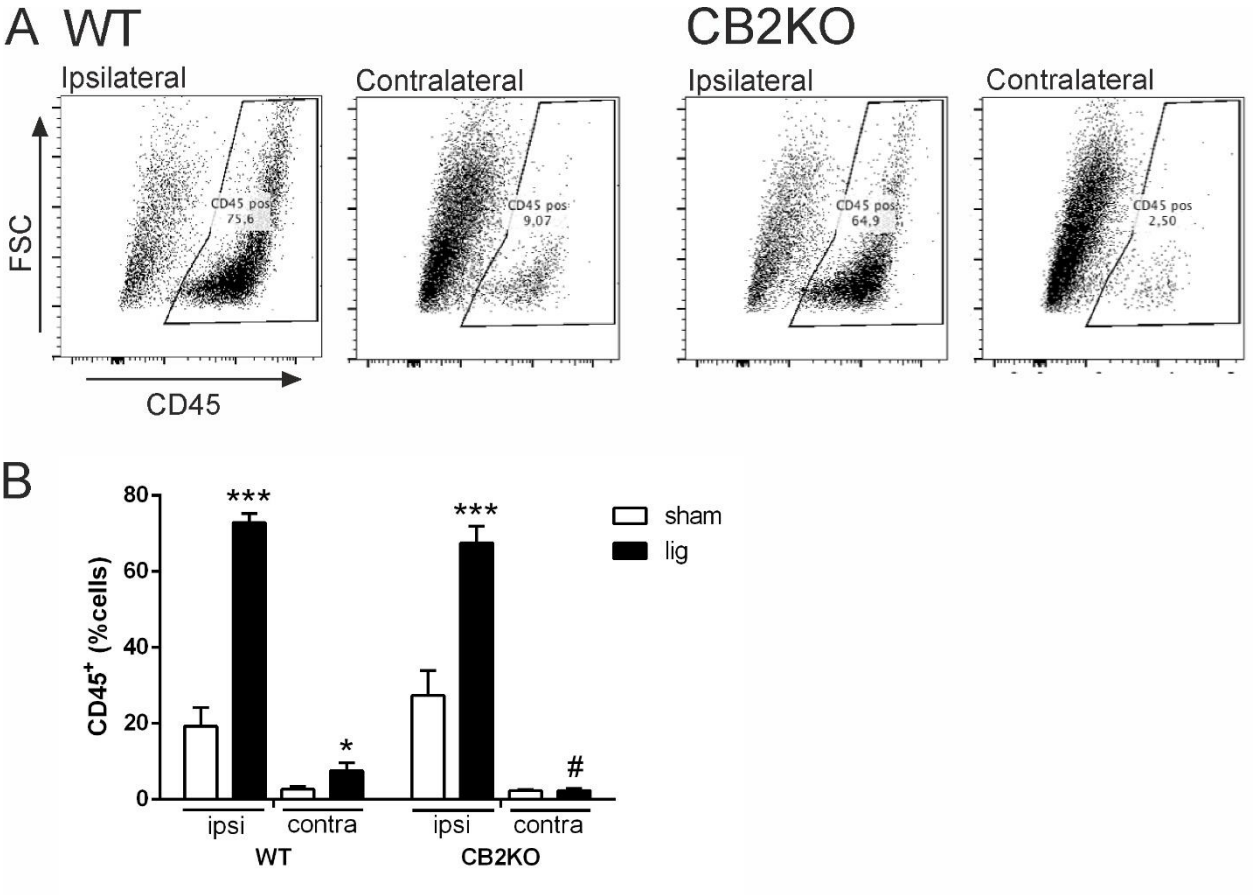

Figure 16 Analyzing for CD45⁺ cells in sciatic nerves three days post PSNL. A) Scatter blot of measured events. Cells were differentiated through forward scatter and a CD45 marker. The same gate was applied to all samples. B) Statistical comparison of cell percentages between treatment and genotype. Highest amount of CD45⁺ cells were measured in ligated ipsilateral samples for both genotypes. Data is shown in mean +/- SEM. Statistical analysis with 2-way ANOVA and a Tukey's post-hoc test. * p < 0.05; *** p < 0.001; * equals difference between treatments. # < 0.05; # shows difference between genotypes. n = 4

Moreover, the amount of CD45⁺ cells increased significantly on the contralateral side for WT but not for CB2KO animals [WT p = 0.0486; CB2KO p > 0.9999], which led to a

significant difference between genotypes for the ligated contralateral nerve [WT vs. CB2KO p = 0.035]I further analyzed all $CD45^+$ cells for CD11b and Ly-6B. CD11b is also known as Integrin αM and is involved in adherence of monocytes, macrophages and granulocytes. It serves as a more specific marker for macrophages or dendritic cells (Murray & Wynn 2011). Ly-6B on the other hand, is found on neutrophils or M1 monocytes and is lost upon differentiation into resident M2 macrophages. Therefore, it can be used to separate cell populations into neutrophils and M1 macrophages ($Ly\text{-}6B^{high}$) or into M2 macrophages ($Ly\text{-}6B^{low}$). I found two populations of $CD45^+$ cells; $CD11b^+$ and $Ly\text{-}6B^{low}$ expressing cells and $CD11b^+$ $Ly\text{-}6B^{high}$ expressing cells (Figure 17 A). In sham contralateral samples of WT and CB2KO mice, amount of $Ly\text{-}6B^{low}$ cells was around 11 – 13% for both genotypes (Figure 17 B). In WT animals, the ipsilateral side contained higher numbers of $Ly\text{-}6B^{low}$ cells than on the contralateral side. Ligated ipsilateral levels reached up to 35% of all $CD45^+$ cells but did not differ statistically between treatment nor genotype, since CB2KO ipsilateral samples contained similar amounts of $CD45^+$ cells [*treatment* $F_{1,12} = 0.9151$, p = 0.3576; *genotype* $F_{1,12} = 0.3511$, p = 0.5645].

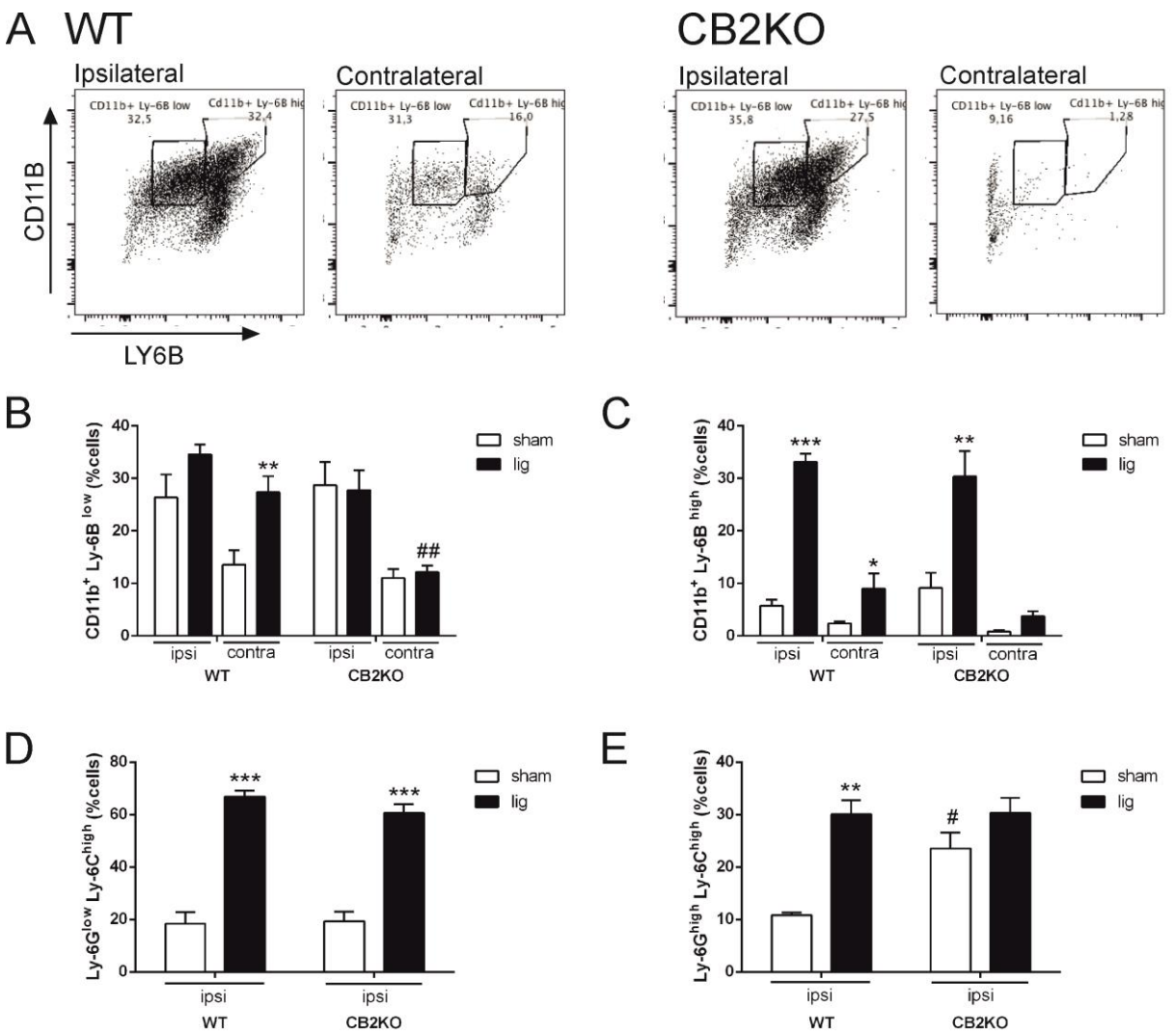

Figure 17 Percentage of different immune cells in sciatic nerves three days after PSNL. A) Scatter blot of cells analyzed for CD11b and Ly-6B in ligated ipsilateral and contralateral samples of both genotypes. Blots show a clear difference of cell percentages between ipsi- and contralateral sides. B) Differences in percentage of $CD11b^+$ and $Ly\text{-}6B^{low}$ cells. Ipsilateral and contralateral ligated samples showed an increased amount of cells, whereas both contralateral nerve samples of CB2KO animals revealed only reduced amounts of $CD11b^+$ and $Ly\text{-}6B^{low}$ cells. C) $CD11b^+$ and $Ly\text{-}6B^{high}$ cell percentages of all samples. Ipsilateral samples show an equal increase after ligation, which was not observed for the contralateral side. Further analysis for Ly-6G and Ly-6C revealed populations of M1 macrophages (D) and neutrophils (E). This analysis was only possible on the ligated ipsilateral side, since other samples contained too few cells to analyze. For both cell populations, percentages were increased after nerve ligation in WT and CB2KO animals. Data is expressed as mean +/- SEM. Statistical analysis was performed with a two-way ANOVA and a Tukey's post-hoc test. ** $p < 0.01$; *** $p < 0.001$ * shows differences in treatment. # $p < 0.05$ # indicates differences between both genotypes. n = 4

This was in contrast to the ligated, contralateral side, where $Ly\text{-}6B^{low}$ cell number significantly increased in WT animals after nerve ligation [p = 0.0057] but remained on basal levels in CB2KO mice [*treatment* $F_{1,12}$ =10.37, p = 0.0073; *genotype* $F_{1,12}$ = 14.70, p = 0.0024].

I detected an equal increase on the ipsilateral side for $CD11b^+$ $Ly\text{-}6B^{high}$ cells in both genotypes after nerve ligation (Figure 17 C). Around 30% of all $CD45^+$ cells in ligated,

ipsilateral sciatic nerves expressed Ly-6B and CD11b. This rise was independent from the genotype but dependent from treatment [*treatment* $F_{1,12}$ = 67.10, p < 0.0001 ; *genotype* $F_{1,12}$ = 0.0113, p = 0.9170], as sham operated animals exhibited only minor increase in Ly-6B^{high} cells on the ipsilateral side and almost no change on the contralateral side. Contralateral ligated nerve samples of WT animals contained three times more Ly-6B^{high} cells than their respective sham controls [WT p = 0.0463] and two times more than CB2KO mice. Therefore, I detected a statistical significant *genotype* [$F_{1,12}$ = 4.828, p = 0.0484] and *treatment* [$F_{1,12}$ = 9.455, p = 0.0096] effect but no interaction of these two.

I further analyzed CD11b^{+} and Ly-6B^{high} cells for the markers Ly-6C and Ly-6G to differentiate M1 macrophages and neutrophil populations among the analyzed cells (Figure 17 D, E). Ly-6G is a common marker for neutrophils and Ly-6C is expressed in both, macrophages and neutrophils. (Rose et al. 2012). Ly-6C^{high} and Ly-6G^{high} cells could be assigned as neutrophils and the percentages of these cells were increased in ipsilateral samples after ligation for both genotypes but significantly differed only in WT mice (Figure 17 E) [WT p = 0.0024]. Ipsilateral nerves of sham treated CB2KO mice exhibited a higher percentage of these cells than in WT animals [p = 0.0350]. Overall, I found a significant *treatment* [$F_{1,11}$ = 23.39, p= 0.0005] and *genotype* effect [$F_{1,11}$ = 5.836, p = 0.0343] for neutrophil populations in ipsilateral samples. Additionally, the interaction of these two effects was significant, too [$F_{1,11}$ = 5.354, p = 0.0410]. Cell number of CD11b^{+} Ly-6B^{high} cells was too low in contralateral samples for further analysis. M1 macrophages were determined as Ly-6C^{high} and Ly-6G^{low} cells and represented 60% – 66% of all previously analyzed CD11b^{+} and Ly-6B^{high} cells in ligated, ipsilateral samples. Sham ipsilateral nerves comprised only around 20% of these cell populations and were statistical significant to the ligated samples [WT lig p < 0.0001; CB2KO lig p < 0.0001]. Therefore, I detected a *treatment* [$F_{1,12}$ = 162.6, p < 0.0001] but no *genotype* effect [$F_{1,12}$ = 0.5388, p = 0.4770] when analyzing the results with a two-way ANOVA. Again, contralateral samples did not contain enough cells to be analyzed.

Overall, I detected a statistical difference only for the contralateral samples between CB2KO and WT mice on day 3 after PSNL, showing a reduced amount of immune cells in contralateral nerves of CB2KO mice. I was further interested in this difference and since the contralateral pain in CB2KO animals is robust from day 8 on (see Figure 11), I evaluated immune cells on day 8 after nerve ligation in sciatic nerves of both genotypes.

After analyzing all living cells for CD45, a difference between treatments became obvious (Figure 18 A). Again, ipsilateral samples of ligated animals contained most of all analyzed CD45⁺ cells and were significantly increased after nerve ligation [WT p = 0.0001 ; CB2KO p = 0.0003], but the overall amount of CD45⁺ cells (30-40%) was less than on day 3 (60-70%; see Figure 16 B). Consequently, I detected a *treatment* [$F_{1,12}$ = 81.22, p < 0.0001] but no *genotype* effect [$F_{1,12}$ = 0.2219, p = 0.6460] when analyzing the results with a two-way ANOVA. Ligated contralateral or both sham treated samples did not comprise more than 10% of these cell populations and showed no significant effect for treatment or genotype. This was in contrast to CD45⁺ cell numbers on day 3, when even ipsilateral sham samples showed an increased amount of CD45⁺ cells.

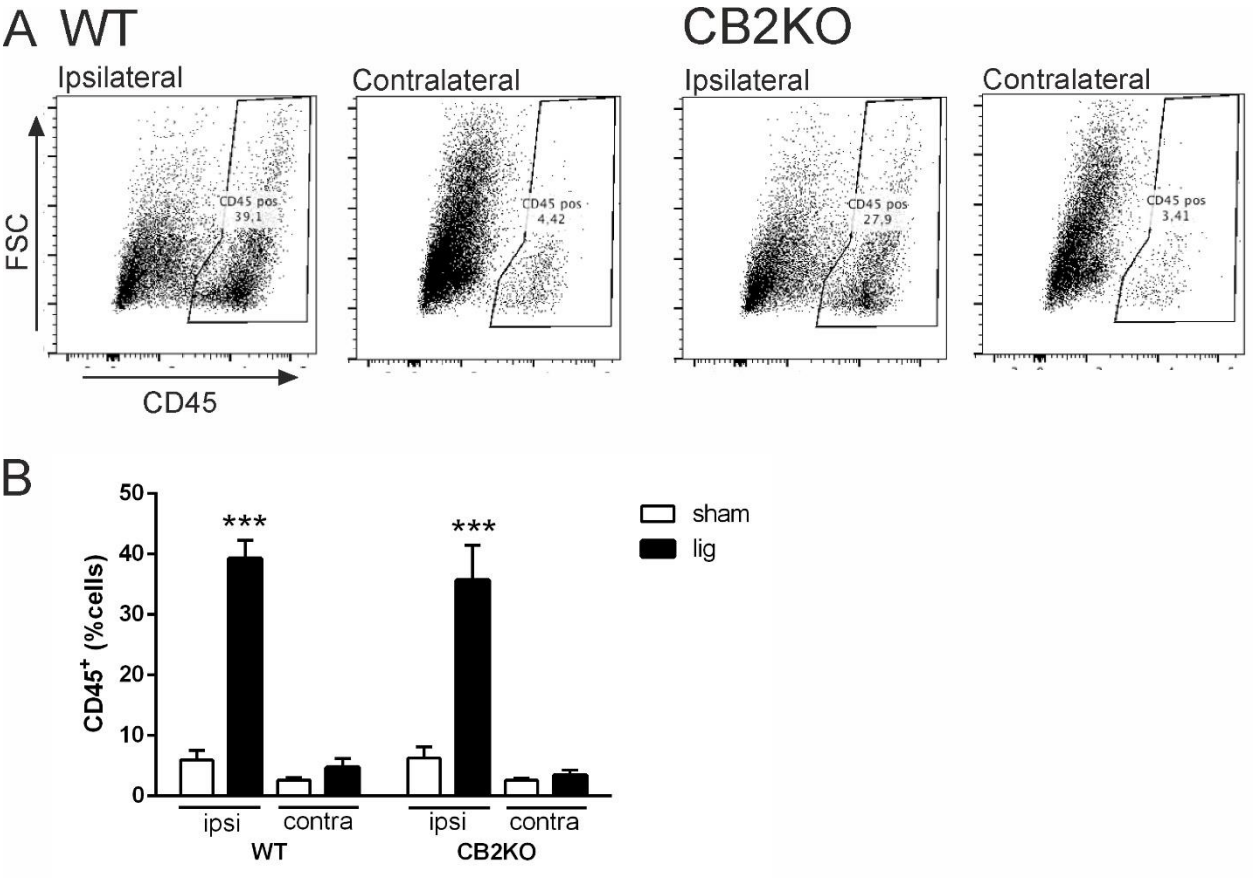

Figure 18 Analysis of viable CD45⁺ cells in sciatic nerves eight days after PSNL. A) Scatter blot of measured events. Cells were differentiated through forward scatter and a CD45 marker. The same gate was applied to all samples. B) Statistical comparison of cell percentages between treatment and genotype. Highest amount of CD45⁺ cells were measured in ligated ipsilateral samples for both genotypes. Data is shown in mean +/- SEM. Statistical analysis with two-way ANOVA and a Tukey's post-hoc test. *** p < 0.001; * equals difference between treatments. n = 4

Because of the low amount of CD45$^+$ cells measured on day 8, further analysis of CD11b and Ly-6B was difficult. Analysis of these two markers was only possible in ligated ipsilateral samples, as other nerve samples did not contain enough CD45$^+$ cells (Figure 19). CD11b$^+$ and Ly-6B^{low} cells reached a percentage of around 18 - 21% in both, WT and CB2KO samples. CD11b$^+$ and Ly-6B^{high} cells only comprised 12 - 13% of all CD45$^+$ cells. Unfortunately, the amount of analyzed cells was too low to further analyze for Ly-6G and Ly-6G, as on day 3. Again, I did not detect any statistical differences between WT and CB2KO animals in measured cell percentages.

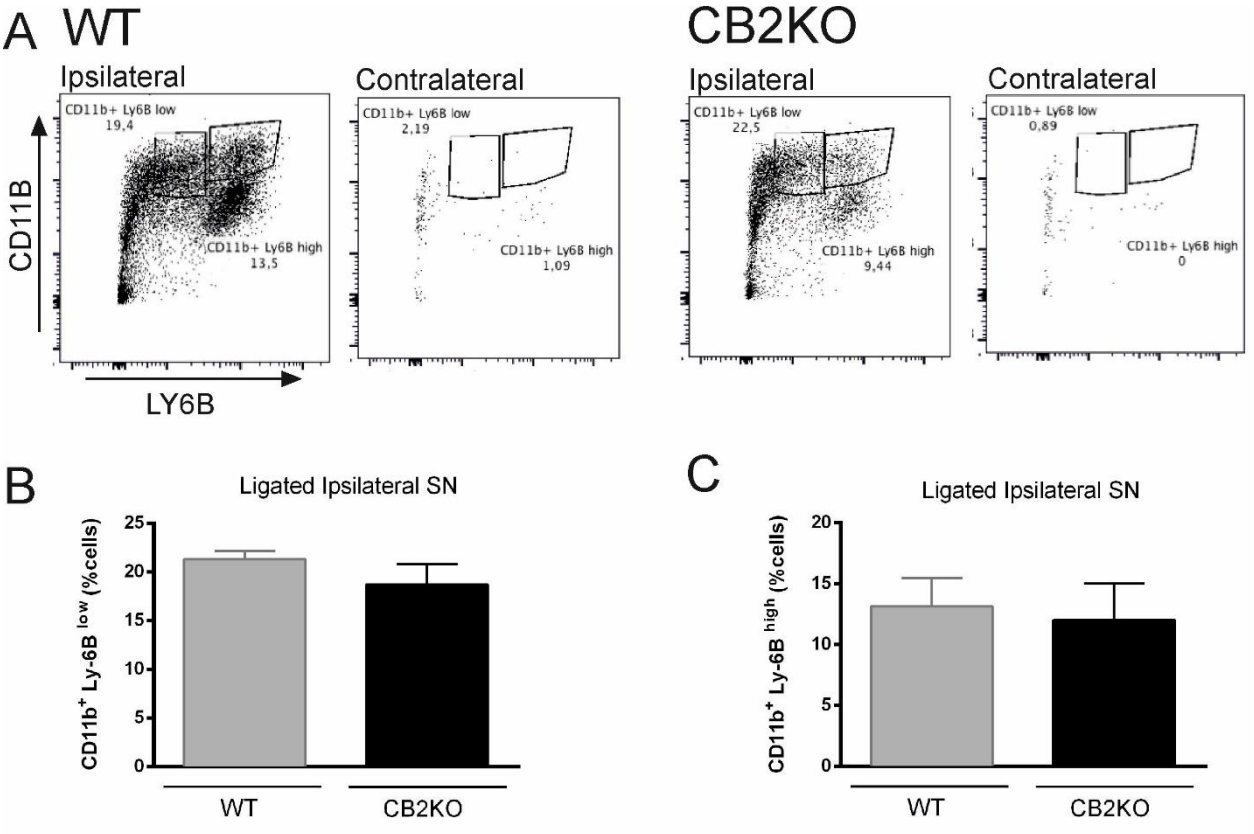

Figure 19 Amount of different immune cells in sciatic nerves eight days after PSNL. A) Scatter blot of cells analyzed for CD11b and Ly-6B in ligated ipsilateral and contralateral samples of both genotypes. Blots show a clear difference of cell percentages between ipsi- and contralateral sides. B) No statistical differences in percentage of CD11b$^+$ and Ly-6B^{low} cells in ligated ipsilateral samples between WT and CB2KO animals C) CD11b$^+$ and Ly-6B^{high} cell percentages in ligated ipsilateral samples. There was no significant difference of cell

percentages between both genotypes. Data is expressed as mean +/- SEM. Statistical analysis was performed with student's t-test. n = 4

4.3 Leptin receptor expression in the sciatic nerve of ligated mice

Previous studies showed a relation between leptin and the CB2 receptor (Lopez-Rodriguez et al. 2016). To investigate this relation, leptin receptor expression was analyzed by immunohistochemistry in the ipsi- and contralateral sciatic nerve of WT and CB2KO mice (Figure 19).

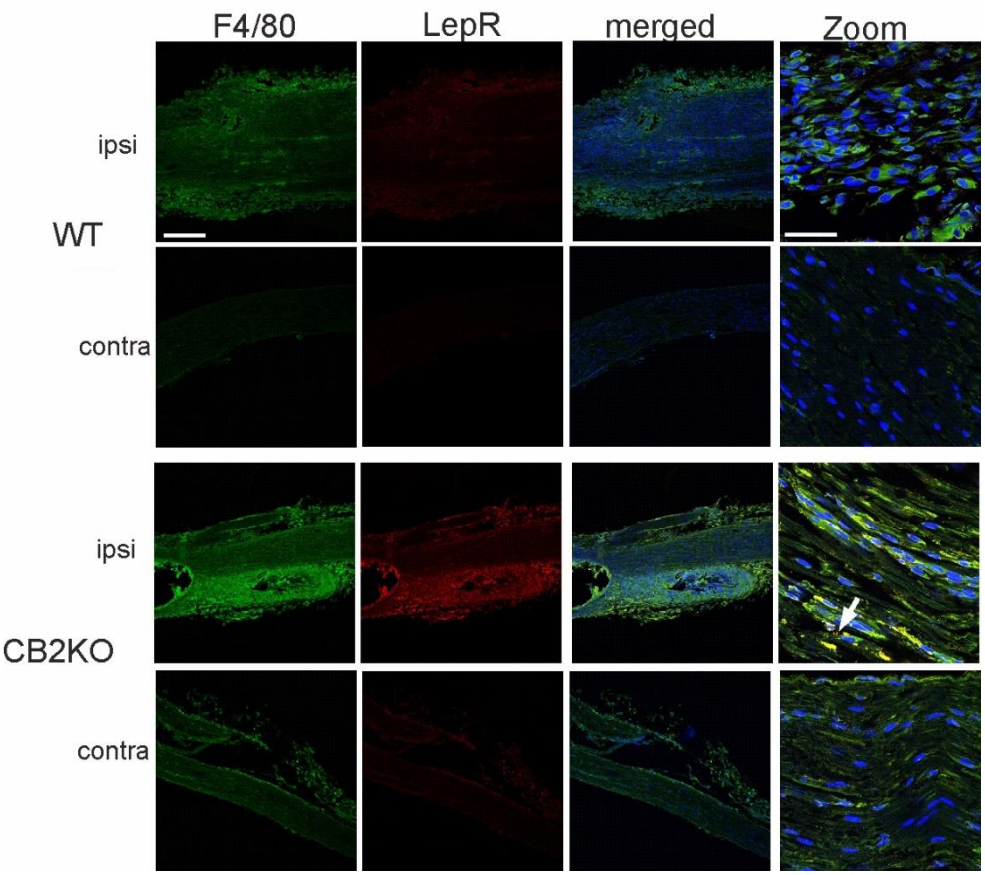

Figure 16 Coexpression of leptin receptor (red) with F4/80 (green) 14 days post PSNL in the sciatic nerve in WT and CB2KO mice. Leptin receptor signal was highest and colocalized with the macrophage marker F4/80 in ipsilateral sciatic nerve of CB2KO mice compared to WT mice. Cell nuclei were stained with DAPI (blue). Arrows show coexpressing cells. (scale = 250 µm, zoom scale = 50 µm).

Signal of leptin receptor was increased in the ipsilateral sciatic nerve of CB2KO mice, in contrast to WT animals, which did not show any staining of the leptin receptor. Moreover, leptin receptor signal overlapped with F4/80, showing a coexpression of these two

proteins. F4/80 signal was increased as well on the ipsilateral side of CB2KO mice compared to the contralateral side or to samples from WT animals.

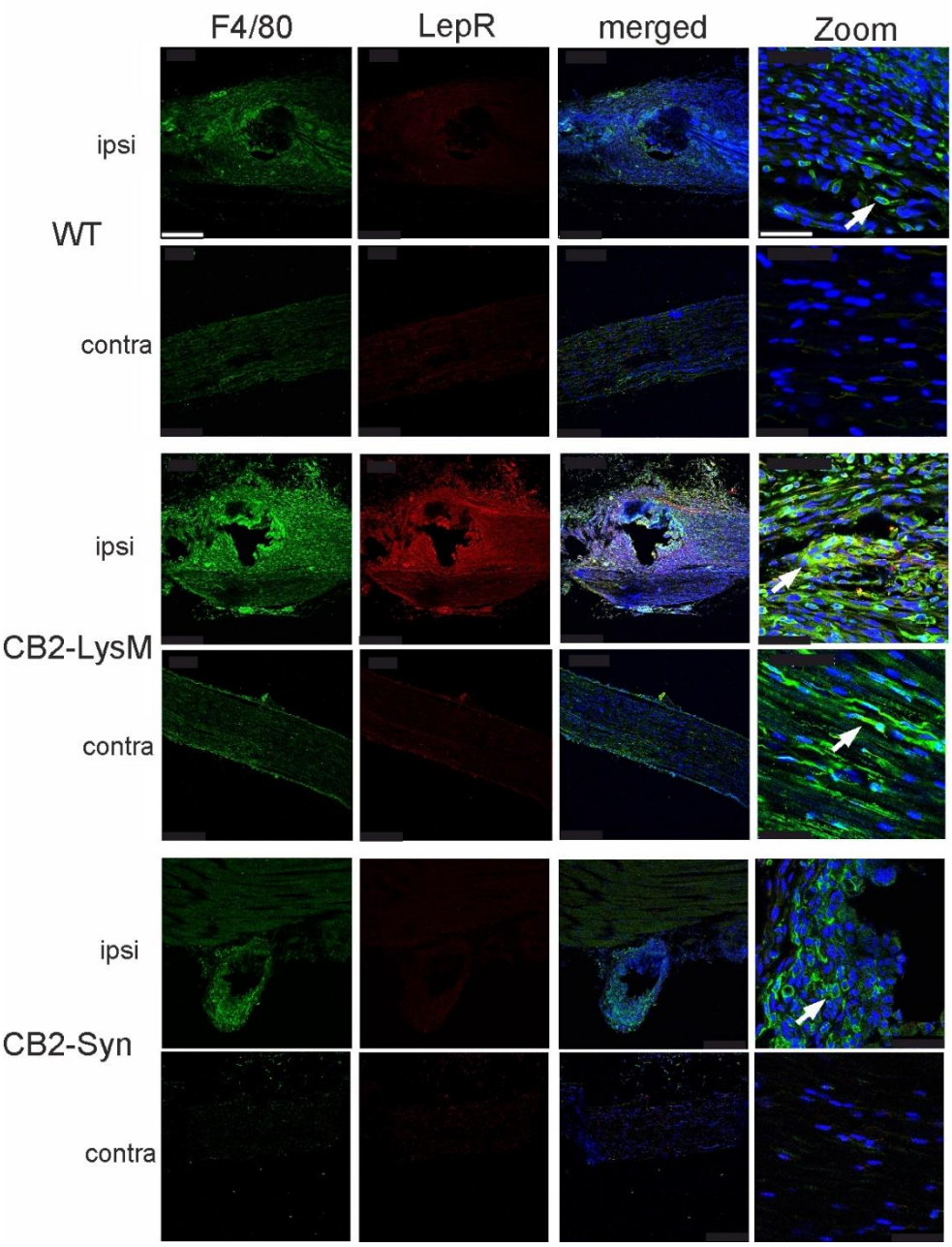

Figure 170 Coexpression of leptin receptor (red) with F4/80 (green) 14 days post PSNL in the sciatic nerve in WT, CB2-LysM and CB2-Syn mice. Leptin receptor signal was highest in ipsilateral sciatic nerve of CB2-LysM mice compared to WT or CB2-Syn mice and colocalized with the macrophage marker F4/80 (see white arrows). Cell nuclei were stained with DAPI (blue) Ipsilateral ruptures of the nerve indicate the site of ligation. (scale = 250 µm, 63x zoom scale = 50 µm).

To examine if conditional CB2 knock-out mice share this phenotype, leptin receptor expression was analyzed by immunohistochemistry in the ipsi- and contralateral sciatic

nerve of WT, CB2-LysM and CB2-Syn mice (Figure 20). Similar to the previous findings of CB2KO mice, leptin receptor expression increased on the ipsilateral side of CB2-LysM animals. Moreover, signal of leptin receptors colocalized with the common macrophage marker F4/80. As expected, CB2-Syn and WT mice did not show any differences in leptin receptor expression.

4.4 Daglα in neuroinflammation and pain

Since Daglα is the main enzyme in the biosynthesis of 2-AG, a major ligand for the CB2 receptor, I suspected this enzyme to have an important role in inflammation and pain. Therefore, Daglα KO mice were as well analyzed for their phenotype in neuropathic pain processing.

4.4.1 Daglα in neuropathic mice

To investigate the relation between the two main endocannabinoids AEA and 2-AG, the CB2 receptor and the synthesizing enzyme Daglα, I measured endocannabinoid levels in WT, CB2KO and Daglα KO mice (Figure 21). Spinal cord tissue was analyzed ipsi- and contralateral, 14 days after nerve ligation for 2-AG, arachidonic acid and anandamide levels.

Levels of 2-AG did not differ between both sides or between treatments in CB2KO animals. Ligated Daglα KO mice showed a tendency of higher 2-AG amounts compared to sham mice, which was more obvious on the contralateral side [p = 0.0507]. When analyzed with a two-way ANOVA, I detected an overall significant *treatment* effect for these samples [$F_{1,4}$ = 27.02 p = 0.0065]. Nerve ligation in WT mice increased 2-AG levels. After analysis with a two-way ANOVA, I detected a clear *treatment* effect [F1,4 = 9.127 p = 0.0391]. Moreover, WT animals contained over three times more 2-AG than Daglα mice.

Arachidonic acid levels were equally changed as 2-AG. Again, I could not detect any differences in CB2KO mice. Levels of Daglα KO animals were reduced but did not differ between treatments. Arachidonic acid levels slightly increased after nerve ligation in WT mice on the ipsilateral side of the spinal cord and significantly increased on the contralateral side [p = 0.0155]. Consequently, I detected a small *treatment* effect for AA in WT mice [$F_{1,4}$ = 10.88 p = 0.0300].

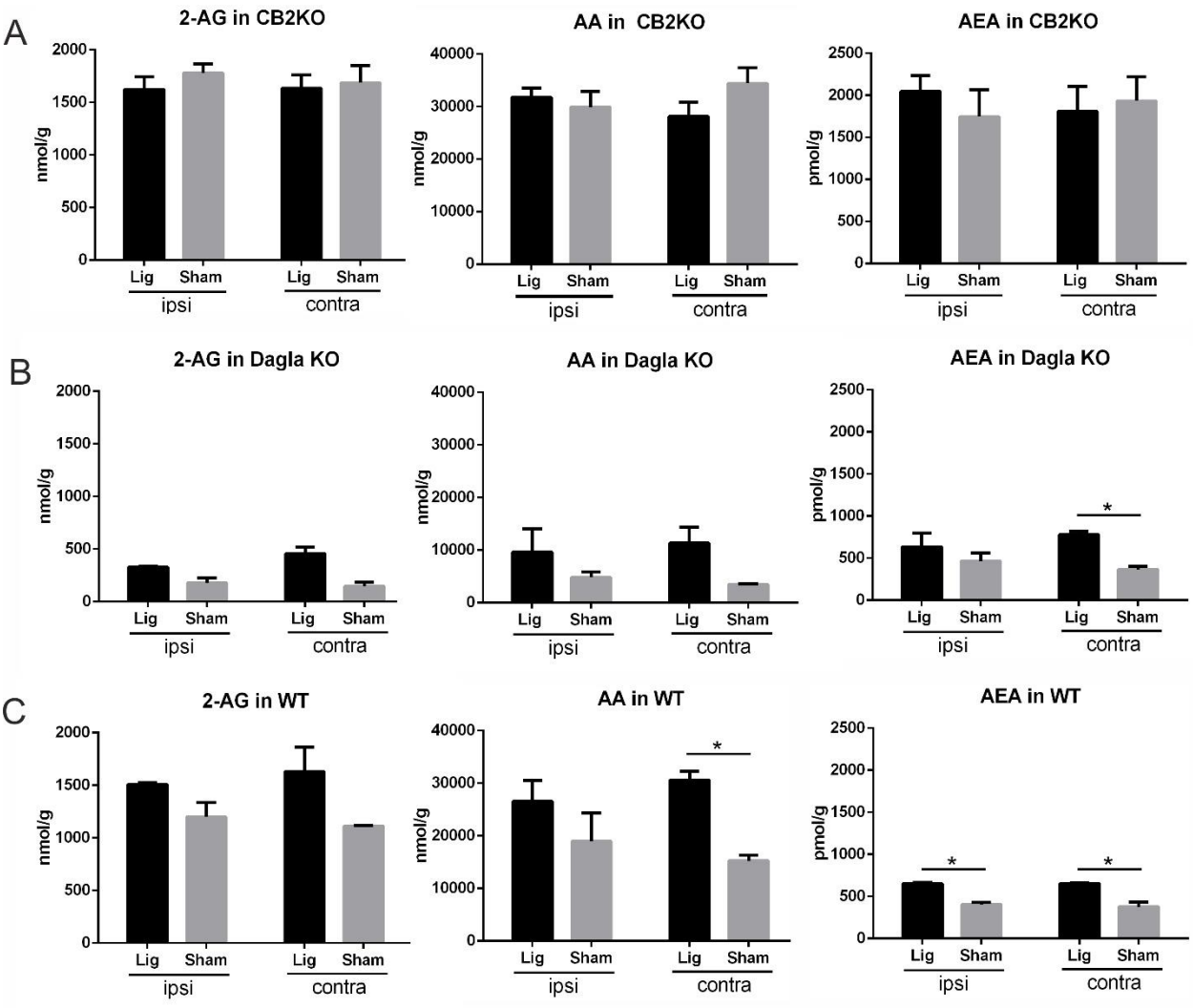

Figure 181 Endocannabinoid levels measured in the ipsi- and contralateral spinal cord of CB2KO, Daglα KO and WT mice 14 days after nerve ligation or sham surgery. Anandamide, 2-AG and arachidonic acid levels were measured with mass spectrometry and compared between treatments and sides of the spinal cord. In general, nerve ligation induced increased levels of all endocannabinoids in WT and Daglα KO mice but failed to induce a difference in CB2KO animals. Overall, levels were reduced in Daglα KO mice. Statistical significance was measured with multiple t-tests using the Holm-Sidak method and a two-way ANOVA. * $p < 0.05$, Data is expressed in mean +/- SEM. n = 2

The endocannabinoid anandamide did not change in CB2KO mice after nerve ligation, but overall levels of anandamide were higher than in WT or Daglα KO animals. Daglα KO and WT mice both showed significant differences of anandamide levels between treatments [*treatment* effect in Daglα KO $F_{1,4} = 8.706$ $p = 0.0419$; WT $F_{1,4} = 62.91$ $p = 0.0014$]. Daglα KO mice revealed significant increases in anandamide on the contralateral side [$p = 0.0172$]. In WT mice, both sides showed a significant increase of anandamide levels after nerve ligation [ipsi $p = 0.0158$; contra $p = 0.0414$].

Overall, endocannabinoid levels of CB2KO mice were not changed. Daglα KO mice showed reduced levels of all three measured endocannabinoids, whereas levels of WT mice always increased after nerve ligation. Endocannabinoid levels could not be analyzed statistically between each genotype, since the measurements of endocannabinoids were performed in different experiments.

4.4.2 Behavioral analysis of Daglα KO mice in pain

To analyze inflammatory pain in Daglα KO mice, I performed the formalin test (Figure 22). Pain responses such as licking or shaking were counted in Daglα KO and Daglα FL mice after formalin injection.

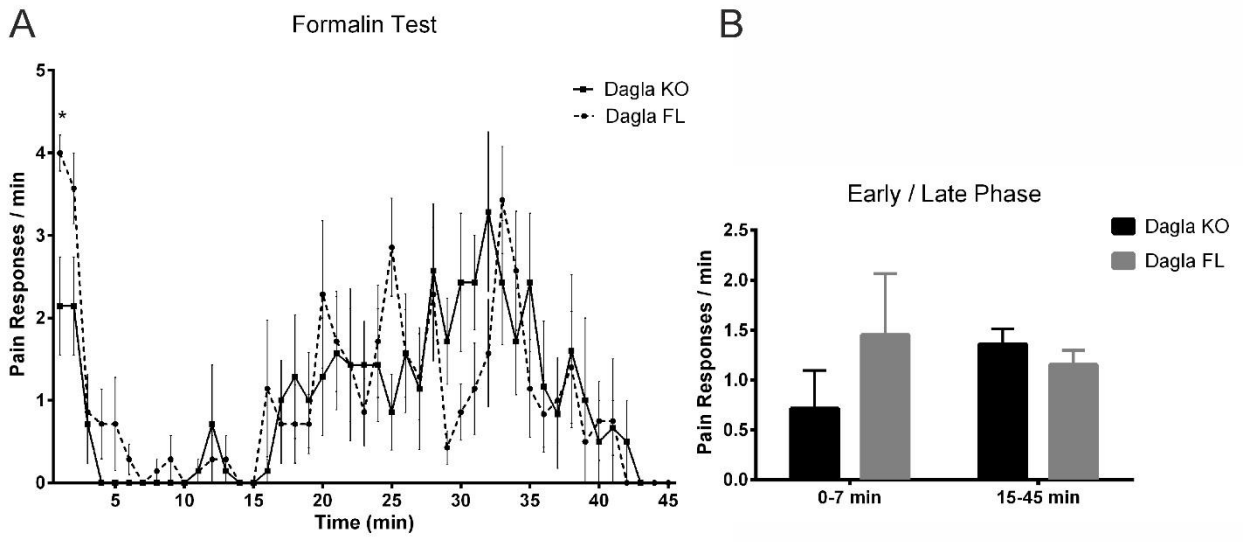

Figure 192 Inflammatory pain in Daglα KO and Dala FL mice. A) Pain responses were recorded and averaged for every minute over a total of 45 minutes. Except for the first minute, no statistical difference was observed between both genotypes. B) Differentiation into early and late phase did not reveal any statistical differences between Dagla KO and FL mice. n = 7 Statistical significance was calculated using 2-way ANOVA and multiple t tests. * $p < 0.05$

Overall, I could not detect any differences between both genotypes but only found a strong *time* effect [*time* $F_{34,420} = 6.158$ $p < 0.0001$ genotype $F_{1,420} = 0.3375$ $p = 0.5616$]. Even after separating the two inflammatory phases into early (0-7 min) and late (15-45 min) phase, no statistical significant difference was found between Daglα KO and Daglα FL mice.

Thermal nociception was studied with a hot plate test in Daglα KO and Daglα FL animals (Figure 23). Mice were placed on a hot surface and nociceptive responses such as shacking, licking or jumping were measured. Latency until the first reaction did not differ significantly between genotypes [$p = 0.3495$], whereas Daglα KO mice had a slightly reduced latency. When comparing between the different reactions, I detected a significant

difference in the licking reaction between both genotypes [p = 0.0231]. Daglα KO mice seemed to response in a different way to thermal pain as Daglα FL mice.

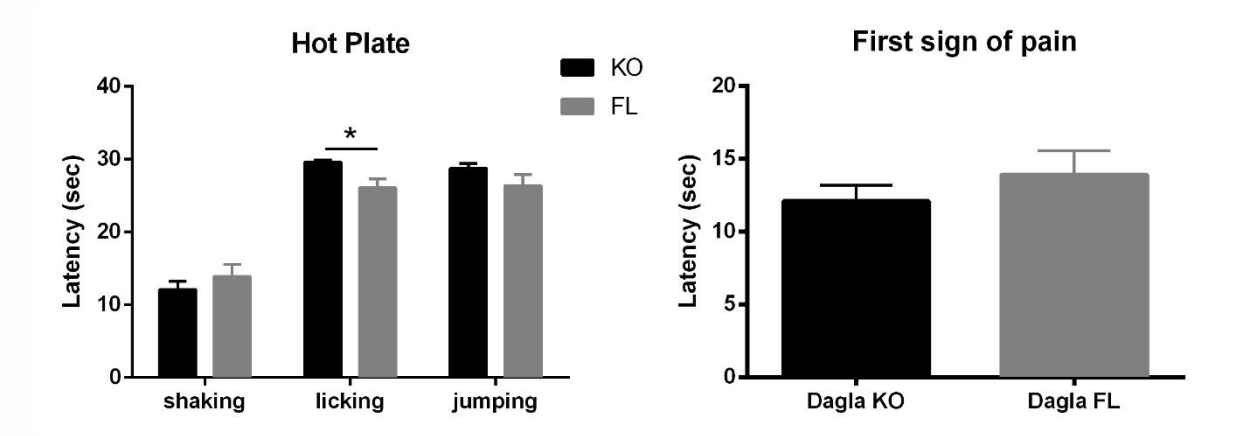

Figure 23 Thermal nociception in Daglα KO and Daglα FL mice. Latency in seconds was measured on a 52°C hot surface for 30 seconds or until a jumping reaction. Daglα KO mice showed a slight increased preference for licking behavior as a nociceptive response but overall did not differ significantly to Daglα FL mice in the latency for the first sign of pain. Data is expressed as mean +/- SEM. Statistical significance was analyzed with multiple t-tests using the Holm-Sidak method or an unpaired t-test for first sign of pain. * $p < 0.05$; n = 13 (WT), n = 18 (KO)

Since I could not determine a strong genotype effect in the hot plate test, I analyzed the thermal nociceptive threshold via a plantar test (Hargreaves method) (Figure 24). This method allows mice to react to increasing thermal stimuli on the hind paw and is more sensitive.

In contrast to the results of the hot plate test, Daglα KO mice seemed to react slower than Daglα FL mice. Their withdrawal latency was slightly increased, but this difference was not statistical significant when analyzed with an unpaired t-test [p = 0.0833].

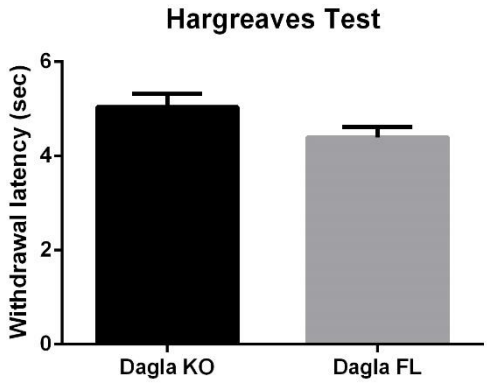

Figure 204 Hargreaves test for thermal nociception in Daglα KO and FL mice. Latency in seconds was measured until first nociceptive behavior. There was no statistical significant difference between both genotypes. Statistical

analysis was calculated with an unpaired t-test. Data is expressed as mean +/- SEM n = 28 (Daglα FL) n = 32 (Daglα KO).

Finally, mechanical allodynia was assessed with an aesthesiometer in Daglα KO and Daglα FL animals after PSNL (Figure 25). I measured the applied force of an automated filament, which elevated with increasing strength against the hind paw of the animal. Basal values before the surgery were set as 100%. The ipsilateral hind paw of ligated animals, both Daglα KO and FL, reacted already to low levels of applied force. Consequently, I detected a significant *treatment* effect for the ipsilateral side [Daglα KO $F_{1,92}$ = 29.70 p < 0.0001; Daglα FL $F_{1,92}$ = 21.20 p < 0.0001]. The increased mechanical allodynia after PSNL was observed for the whole period of 14 days. Therefore, both genotypes showed a significant *time* effect when measured with a two-way ANOVA [Daglα KO $F_{3,92}$ = 5.323 p = 0.002; Daglα FL $F_{3,92}$ = 7.627 p = 0.0001]. Neither Daglα FL nor Daglα KO mice showed any contralateral mechanical allodynia [*treatment* effect: Daglα FL $F_{1,92}$ = 0.4804 p = 0.4900; Daglα KO $F_{1,92}$ = 2.979 p = 0.0877]. Additionally, sham treated mice did not show any signs of neuropathic pain after nerve ligation.

Overall, Daglα KO mice did not react different than control Daglα FL mice and showed no abnormal pain phenotype.

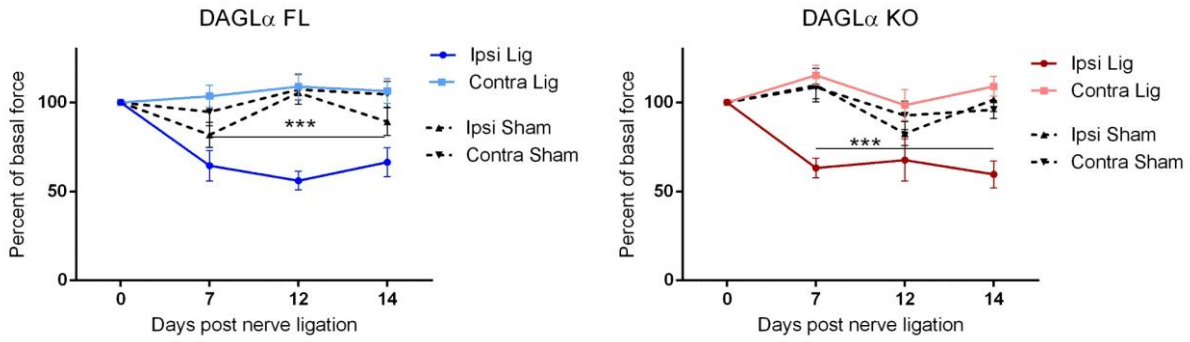

Figure 25 Mechanical allodynia in Daglα KO and Daglα FL mice assessed with an aesthesiometer basal and during 14 days post PSNL in ipsi- and contralateral hind paws. Ligated animals showed increased ipsilateral allodynia compared to sham treated mice. No statistical significant difference between genotypes, nor an increased mechanical allodynia on the contralateral side was detected. n=7-15 Statistical significance was determined with a two-way ANOVA and Bonferroni post-hoc test. Stars represent differences between ligated ipsilateral and ligated contralateral paws. *p<0.05, ** p<0.01, ***p<0.001 Error bars show SEM.

5 Discussion

In this study, different transgenic CB2 receptor mouse lines were used to address the role of CB2 in neuroinflammation and neuropathic pain induced by PSNL. The localization of

the CB2 receptor on microglia and macrophages was confirmed in colocalization studies of CB2-GFP mouse tissue with Iba1 or NeuN antibodies. Moreover, it was shown that the development of contralateral pain is not limited to constitutive CB2KO animals but appears in a similar manner in myeloid-specific CB2-LysM mice. Additionally, these contralateral effects were absent in neuron-specific CB2-Syn animals. According to this, CB2KO and CB2-LysM mice exhibited the same phenotype in mechanical allodynia of their hind paws and in microgliosis of the lumbar spinal cord, indicating a stronger inflammation on the ipsilateral side and a weak but consistent contralateral inflammation. On top of this, CB2-LysM animals showed the same increase in leptin receptor signal in the sciatic nerve as seen before in CB2KO mice. In the second part, the influence of DAGLα, the main synthesizing enzyme for 2-AG, was investigated on thermal, mechanical and inflammatory pain.

5.1 CB2-GFP expression in microglia and neurons

Using the CB2-GFP mouse strain that was recently generated (Schmöle et al. 2015), is an elaborate way to visualize CB2 receptor expression. As known since some years ago, the CB2 receptor is detected on peripheral immune cells, with the highest expression in B cells and natural killer cells, to a lesser extent in monocytes and neutrophils and with the lowest expression found in T lymphocytes (Fernández-Ruiz et al. 2007, Galiègue et al. 1995). Analysis of GFP expression revealed a generally low level in nervous tissue but showed an increase of GFP signal after PSNL, with the highest levels found in the ipsilateral ligated sciatic nerve. An increase of GFP signal after nerve ligation was expected, as several studies already showed an inflammation dependent upregulation of the CB2 receptor in the spinal cord after chronic pain (Zhang et al. 2003) and after brachial plexus avulsion (Paszcuk et al. 2011). Through colocalization studies with Iba1 and NeuN antibodies, I could detect CB2 receptor expression in nervous tissue on microglia and macrophages but not on neuronal cells. Expression of the CB2 receptor on microglia was proposed before, through ISH in the spinal cord (Zhang et al. 2003) or through analysis of CB2 expression in microglia and macrophage cell culture. In the latter study, CB2 mRNA and protein was detected in activated monocytes (Carlisle et al. 2002). CB2 mRNA was also found in DRG and spinal cord tissue, as well as in microglia cells cultured from the spinal cord (Beltramo et al. 2006). A study by Wotherspoon suggested

CB2 protein expression on sensory neurons in the proximal side of the sciatic nerve (Wotherspoon et al. 2005), but since the efficiency of CB2 antibodies is highly debatable (Ashton 2011, Marchalant et al. 2014), these results have to be interpreted with caution. In contrast to previous studies, analysis of CB2-GFP animals successfully confirmed Iba1-colocalized GFP signal in the DRG, spinal cord and sciatic nerves through immunohistochemistry. Additional to GFP-Iba1 positive cells, a GFP signal was detected in cells, which were negative for Iba1 and NeuN. These other GFP positive cells can be T lymphocytes, as they are known to infiltrate the inflamed tissue, too and CB2 expression was confirmed on T cells before (Schatz et al. 1997). Other possible CB2 – expressing cell types would include Schwann cells, where CB2 expression was not confirmed yet. Neutrophils are as well known to express the CB2 receptor but are vanished 8 days after nerve injury (Perkins & Tracey 2000).

By utilizing the CB2-GFP mouse strain, CB2 expression was specifically located to microglia and macrophages in DRG, spinal cord and sciatic nerve tissue after induction of neuropathic pain. In contrast, no colocalization of CB2 was found with the neuronal marker NeuN. Moreover, an upregulation of the CB2 receptor after nerve injury was confirmed, which was most profound in the ipsilateral sciatic nerve.

5.2 Mechanical allodynia in constitutional or conditional CB2KO mice

In accordance to the immunohistological findings, a distinguishable phenotype after nerve ligation was detected in myeloid-specific CB2-LysM mice that was similar to the previously reported phenotype of CB2KO animals (Racz et al. 2008a).

CB2-LysM animals have a cell-sepcific deletion of the *Cnr2* gene in monocytes, mature macrophages, microglia and granulocytes. Even though it was shown that the promoter is only active in ~40% of all microglia (Goldmann et al. 2013), I could still detect a distinct phenotype. This indicates a strong response of the CB2 deletion, as already a 40% loss of CB2 induces increased mechanical allodynia. It should be noted, that the LysM Cre is also active in neutrophils. Whether CB2 is expressed on neutrophils, is still under debate. Some studies did not find any CB2 protein expression in neutrophils (Deusch et al. 2003), but others did detect CB2 cell surface expression in human samples by flow cytometry (Kurihara et al. 2006). Further analysis of CB2 on neutrophils is still needed.

As I expected the CB2 expression on microglia and macrophages to be more relevant in the development of neuropathic pain, I concentrated on the aspect of microglial (and macrophage) CB2 deletion.

After induction of neuropathic pain, both CB2KO and CB2-LysM mice developed significant mechanical allodynia on the contralateral side and showed increased ipsilateral pain compared to WT mice as well. A detectable increase in pain hypersensitivity on the ipsilateral side of WT mice after partial sciatic nerve ligation was described earlier by Malmberg and Basbaum (Malmberg & Basbaum 1998), but an increased sensitivity on the contralateral hind paw was first detected in 2008 in CB2KO mice (Racz et al. 2008a). In this study, I could confirm the contralateral allodynia in CB2KO mice and even detect a slightly increased ipsilateral pain as well. Moreover, CB2-LysM mice developed the same phenotype as seen in CB2KO animals. Additionally, behavioral results obtained by the neuronal-specific CB2-Syn mice confirm the hypothesis that CB2 expression on neurons has no relevance for the development of contralateral pain.

5.3 Microglia expression in the dorsal spinal cord

Before, I could demonstrate that CB2-LysM mice developed a similar neuropathic pain reaction as seen in CB2KO animals. Meanwhile, CB2-Syn mice showed no distinct pain phenotype, comparable to the WT controls. To address the phenotype of both conditional CB2 mouse lines further, I analyzed microgliosis in the lumbar dorsal horn after nerve lgation. Since previous studies showed an increase in microgliosis of CB2KO animals on the contralateral side (Racz et al. 2008a), I hypothesized to see the same appearance of contralateral microgliosis in CB2-LysM animals, too. When analyzing the ipsi- and contralateral dorsal horns 14 days after nerve ligation, Iba1 signal was increased on the ipsilateral side of all measured genotypes (WT, CB2KO, CB2-LysM and CB2-Syn) and additionally increased on the contralateral side of CB2KO and CB2-LysM mice. It was shown before that microglia signal is increased in the ipsilateral dorsal horn after neuropathic pain, since this cell type is essential for the induction and persistence of chronic pain (Zhang et al. 2003). After peripheral nerve damage, signal molecules that activate microglia are released from injured neurons in the spinal cord. This results in a shift of the inflammation from peripheral to central sites and the development of a chronic

disease (Scholz & Woolf 2007). The contralateral increase in microglial signal confirms the development of contralateral neuroinflammation in CB2KO and CB2-LysM mice, as it was detected before by an increased mechanical allodynia on the contralateral side.

The phenomenon of contralateral or mirror-image pain, which was detected in CB2KO and CB2-LysM mice, has already been described in humans and rodents in several publications (Huang & Yu 2010, Koltzenburg et al. 1999). Even though the molecular mechanism are still unclear, studies suggested a role of microglia in the development of mirror-image pain (Milligan et al. 2003, Schreiber et al. 2008). It is important to note that all studies on mirror-image pain so far were conducted on wild-type mice or rats, which were missing any transgenic modification. This proves the fact that contralateral pain is generally able to develop independently from any modification of the CB2 receptor. It also should be noted that mirror-image pain was never observed in WT animals who developed neuropathic pain through a partial sciatic nerve ligation but rather after spinal nerve ligation, chronic construction injury or unilateral construction of the infraorbital nerve (ARGUIS et al. 2008, Chichorro et al. 2006, Paulson et al. 2000). It is highly plausible that these pain models induce a stronger inflammation than the partial sciatic nerve ligation, which then causes the mirror-image pain even in WT animals. A possible explanation for the observed contralateral pain in CB2KO and CB2-LysM mice might be an increased inflammation to the nerve ligation as a consequence of a missing anti-inflammatory CB2 response. Our results suggest that the absent suppression of inflammation by CB2 enhances the inflammation and consequently induces contralateral pain. Moreover, I suspect an important role for microglia in this process, since contralateral pain was observed in the microglia-specific KO mice (CB2-LysM) as well.

The anti-inflammatory effects of CB2 receptor activation were already described before. In 1996, Coffey observed a reduced production of proinflammatory nitric oxide (NO) by macrophages, after stimulation with THC (Coffey et al. 1996). A similar reduction of NO release by microglia and an increased expression of M2 markers was observed in response to anandamide treatment (Malek et al. 2015). Furthermore, selective CB2 activation reduced extracellular signal-regulated kinase, tumor necrosis factor alpha (TNF-α) expression, and microglial migration (Romero-Sandoval et al. 2009). Since CB2 receptor activation acts anti-inflammatory on macrophages and microglia, an increase of inflammation in mice lacking CB2 was suspected. Indeed, several studies demonstrated an increased inflammation in CB2KO mice, comprising an increase of TNF-α, inducible

nitric oxide synthase (iNOS), and intercellular adhesion molecule 1 mRNA. Additionally, CB2KO mice showed an increased permeability of the blood-brain barrier after traumatic brain injury (Amenta et al. 2014). After myocardial ischemia-reperfusion injury, CB2KO animals developed a stronger inflammation and an increased infiltration of macrophages (Duerr et al. 2015). In a study of trinitrobenzene sulfonic acid (TNBS) – induced colitis, CB2KO animals produced a stronger colitis reaction and an increased secretion of TNF-α and interleukin-β (Engel et al. 2010). Overall, clear evidence supports the hypothesis that the induction of contralateral pain is promoted by the lack of the anti-inflammatory CB2 receptor.

5.4 Analysis of immune cells in the sciatic nerve

To compare immune cells in inflamed sciatic nerve tissue between WT and CB2KO animals, nerve samples were isolated and immune cells were measured by flow cytometry. I suspected to see a large difference in cell amount and types three days after nerve ligation, as the first symptoms of neuropathic pain were already measured after three days. Since the CB2 receptor is important for immune cell activation and migration (Turcotte et al. 2016), a lack of CB2 should interfere with the profile of measured cells in the inflamed sciatic nerve. The percentage of $CD45^+$ cells showed a strong increase on the ipsilateral side after nerve ligation but were on equally high levels in both genotypes. In general, an increase of $CD45^+$ cells, like monocytes or neutrophils, at the site of inflammation was shown before (Nadeau et al. 2011). Surprisingly, ipsilateral samples of sham treated mice also contained around 20% of $CD45^+$ cells, which might be a result of the surgical procedure itself. A small increase was as well observed in contralateral samples of WT mice after ligation, which was significantly higher than in CB2KO animals.

Cells were further analyzed for “M1 and M2“ monocytes and neutrophils. The clear definition of M1 or M2 macrophages rather reflects the case *in vitro* but cannot be applied to the real situation *in vivo*. Research in the past years has discovered many more activation states in between the M1 and M2 states (M2a, M2b,..), whereas cells with a M1-like state express more proinflammatory genes and M2-like cells induce rather anti-inflammatory responses (Martinez & Gordon 2014). Recent publications suggest a new nomenclature that reflects the spectrum of different activation states more efficiently. In this nomenclature, macrophages should be named according to their stimulation factors

(in case of *in vitro* experiments) or characterized markers (for *ex vivo* samples)(Murray et al. 2014). For convenience, the analyzed cells in the following paragraph will be still called M1-like or M2-like but at the same time referring to the markers, which characterized these cell populations.

A distinguishable difference of all measured cells was detected between both genotypes. Independent of the treatment, ipsilateral samples contained increased amounts of $CD11b^{+}$ and $Ly\text{-}6B^{low}$ (M2-like) cells compared to their respective contralateral samples In CB2KO animals, no differences between ligated and sham treatment were measured. In contrast, an increase of M2-like cells was measured after nerve ligation in WT mice. Infiltration of M2-like as well as M1-like macrophages to a peripheral nerve after nerve injury was published before by Komori and colleagues (Komori et al. 2011). Surprisingly, an increased amount of M2-like cells was measured as well on the contralateral side of ligated WT samples. These levels were above the basal amount of resident M2-like cells, which was around 10% of all measured cells. On the contrary, the amount of M2-like cells in contralateral ligated samples of CB2KO mice remained on basal levels. A possible explanation for the elevated M2-like cell levels in WT mice may be a CB2 receptor promoted shift from M1-like to M2-like, which would be lacking in CB2 deficient mice. A CB2-dependent shift from M1 to M2 was already observed in liver macrophages after stimulating with the CB2 agonist JWH-133 (Tomar et al. 2015). In another study, a favor of the M2 state in microglia culture after addition of endocannabinoids and on the contrary a lack of M2 markers in microglia of CB2KO mice supports a CB2-dependent shift to the M2 state (Mecha et al. 2015).

In contrast to this hypothesis are the relatively high levels of M2-like cells in ligated ipsilateral samples of CB2KO mice, which would be expected to be reduced as well. Additionally, I would expect more M1-like cells in CB2KO mice, which would reflect in increased cell percentages of $CD11b^{+}$ and $Ly\text{-}6B^{high}$ cells, but this increase was not detected. The levels of $CD11b^{+}$ and $Ly\text{-}6B^{high}$ cells were generally lower in CB2KO mice compared to WT animals. On the contralateral side, WT mice showed even an increase of $CD11b^{+}$ and $Ly\text{-}6B^{high}$ cells after nerve ligation. In general, this cell population includes M1-like macrophages and neutrophils. Neutrophils are known to be one of the first type of infiltrating immune cells after peripheral nerve injury (Perkins & Tracey 2000). After release of cytokines, like CCL2 or macrophage inflammatory protein-1α from neutrophils and damaged neurons, infiltration of macrophages into the inflamed tissue follows

(Scholz & Woolf 2007). Therefore, this augmentation was surprising, since no sign of contralateral hypersensitivity was measured in WT animals. After characterizing for the marker Ly-6G, which differentiates between M1-like macrophages and neutrophils, no statistical difference between WT and CB2KO animals was detected in any ligated, ipsilateral samples. Contralateral sciatic nerve tissue contained not enough cells to further differentiate between these two cell types and was neglected.

Immune cells were also investigated 8 days after nerve ligation but contained less cells than on day 3. $CD45^+$ cells were as well increased in ipsilateral ligated samples but showed much lower amounts than on day 3. Because of the overall reduced cell numbers, further analysis was only possible for ligated ipsilateral samples. In general, cell percentages of monocytes and neutrophils were lower than on day 3 and did not show any statistical difference between both genotypes. It is highly possible that the amount of immune cells decreases already from day 3 to day 8 after nerve injury, since infiltrating immune cell start to phagocyte cell debris and resolve the inflammation for further regeneration of the nerve (Gaudet et al. 2011). Nevertheless, chronic neuropathic pain endures even after resolution of the inflammatory environment at the sciatic nerve, since inflammation spreads to central sites, and thereby promoting a general hypersensitivity. The lack of a genotype difference in immune cell infiltration between WT and CB2KO mice on day 3 and day 8 in the sciatic nerve is an indicator for a different mechanism, which is leading to an increased inflammation in CB2KO mice. Possibly, inflammation is only stronger on central rather than peripheral sites in CB2KO mice, which is reflected in the increased Iba1 signal that was measured in the spinal cord of C2KO mice.

5.5 Leptin receptor expression in sciatic nerves

Just recently, a contribution of leptin and leptin receptor in the development of neuropathic pain was discovered in CB2KO animals. After nerve ligation, protein expression of the leptin receptor drastically increased on the ipsilateral sciatic nerve of CB2KO mice but not in WT control nerves (unpublished results). A link between leptin and neuropathic pain was already shown before (Maeda et al. 2009). In this study, neuropathic pain development was promoted by leptin-stimulated macrophages that were shown to express the leptin receptor as well. Furthermore, administration and stimulation of peritoneal macrophages with leptin could restore the loss of allodynia in

leptin deficient *ob/ob* mice (Maeda et al. 2009). In a different study, leptin induced neuroprotective effects in a model of traumatic brain injury that in turn were attenuated after administration of the CB2 antagonist AM630 (Lopez-Rodriguez et al. 2016). Our study suggests, that an increased expression of the leptin receptor is somehow related to an increased inflammation in CB2KO mice. This increase in expression is normally missing under physiological conditions or in WT mice. The measured upregulation of the leptin receptor in CB2-LysM mice similar to CB2KO mice supports the hypothesis of a CB2-dependent mechanism in microglia and macrophages, which increases inflammation in neuropathic pain.

5.6 Daglα in neuroinflammation and pain

In section 4, I could show that the endocannabinoid system has an important impact in the regulation of neuropathic pain. Therefore, the effect of nerve ligation on the endocannabinoid levels in the spinal cord was analyzed. Surprisingly, no significant differences in endocannbinoid levels were detected between ligated and sham CB2KO mice. In contrast to this, levels of all measured endocannabinoids were increased in ligated WT animals, compared to sham treated WT mice. An increase in the spinal cord of anandamide after chronic construction injury (Starowicz et al. 2013) or of 2-AG after nerve ligation in rats (Petrosino et al. 2007) was shown before. Increased endocannabinoid levels in chronic pain models were as well measured in the affected hind paw (Jhaveri et al. 2007) or the dorsal root ganglion (Mitrirattanakul et al. 2006). The dual roles of anandamide and 2-AG in inflammation were shown in several studies. Whereas 2-AG was proven to induce proinflammatory effects, like microglial migration (Walter et al. 2003) or T cell adhesion (Gasperi et al. 2014), AEA increased production of the anti-inflammatory cytokine IL-10 (Correa et al. 2010) or mitogen-activated protein kinase phosphatase- 1 in microglia (Eljaschewitsch et al. 2006). Contradictory to this, anandamide levels were much lower in WT than in CB2KO mice, even though WT animals showed less mechanical allodynia and microgliosis than CB2KO mice. Since the endocannabinoid levels were never measured in neuropathic CB2KO mice before, no literature exists yet to explain this observation. It is possible that endocannabinoid levels are dysregulated in CB2KO mice, resulting in generally elevated levels compared to WT

animals. Potentially, the active CB2 receptor in WT mice contributes to the regulation of the endocannabinoid levels in neuropathic pain conditions.

One of the main ligands for the CB2 receptor is 2-AG, which is synthesized by the enzyme Daglα (Sugiura et al. 2002). Therefore, Daglα KO mice were as well investigated for their endocannabinoid levels and later on for their pain phenotype. As already published, 2-AG levels were strongly decreased in Daglα KO mice. Arachidonic acid, the breakdown product of 2-AG was as well decreased, when compared to levels of WT mice. A reduction of 2-AG and AEA in the brain of Daglα KO mice was published earlier (Jenniches et al. 2016). It is therefore not surprising, that the similar reductions were detected in the spinal cord, too. An interesting result is the small increase of all measured endocannabinoids on both sides of Daglα KO mice after nerve ligation. The same elevations on both sides after induction of neuropathic pain were measured in WT mice as well, even though not all differences were statistically significant. This finding could imply a regulatory function of endocannabinoids, which even appear on the contralateral side. Possibly, regulatory changes do appear on the non-injured side after nerve ligation but do not develop into an inflammation.

Since the observed dysregulation of endocannabinoid levels in CB2KO mice was not seen in Daglα KO mice, the mechanism behind this observation is likely to be located downstream of the CB2 receptor and thereby unaffected by the 2-AG reduction in Daglα KO animals. The enzyme Daglα was therefore neither expected to be relevant in pain processing nor would deletion of Daglα induce contralateral pain as observed in CB2KO mice. To prove this hypothesis, Daglα KO mice were analyzed through different behavioral pain tests, regarding physiological and pathological pain processing.

Naïve Daglα KO and FL mice were analyzed in a formalin test to observe their reaction to inflammatory pain. Inflammation of the nerve is an essential process in the development of neuropathic pain. Since the CB2 receptor is highly involved in inflammatory processes and showed a clear phenotype in the formalin test before (Klauke et al. 2014), the behavior of Daglα KO mice was of interest, too. Even though Daglα KO mice showed less pain responses than control FL mice in the first minute, the overall reaction was not statistical different between both genotypes. Since mice treated with a CB2 agonist showed a reduced reaction in the formalin test (Beltramo et al. 2006), an increased reaction to inflammatory pain in Daglα KO mice would have been expected. The

observed result supports the hypothesis, that a 2-AG independent mechanism is regulating pathological pain processing in CB2KO animals.

When analyzing Daglα KO mice for thermal pain processing in the hot plate test, no statistical difference between both genotypes was measured. The only difference observed was an increased licking reaction in Daglα KO mice, without affecting the overall pain reaction. The Hargreaves test was further used as a more sensitive approach to analyze thermal pain. Daglα KO mice appeared to have a slightly increased withdrawal latency, which would represent a reduced pain perception but overall did not show a significant different response to Daglα FL mice. Previous publications supported this finding, revealing no difference in thermal pain perception between Daglα KO mice and WT animals (Jenniches et al. 2016). In contrast to this, latency of mice stimulated with a CB2 receptor agonist increased significantly in the Hargreaves test, indicating less thermal pain in these animals (Ibrahim et al. 2005). It is highly possible, that thermal pain perception is 2-AG independent as well, which would explain the missing phenotype of Daglα KO mice.

Finally, I measured neuropathic pain development induced by PSNL in Daglα KO and FL mice, to test for the contralateral pain as seen before in CB2KO mice. Daglα KO mice did neither show an increased mechanical allodynia on the ipsilateral side nor on the contralateral side. It is worth mentioning that due to a change in the experimental setup, mechanical allodynia in Daglα KO mice was assessed with an automated aesthesiometer, instead of the manual von Frey filaments, used for CB2KO animals. Manual von Frey filaments are thought to be more sensitive in detecting small differences in mechanical allodynia, but the overall result is supposed to be equal to an automated aesthesiometer (Nirogi et al. 2012).

As a conclusion, Daglα KO mice did not develop any pain phenotype in thermal, inflammatory or induced neuropathic pain. This finding adds to the hypothesis of a 2-AG independent mechanism for CB2 regulation of pain processing. As mentioned earlier, the endocannabinoid anandamide is known to induce anti-inflammatory effects and was shown before to promote the M2 state of microglia by activating the microglial CB2 receptor (Malek et al. 2015). Therefore, an anandamide–dependent mechanism in CB2 pain processing is highly possible. Another possible explanation may derive from Daglβ, the second enzyme known to synthesize 2-AG. The reduced levels of 2-AG in Daglα KO

mice may have still been high enough to activate the CB2 receptor. To test this hypothesis, a dual inhibition of Daglα and Daglβ would be necessary.

6 Conclusion

In this study I could confirm the microglial expression of the CB2 receptor. Through behavioural experiments, I demonstrated a similar pain phenotype of the myeloid-specific CB2 deletion in CB2-LysM mice as seen in CB2KO mice. This observation was confirmed by an equal increase of microgliosis in the spinal cord of both mouse strains. Through immunohistological analysis of CB2-GFP mice, microglial expression of CB2 in the spinal cord, sciatic nerve and DRG was confirmed as well. Therefore, a role of the microglial CB2 receptor in neuropathic pain processing is strongly suggested.

Additional to the CB2 localization, a specific CB2 pain phenotype was revealed. CB2KO and CB2-LysM mice both showed increased ipsilateral and contralateral mechanical allodynia after PSNL. One hypothesis is that neuroinflammation is increased in CB2KO and CB2-LysM animals, which in turn would induce the observed contralateral pain. This phenomenon was not detected in WT or CB2-Syn mice and is therefore specific for CB2 on myeloid cells. To test the increased neuroinflammation in CB2KO and CB2-LysM mice, further analysis of immune cells in the sciatic nerves and spinal cord on day 14 are needed. Moreover, a conditional deletion of CB2 in cells expressing the CX_3CR1 promoter is useful, to exclude any interference of a CB2 deletion in neutrophils.

Interestingly, the leptin receptor was shown to be modulated after PSNL in CB2KO and CB2-LysM mice as well. I hypothesize that the CB2 receptor on myeloid cells interferes with leptin receptor expression. The exact mechanism and connection between the leptin receptor and the CB2 receptor still has to be revealed.

When I analyzed pain behavior in Daglα KO mice, which are lacking the main 2-AG producing enzyme, no pain phenotype was detected. This suggests that the modulation of CB2 in pain processing is 2-AG independent or at least Daglα independent. To further confirm this, Daglβ KO mice are needed to be analyzed after PSNL as well. Moreover, it would be interesting to see the contribution of the other main endocannabinoid, AEA. Therefore, mice with reduced AEA levels could be also investigated after PSNL. In conclusion, our results suggest that CB2 receptors on myeloid cells but not on neurons are essential for neuropathic pain development.

7 References

Agarwal N, Pacher P, Tegeder I, Amaya F, Constantin CE, et al. 2007. Cannabinoids mediate analgesia largely via peripheral type 1 cannabinoid receptors in nociceptors. *Nat. Neurosci.* 10(7):870–79

Amenta PS, Jallo JI, Tuma RF, Hooper DC, Elliott MB. 2014. Cannabinoid receptor type-2 stimulation, blockade, and deletion alter the vascular inflammatory responses to traumatic brain injury. *J. Neuroinflammation*. 11(1):191

Anand P, Whiteside G, Fowler CJ, Hohmann AG. 2009. Targeting CB2 receptors and the endocannabinoid system for the treatment of pain. *Brain Res. Rev.* 60(1):255–66

Anand U, Otto WR, Sanchez-Herrera D, Facer P, Yiangou Y, et al. 2008. Cannabinoid receptor CB2 localisation and agonist-mediated inhibition of capsaicin responses in human sensory neurons. *Pain*. 138(3):667–80

ARGUIS M, PEREZ J, MARTINEZ G, UBRE M, GOMAR C. 2008. Contralateral Neuropathic Pain Following a Surgical Model of Unilateral Nerve Injury in Rats. *Reg. Anesth. Pain Med.* 33(3):211–16

Ashton JC. 2011. Knockout controls and the specificity of cannabinoid CB $_2$ receptor antibodies. *Br. J. Pharmacol.* 163(6):1113–1113

Attal N, Cruccu G, Baron R, Haanpää M, Hansson P, et al. 2010. EFNS guidelines on the pharmacological treatment of neuropathic pain: 2010 revision. *Eur. J. Neurol.* 17(9):1113-e88

Attal N, Gaudé V, Brasseur L, Dupuy M, Guirimand F, et al. 2000. Intravenous lidocaine in central pain: a double-blind, placebo-controlled, psychophysical study. *Neurology*. 54(3):564–74

Atwood BK, Mackie K. 2010. CB2: a cannabinoid receptor with an identity crisis. *Br. J. Pharmacol.* 160(3):467–79

Basbaum AI, Bautista DM, Scherrer G, Julius D. 2009. Cellular and molecular mechanisms of pain. *Cell*. 139(2):267–84

Beltramo M, Bernardini N, Bertorelli R, Campanella M, Nicolussi E, et al. 2006. CB2 receptor-mediated antihyperalgesia: Possible direct involvement of neural mechanisms. *Eur. J. Neurosci.* 23(6):1530–38

Bifulco M, Pisanti S. 2015. Medicinal use of cannabis in Europe: The fact that more countries legalize the medicinal use of cannabis should not become an argument for

unfettered and uncontrolled use. *EMBO Rep.* 16(2):130–32

Boychuk DG, Goddard G, Mauro G, Orellana MF. 2015. The Effectiveness of Cannabinoids in the Management of Chronic Nonmalignant Neuropathic Pain: A Systematic Review. *J. Oral Facial Pain Headache*. 29(1):7–14

Buckley NE, Mccoy KL, Mezey É, Bonner T, Zimmer A, et al. 2000. Immunomodulation by cannabinoids is absent in mice deficient for the cannabinoid CB2 receptor. *Eur. J. Pharmacol.* 396(2–3):141–49

Calignano A, La Rana G, Giuffrida A, Piomelli D. 1998. Control of pain initiation by endogenous cannabinoids. *Nature*. 394(6690):277–81

Carlisle SJ, Marciano-Cabral F, Staab A, Ludwick C, Cabral GA. 2002. Differential expression of the CB2 cannabinoid receptor by rodent macrophages and macrophage-like cells in relation to cell activation. *Int. Immunopharmacol.* 2(1):69–82

Carrier EJ, Kearn CS, Barkmeier AJ, Breese NM, Yang W, et al. 2004. Cultured Rat Microglial Cells Synthesize the Endocannabinoid 2-Arachidonylglycerol, Which Increases Proliferation via a CB2 Receptor-Dependent Mechanism. *Mol. Pharmacol.* 65(4):999–1007

Caterina MJ, Schumacher M a, Tominaga M, Rosen T a, Levine JD, Julius D. 1997. The capsaicin receptor: a heat-activated ion channel in the pain pathway. *Nature*. 389(6653):816–24

Chaplan SR, Bach FW, Pogrel JW, Chung JM, Yaksh TL. 1994. Quantitative assessment of tactile allodynia in the rat paw. *J. Neurosci. Methods*. 53(1):55–63

Cheng C-F, Cheng J-K, Chen C-Y, Rau R-H, Chang Y-C, Tsaur M-L. 2015. *NGF-Induced Synapse-like Structures in Contralateral Sensory Ganglia Contribute to Chronic Mirror-Image Pain*

Chevaleyre V, Takahashi KA, Castillo PE. 2006. Endocannabinoid-mediated synaptic plasticity in the CNS. *Annu. Rev. Neurosci.* 29(1):37–76

Chichorro JG, Zampronio AR, Rae GA. 2006. Endothelin ET(B) receptor antagonist reduces mechanical allodynia in rats with trigeminal neuropathic pain. *Exp. Biol. Med. (Maywood).* 231(6):1136–40

Choi H, Roh D, Yoon S, Moon J, Choi S, Kwon S. 2015. Microglial interleukin-1 b in the ipsilateral dorsal horn inhibits the development of mirror-image contralateral mechanical allodynia through astrocyte activation in a rat model of inflammatory

pain. . 156:1046–59

Clark AK, Old E a, Malcangio M. 2013. Neuropathic pain and cytokines: current perspectives. *J. Pain Res.* 6:803–14

Clausen BE, Burkhardt C, Reith W, Renkawitz R, Förster I. 1999. Conditional gene targeting in macrophages and granulocytes using LysMcre mice. *Transgenic Res.* 8(4):265–77

Coffey RG, Yamamoto Y, Snella E, Pross S. 1996. Tetrahydrocannabinol inhibition of macrophage nitric oxide production. *Biochem. Pharmacol.* 52(5):743–51

Correa F, Hernangómez M, Mestre L, Loría F, Spagnolo A, et al. 2010. Anandamide enhances IL-10 production in activated microglia by targeting CB(2) receptors: roles of ERK1/2, JNK, and NF-kappaB. *Glia*. 58(2):135–47

De Petrocellis L, Bisogno T, Maccarrone M, Davis JB, Finazzi-Agro A, Di Marzo V. 2001. The activity of anandamide at vanilloid VR1 receptors requires facilitated transport across the cell membrane and is limited by intracellular metabolism. *J. Biol. Chem.* 276(16):12856–63

Deusch E, Kraft B, Nahlik G, Weigl L, Hohenegger M, Kress HG. 2003. No evidence for direct modulatory effects of delta 9-tetrahydrocannabinol on human polymorphonuclear leukocytes. *J. Neuroimmunol.* 141(1–2):99–103

Devane WA, Hanus L, Breuer A, Pertwee RG, Stevenson LA, et al. 1992. Isolation and structure of a brain constituent that binds to the cannabinoid receptor. *Science*. 258(5090):1946–49

Devane W a, Dysarz F a 3Rd, Johnson MR, Melvin LS, Howlett a C. 1988. Determination and characterization of a cannabinoid receptor in rat brain. *Mol. Pharmacol.* 34(5):605–13

Di Marzo V, Fontana A, Cadas H, Schinelli S, Cimino G, et al. 1994. Formation and inactivation of endogenous cannabinoid anandamide in central neurons. *Nature*. 372(6507):686–91

Di Marzo V, Goparaju SK, Wang L, Liu J, Bátkai S, et al. 2001. Leptin-regulated endocannabinoids are involved in maintaining food intake. *Nature*. 410(6830):822–25

Dinh TP, Carpenter D, Leslie FM, Freund TF, Katona I, et al. 2002. Brain monoglyceride lipase participating in endocannabinoid inactivation. *Proc. Natl. Acad. Sci. U. S. A.* 99(16):10819–24

Dixon WJ. 1965. The up-and-down method for small samples. *J. Am. Stat. Assoc.* 60(312):967–978

Dominguez E, Mauborgne A, Mallet J, Desclaux M, Pohl M. 2010. SOCS3-mediated blockade of JAK/STAT3 signaling pathway reveals its major contribution to spinal cord neuroinflammation and mechanical allodynia after peripheral nerve injury. *J. Neurosci.* 30(16):5754–66

Dubin AE, Patapoutian A. 2010. Nociceptors: The sensors of the pain pathway. *J. Clin. Invest.* 120(11):3760–72

Duerr GD, Heinemann JC, Gestrich C, Heuft T, Klaas T, et al. 2015. Impaired border zone formation and adverse remodeling after reperfused myocardial infarction in cannabinoid CB2 receptor deficient mice. *Life Sci.* 138:8–17

Eddy NB, Leimbach D. 1953. SYNTHETIC ANALGESICS. II. DITHIENYLBUTENYL- AND DITHIENYLBUTYLAMINES. *J. Pharmacol. Exp. Ther.* 107(3):

Eljaschewitsch E, Witting A, Mawrin C, Lee T, Schmidt PM, et al. 2006. The Endocannabinoid Anandamide Protects Neurons during CNS Inflammation by Induction of MKP-1 in Microglial Cells. *Neuron*. 49(1):67–79

Engel MA, Kellermann CA, Burnat G, Hahn EG, Rau T, Konturek PC. 2010. Mice lacking cannabinoid CB1-, CB2-receptors or both receptors show increased susceptibility to trinitrobenzene sulfonic acid (TNBS)-induced colitis. *J. Physiol. Pharmacol.* 61(1):89–97

Fernández-Ruiz J, Romero J, Velasco G, Tolón RM, Ramos JA, Guzmán M. 2007. Cannabinoid CB2 receptor: a new target for controlling neural cell survival? *Trends Pharmacol. Sci.* 28(1):39–45

Fine PG, Rosenfeld MJ. 2013. The endocannabinoid system, cannabinoids, and pain. *Rambam Maimonides Med. J.* 4(4):e0022

Galiègue S, Mary S, Marchand J, Dussossoy D, Carrière D, et al. 1995. Expression of central and peripheral cannabinoid receptors in human immune tissues and leukocyte subpopulations. *Eur. J. Biochem.* 232(1):54–61

Gammon CM, Allen AC, Morell P. 1989. Bradykinin Stimulates Phosphoinositide Hydrolysis and Mobilization of Arachidonic Acid in Dorsal Root Ganglion Neurons. *J. Neurochem.* 53(1):95–101

Gasperi V, Evangelista D, Chiurchiù V, Florenzano F, Savini I, et al. 2014. 2-Arachidonoylglycerol modulates human endothelial cell/leukocyte interactions by

controlling selectin expression through CB1 and CB2 receptors. *Int. J. Biochem. Cell Biol.* 51:79–88

Gaudet AD, Popovich PG, Ramer MS. 2011. Wallerian degeneration: gaining perspective on inflammatory events after peripheral nerve injury. *J. Neuroinflammation*. 8:110

Giordano C, Cristino L, Luongo L, Siniscalco D, Petrosino S, et al. 2012. TRPV1-dependent and -independent alterations in the limbic cortex of neuropathic mice: impact on glial caspases and pain perception. *Cereb. Cortex*. 22(11):2495–2518

Goldmann T, Wieghofer P, Müller PF, Wolf Y, Varol D, et al. 2013. A new type of microglia gene targeting shows TAK1 to be pivotal in CNS autoimmune inflammation. *Nat. Neurosci.* 16(11):1618–26

Guindon J, Hohmann AG. 2008. Cannabinoid CB2 receptors: a therapeutic target for the treatment of inflammatory and neuropathic pain. *Br. J. Pharmacol.* 153(2):319–34

Guo W, Wang H, Watanabe M, Shimizu K, Zou S, et al. 2007. Glial-cytokine-neuronal interactions underlying the mechanisms of persistent pain. *J. Neurosci.* 27(22):6006–18

Hanus L, Breuer A, Tchilibon S, Shiloah S, Goldenberg D, et al. 1999. HU-308: a specific agonist for CB(2), a peripheral cannabinoid receptor. *Proc. Natl. Acad. Sci. U. S. A.* 96(25):14228–33

Hargreaves K, Dubner R, Brown F, Flores C, Joris J. 1988. A new and sensitive method for measuring thermal nociception in cutaneous hyperalgesia. *Pain*. 32(1):77–88

Hashimotodani Y, Ohno-Shosaku T, Kano M. 2007. Endocannabinoids and synaptic function in the CNS. *Neuroscientist*. 13(2):127–37

Hoess RH, Abremski KEN. 1984. Interaction of the bacteriophage. *Biochemistry*. 81(February):1026–29

Howlett AC, Blume LC, Dalton GD. 2010. CB(1) cannabinoid receptors and their associated proteins. *Curr. Med. Chem.* 17(14):1382–93

Hsu K-L, Tsuboi K, Adibekian A, Pugh H, Masuda K, Cravatt BF. 2012. DAGLβ inhibition perturbs a lipid network involved in macrophage inflammatory responses. *Nat. Chem. Biol.* 8(12):999–1007

Huang D, Yu B. 2010. The mirror-image pain: An unclered phenomenon and its possible mechanism. *Neurosci. Biobehav. Rev.* 34(4):528–32

Ibrahim MM, Porreca F, Lai J, Albrecht PJ, Rice FL, et al. 2005. CB2 cannabinoid receptor activation produces antinociception by stimulating peripheral release of

endogenous opioids. *Proc. Natl. Acad. Sci. U. S. A.* 102(8):3093–98

Ikeda H, Ikegami M, Kai M, Ohsawa M, Kamei J. 2013. Activation of spinal cannabinoid cb2 receptors inhibits neuropathic pain in streptozotocin-induced diabetic mice. *Neuroscience*. 250:446–54

Iversen LL. 2007. *The Science of Marijuana*. Oxford University Press

Jancalek R. 2011. Signaling mechanisms in mirror image pain pathogenesis. *Ann. Neurosci.* 18(3):123–27

Jenniches I, Ternes S, Albayram O, Otte DM, Bach K, et al. 2016. Anxiety, Stress, and Fear Response in Mice with Reduced Endocannabinoid Levels. *Biol. Psychiatry*. 79(10):858–68

Jensen B, Chen J, Furnish T, Wallace M. 2015. Medical Marijuana and Chronic Pain: a Review of Basic Science and Clinical Evidence. *Curr. Pain Headache Rep.* 19(10):1–9

Jhaveri MD, Richardson D, Chapman V. 2007. Endocannabinoid metabolism and uptake: novel targets for neuropathic and inflammatory pain. *Br. J. Pharmacol.* 152(5):624–32

Kalant H. 2004. Adverse effects of cannabis on health: An update of the literature since 1996

Kandel ER, Schwartz JH, Jessell TM. 2000. *Principles of Neural Science*, Vol. 3. New York: McGraw-Hill, Health Professions Division. 4th ed.

Kendall DA, Yudowski GA. 2017. Cannabinoid Receptors in the Central Nervous System: Their Signaling and Roles in Disease. *Front. Cell. Neurosci.* 10:294

Kierdorf K, Prinz M. 2013. Factors regulating microglia activation. *Front. Cell. Neurosci.* 7(April):1–8

Kiguchi N, Maeda T, Kobayashi Y, Fukazawa Y, Kishioka S. 2010. Macrophage inflammatory protein-1?? mediates the development of neuropathic pain following peripheral nerve injury through interleukin-1?? up-regulation. *Pain*. 149(2):305–15

Klauke A-LL, Racz I, Pradier B, Markert a., Zimmer AM, et al. 2014. The cannabinoid CB2 receptor-selective phytocannabinoid beta-caryophyllene exerts analgesic effects in mouse models of inflammatory and neuropathic pain. *Eur. Neuropsychopharmacol.* 24(4):608–20

Kohnz RA, Nomura DK, Vann RE, Walentiny DM, Booker L, et al. 2014. Chemical approaches to therapeutically target the metabolism and signaling of the endocannabinoid 2-AG and eicosanoids. *Chem. Soc. Rev.* 43(19):6859–69

Koltzenburg M, Wall PD, McMahon SB. 1999. Does the right side know what the left is doing? *Trends Neurosci.* 22(3):122–27

Komori T, Morikawa Y, Inada T, Hisaoka T, Senba E. 2011. Site-specific subtypes of macrophages recruited after peripheral nerve injury. *Neuroreport*. 22(17):911–17

Koppel BS, Brust JCM, Fife T, Bronstein J, Youssof S, et al. 2014. Systematic review: Efficacy and safety of medical marijuana in selected neurologic disorders: Report of the Guideline Development Subcommittee of the American Academy of Neurology. *Neurology*. 82(17):1556–63

Kurihara R, Tohyama Y, Matsusaka S, Naruse H, Kinoshita E, et al. 2006. Effects of Peripheral Cannabinoid Receptor Ligands on Motility and Polarization in Neutrophil-like HL60 Cells and Human Neutrophils. *J. Biol. Chem.* 281(18):12908–18

La Cava A, Matarese G. 2004. The weight of leptin in immunity. *Nat Rev Immunol*. 4(5):371–79

Lallemand Y, Luria V, Haffner-Krausz R, Lonai P. 1998. Maternally expressed PGK-Cre transgene as a tool for early and uniform activation of the Cre site-specific recombinase. *Transgenic Res.* 7(2):105–12

Landry RP, Martinez E, DeLeo JA, Romero-Sandoval EA. 2012. Spinal cannabinoid receptor type 2 agonist reduces mechanical allodynia and induces mitogen-activated protein kinase phosphatases in a rat model of neuropathic pain. *J. Pain*. 13(9):836–48

Lomazzo E, Bindila L, Remmers F, Lerner R, Schwitter C, et al. 2015. Therapeutic potential of inhibitors of endocannabinoid degradation for the treatment of stress-related hyperalgesia in an animal model of chronic pain. *Neuropsychopharmacology*. 40(2):488–501

Lopez-Rodriguez AB, Mela V, Acaz-Fonseca E, Garcia-segura LM, Viveros M. 2016. CB2 cannabinoid receptor is involved in the anti-in fl ammatory effects of leptin in a model of traumatic brain injury. *Exp. Neurol.* 279:274–82

Lynch ME, Campbell F. 2011. Cannabinoids for treatment of chronic non-cancer pain; a systematic review of randomized trials. *Br. J. Clin. Pharmacol.* 72(5):735–44

Maccarrone M, Bab I, Bíró T, Cabral GA, Dey SK. 2014. Community review on Endocannabinoid signaling at the periphery : 50 years after THC. . (October):

Maeda T, Kiguchi N, Kobayashi Y, Ikuta T, Ozaki M, Kishioka S. 2009. Leptin derived from

adipocytes in injured peripheral nerves facilitates development of neuropathic pain via macrophage stimulation. *Proc. Natl. Acad. Sci. U. S. A.* 106(31):13076–81

Maldonado R, Baños JE, Cabañero D, Caban D, Maldonado R, Ban JE. 2016. The endocannabinoid system and neuropathic pain. . 157(2):

Malek N, Popiolek-Barczyk K, Mika J, Przewlocka B, Starowicz K. 2015. Anandamide, Acting via CB2 Receptors, Alleviates LPS-Induced Neuroinflammation in Rat Primary Microglial Cultures. *Neural Plast.* 2015:130639

Malmberg a B, Basbaum AI. 1998. Partial sciatic nerve injury in the mouse as a model of neuropathic pain: behavioral and neuroanatomical correlates. *Pain*. 76(1–2):215–22

Marchalant Y, Brownjohn PW, Bonnet A, Kleffmann T, Ashton JC. 2014. Validating Antibodies to the Cannabinoid CB2 Receptor: Antibody Sensitivity Is Not Evidence of Antibody Specificity. *J. Histochem. Cytochem.* 62(6):395–404

Marks DM, Shah MJ, Patkar AA, Masand PS, Park G-Y, Pae C-U. 2009. Serotonin-norepinephrine reuptake inhibitors for pain control: premise and promise. *Curr. Neuropharmacol.* 7(4):331–36

Marsicano G, Kuner R. 2008. Anatomical Distribution of Receptors, Ligands and Enzymes in the Brain and in the Spinal Cord: Circuitries and Neurochemistry. In *Cannabinoids and the Brain*, pp. 161–201. Boston, MA: Springer US

Martinez FO, Gordon S. 2014. The M1 and M2 paradigm of macrophage activation: time for reassessment. *F1000Prime Rep.* 6:13

Matsuda LA, Lolait SJ, Brownstein MJ, Young AC, Bonner TI. 1990. Structure of a cannabinoid receptor and functional expression of the cloned cDNA. *Nature*. 346(6284):561–64

Mecha M, Feliú A, Carrillo-Salinas FJ, Rueda-Zubiaurre A, Ortega-Gutiérrez S, et al. 2015. Endocannabinoids drive the acquisition of an alternative phenotype in microglia. *Brain. Behav. Immun.*

Mechoulam R, Ben-Shabat S, Hanus L, Ligumsky M, Kaminski NE, et al. 1995. Identification of an endogenous 2-monoglyceride, present in canine gut, that binds to cannabinoid receptors. *Biochem. Pharmacol.* 50(1):83–90

Meyer R a, Ringkamp M, Campbell JN, Raja S. 2006. Peripheral mechanisms of cutaneous nociception. *Wall Melzack's Textb. Pain*. 3–34

Milligan ED, Twining C, Chacur M, Biedenkapp J, O'Connor K, et al. 2003. Spinal glia and

proinflammatory cytokines mediate mirror-image neuropathic pain in rats. *J. Neurosci.* 23(3):1026–40

Mitrirattanakul S, Ramakul N, Guerrero A V., Matsuka Y, Ono T, et al. 2006. Site-specific increases in peripheral cannabinoid receptors and their endogenous ligands in a model of neuropathic pain. *Pain*. 126(1):102–14

Murray PJ, Allen JE, Biswas SK, Fisher EA, Gilroy DW, et al. 2014. Macrophage Activation and Polarization: Nomenclature and Experimental Guidelines. *Immunity*. 41(1):14–20

Murray PJ, Wynn TA. 2011. Protective and pathogenic functions of macrophage subsets. *Nat. Rev. Immunol.* 11(11):723–37

Nadal X, La Porta C, Bura SA, Maldonado R. 2013. Involvement of the opioid and cannabinoid systems in pain control: New insights from knockout studies

Nadeau S, Filali M, Zhang J, Kerr BJ, Rivest S, et al. 2011. Functional recovery after peripheral nerve injury is dependent on the pro-inflammatory cytokines IL-1β and TNF: implications for neuropathic pain. *J. Neurosci.* 31(35):12533–42

Napoli I, Noon LA, Ribeiro S, Kerai AP, Parrinello S, et al. 2012. A Central Role for the ERK-Signaling Pathway in Controlling Schwann Cell Plasticity and Peripheral Nerve Regeneration In Vivo. *Neuron*. 73(4):729–42

Niesters M, Martini C, Dahan A. 2014. Ketamine for chronic pain: risks and benefits. *Br. J. Clin. Pharmacol.* 77(2):357–67

Nirogi R, Goura V, Shanmuganathan D, Jayarajan P, Abraham R. 2012. Comparison of manual and automated filaments for evaluation of neuropathic pain behavior in rats. *J. Pharmacol. Toxicol. Methods*. 66(1):8–13

Pacher P, Mechoulam R. 2011. *Is lipid signaling through cannabinoid 2 receptors part of a protective system?*

Panikashvili D, Simeonidou C, Ben-Shabat S, Hanuš L, Breuer A, et al. 2001. An endogenous cannabinoid (2-AG) is neuroprotective after brain injury. *Nature*. 413(6855):527–31

Paszcuk AF, Dutra RC, da Silva KABS, Quintão NLM, Campos MM, et al. 2011. Cannabinoid agonists inhibit neuropathic pain induced by brachial plexus avulsion in mice by affecting glial cells and MAP kinases. *PLoS One*. 6(9):e24034

Paulson PE, Morrow TJ, Casey KL. 2000. Bilateral behavioral and regional cerebral blood flow changes during painful peripheral mononeuropathy in the rat. *Pain*. 84(2–

3):233–45

Perkins N. M, Tracey D. J. 2000. Hyperalgesia due to nerve injury: role of neutrophils. *Neuroscience*. 101(3):745–57

Petrosino S, Palazzo E, de Novellis V, Bisogno T, Rossi F, et al. 2007. Changes in spinal and supraspinal endocannabinoid levels in neuropathic rats. *Neuropharmacology*. 52(2):415–22

Racz I, Nadal X, Alferink J, Baños JE, Rehnelt J, et al. 2008a. Crucial role of CB(2) cannabinoid receptor in the regulation of central immune responses during neuropathic pain. *J. Neurosci.* 28(46):12125–35

Racz I, Nadal X, Alferink J, Baños JE, Rehnelt J, et al. 2008b. Interferon-gamma is a critical modulator of CB(2) cannabinoid receptor signaling during neuropathic pain. *J. Neurosci.* 28(46):12136–45

Rácz I, Nent E, Erxlebe E, Zimmer A. 2015. CB1 receptors modulate affective behaviour induced by neuropathic pain. *Brain Res. Bull.* 114:

Rahn EJ, Hohmann AG. 2009. Cannabinoids as Pharmacotherapies for Neuropathic Pain: From the Bench to the Bedside. *Neurotherapeutics*. 6(4):713–37

Ren K, Dubner R. 2010. Interactions between the immune and nervous systems in pain. *Nat. Med.* 16(11):1267–76

Romero-Sandoval EA, Horvath R, Landry RP, DeLeo JA. 2009. Cannabinoid receptor type 2 activation induces a microglial anti-inflammatory phenotype and reduces migration via MKP induction and ERK dephosphorylation. *Mol. Pain*. 5:25

Rose S, Misharin A, Perlman H. 2012. A novel Ly6C/Ly6G-based strategy to analyze the mouse splenic myeloid compartment. *Cytometry. A*. 81(4):343–50

Schatz AR, Lee M, Condie RB, Pulaski JT, Kaminski NE. 1997. Cannabinoid Receptors CB1 and CB2: A Characterization of Expression and Adenylate Cyclase Modulation within the Immune System. *Toxicol. Appl. Pharmacol.* 142(2):278–87

Schlosburg JE, Blankman JL, Long JZ, Nomura DK, Pan B, et al. 2010. Chronic monoacylglycerol lipase blockade causes functional antagonism of the endocannabinoid system. *Nat. Neurosci.* 13(9):1113–19

Schmöle A-C, Lundt R, Gennequin B, Schrage H, Beins E, et al. 2015. Expression Analysis of CB2-GFP BAC Transgenic Mice. *PLoS One*. 10(9):e0138986

Scholz J, Woolf CJ. 2007. The neuropathic pain triad: neurons, immune cells and glia. *Nat. Neurosci.* 10(11):1361–68

Schreiber KL, Beitz AJ, Wilcox GL. 2008. Activation of spinal microglia in a murine model of peripheral inflammation-induced, long-lasting contralateral allodynia. *Neurosci. Lett.* 440(1):63–67

Seltzer Z, Dubner R, Shir Y. 1990. A novel behavioral model of neuropathic pain disorders produced in rats by partial sciatic nerve injury. *Pain*. 43(2):205–18

Shubayev VI, Kato K, Myers RR. 2010. *Cytokines in Pain*. CRC Press/Taylor & Francis

Starowicz K, Makuch W, Korostynski M, Malek N, Slezak M, et al. 2013. Full inhibition of spinal FAAH leads to TRPV1-mediated analgesic effects in neuropathic rats and possible lipoxygenase-mediated remodeling of anandamide metabolism. *PLoS One*. 8(4):e60040

Stein C. 2013. Opioids, sensory Systems and chronic Pain. *Eur. J. Pharmacol.*

Stempel AV, Stumpf A, Zhang H-Y, Özdoğan T, Pannasch U, et al. 2016. Cannabinoid Type 2 Receptors Mediate a Cell Type-Specific Plasticity in the Hippocampus. *Neuron*. 90(4):795–809

Sugiura T, Kobayashi Y, Oka S, Waku K. 2002. Biosynthesis and degradation of anandamide and 2-arachidonoylglycerol and their possible physiological significance. *Prostaglandins, Leukot. Essent. Fat. Acids*. 66(2–3):173–92

Szczudlik A, Dobrogowski J, Wordliczek J, Stępień A, Krajnik M, et al. 2014. Diagnosis and management of neuropathic pain: review of literature and recommendations of the Polish Association for the study of pain and the Polish Neurological Society - part one. *Neurol. Neurochir. Pol.* 48(4):262–71

Ternes S. 2013. Investigation of the endocannabinoid system using in vivo and in vitro models. . (April):

Tomar S, E. Zumbrun E, Nagarkatti M, Nagarkatti PS. 2015. Protective Role of Cannabinoid Receptor 2 Activation in Galactosamine/Lipopolysaccharide-Induced Acute Liver Failure through Regulation of Macrophage Polarization and MicroRNAs. *J. Pharmacol. Exp. Ther.* 353(2):369–79

Treede R-D-D, Jensen TS, Campbell JN, Cruccu G, Dostrovsky JO, et al. 2008. Neuropathic pain: redefinition and a grading system for clinical and research purposes. *Neurology*. 70(18):1630–35

Trinchieri G, Sher A. 2007. Cooperation of Toll-like receptor signals in innate immune defence. *Nat. Rev. Immunol.* 7(3):179–90

Tsuda M, Inoue K. 2016. Neuron-microglia interaction by purinergic signaling in

neuropathic pain following neurodegeneration. *Neuropharmacology*. 104:76–81

Tsuda M, Shigemoto-mogami Y, Koizumi S. 2003. P2X 4 receptors induced in spinal microglia gate tactile allodynia after nerve injury. . 424(August):1–6

Turcotte C, Blanchet M-RRR, Laviolette M, Flamand N. 2016. The CB2 receptor and its role as a regulator of inflammation. *Cell. Mol. Life Sci.* 73(23):4449–70

Üçeyler N, Tscharke A, Sommer C. 2007. Early cytokine expression in mouse sciatic nerve after chronic constriction nerve injury depends on calpain. *Brain. Behav. Immun.* 21(5):553–60

Van Hecke O, Austin SK, Khan RA, Smith BH, Torrance N. 2014. Neuropathic pain in the general population: A systematic review of epidemiological studies. *Pain*. 155(4):654–62

Verma V, Singh N, Singh Jaggi A. 2014. Pregabalin in neuropathic pain: evidences and possible mechanisms. *Curr. Neuropharmacol.* 12(1):44–56

Walker K, Fox AJ, Urban LA. 1999. Animal models for pain research. *Mol. Med. Today*. 5(7):319–21

Walter L, Franklin A, Witting A, Wade C, Xie Y, et al. 2003. Nonpsychotropic cannabinoid receptors regulate microglial cell migration. *J. Neurosci.* 23(4):1398–1405

Ware MA, Adams H, Guy GW. 2004. The medicinal use of cannabis in the UK: results of a nationwide survey. *Int. J. Clin. Pract.* 59(3):291–95

Whiteside GT, Gottshall SL, Boulet JM, Chaffer SM, Harrison JE, et al. 2005. A role for cannabinoid receptors, but not endogenous opioids, in the antinociceptive activity of the CB2-selective agonist, GW405833. *Eur. J. Pharmacol.* 528(1–3):65–72

Witting A, Walter L, Wacker J, Moller T, Stella N. 2004. P2X7 receptors control 2-arachidonoylglycerol production by microglial cells. *Proc. Natl. Acad. Sci.* 101(9):3214–19

Woolf CJ, Mannion RJ. 1999. Neuropathic pain: aetiology, symptoms, mechanisms, and management. *Lancet*. 353(9168):1959–64

Wotherspoon G, Fox A, McIntyre P, Colley S, Bevan S, Winter J. 2005. Peripheral nerve injury induces cannabinoid receptor 2 protein expression in rat sensory neurons. *Neuroscience*. 135(1):235–45

Zhang J, Hoffert C, Vu HK, Groblewski T, Ahmad S, O'Donnell D. 2003. Induction of CB2 receptor expression in the rat spinal cord of neuropathic but not inflammatory chronic pain models. *Eur. J. Neurosci.* 17(12):2750–54

Zhu Y, Romero MI, Ghosh P, Ye Z, Charnay P, et al. 2001. Ablation of NF1 function in neurons induces abnormal development of cerebral cortex and reactive gliosis in the brain. *Genes Dev.* 15(7):859–76

8 Acknowledgements/ Danksagung

Hiermit möchte ich mich als Erstes bei Herrn Prof. Andreas Zimmer bedanken. Vielen Dank für die Unterstützung und für all die wissenschaftlichen Diskussionen, die mir bei der Erarbeitung des Projekts und der Thesis sehr geholfen haben. Außerdem bin ich dankbar, meine Doktorarbeit im Institut für molekulare Psychiatrie gemacht zu haben.

Als nächstes danke ich Dr. Chihiro Nozaki für die Betreuung meiner Arbeit. Sie war stets sehr hilfbereit und hat mir, besonders am Anfang, alles ausführlich erklärt und gezeigt. Vielen Dank für die schöne gemeinsame Zeit, die zahlreichen Diskussionen und die Gelassenheit, mit der du mich betreut hast, Chihiro!

Des Weiteren bedanke ich mich bei Herrn Prof. Michael Pankratz, der die Aufgabe des Zweitbetreuers übernommen hat und als Teil meines Thesis Committee der BIGS Graduierten Schule einige hilfreiche Anregungen hatte.

Herrn Prof. Gerhard von der Emde danke ich, dass er die Aufgabe des Drittprüfers übernommen hat und mich so nett während eines Master Moduls betreut hat.

Herrn Prof. Klaus Mohr danke ich, mein fachfremder Prüfer zu sein.

Dr. Laura Bindila danke ich, mir bei der Messung der Endocannabinoide geholfen zu haben.

Auch bedanken möchte ich mich bei Anne Schmöle, die mir besonders bei den Flow Cytometry Experimenten geholfen hat. Unsere kurze gemeinsame Bürozeit fand ich sehr angenehm.

Ildiko Racz, Edda Erxlebe und Astrid Markert möchte ich für die Hilfe bei den von Frey Experimenten danken. Zu zweit ging die Zeit immer schneller vorbei.

Einen besonderen Dank an Ash: Thanks a lot for all the nice, funny, entertaining coffe and lunch breaks and for becoming a good friend of mine!

Außerdem danke ich dem gesamten Labor für die schöne Zeit, in der ich mir sehr wohl gefühlt habe. Vielen Dank an alle, die mir geholfen haben! Außerdem besonderen Dank an Frank, Yves, Till und Gregor für die unterhaltsame Ablenkung in den Mittags und Kaffeepausen (und das gelegentliche Feierabendbier).

Ich danke auch besonders Omar, der mich am Ende mit seinem Elan und seiner Zuversicht immer wieder motiviert hat.

Als Letztes möchte ich mich bei meiner Familie bedanken, für die tolle Unterstützung, den Glaube an mich und den Versuch, mir bei meinen wissenschaftlichen Vorträgen interessiert zuzuhören.

Publications

Elisa Nent

- Racz I, **Nent E**, Erxlebe E, Zimmer A (2015) CB1 receptors modulate affective behavior induced by neuropathic pain. *Brain Res Bull* 114:42–48.

- **Nent, E.**, Frommholz, D., Gajda, M., Bräuer, R., Illges H**.** (2013) Histamine 4 receptor plays an important role in auto-antibody-induced arthritis. *Int Immunol.* 25(7):437-43